NTNU – Trondheim
Norwegian University of
Science and Technology

Removal of Triclocarban (TCC) and Diethyl Phthalate (DEP) from Greywater by Adsorption onto Activated Carbon

Ingrid Frogner Skår

Civil and Environmental Engineering (2 year)
Submission date: Januar 2014
Supervisor: Stein Wold Østerhus, IVM
Co-supervisor: Viggo Bjerkelund, IVM

Norwegian University of Science and Technology
Department of Hydraulic and Environmental Engineering

Norwegian University of Science and Technology
NTN

Department of Hydraulic and Environmental Engineering
Faculty of Engineering Science and Technology

MSc – Thesis

Water and Wastewater Engineering

2013

Stud. techn.: **Ingrid Frogner Skår**

Thesis: **Removal of Triclocarban (TCC) and Diethyl Phthalate (DEP) from Greywater by Adsorption onto Activated Carbon**

Description of thesis

This Thesis is based on the findings from my specialization project, where an investigation of priority micropollutants in greywater from PCPs was conducted (Skår, 2013). The objective of the Master Thesis was to select two or three compounds from the list of priority compounds that was suitable for analyzing and monitoring in a greywater recycling scheme, and investigate the removal of those compounds with adsorption onto activated carbon. This was done by performing kinetic and isotherms study in greywater and pure water. An analytical method for detection and quantification in greywater had to be developed for the chosen compounds.

Specific tasks

1. The candidate is to do a literature search on analytical procedures with HPLC and UV detector used on the selected compounds. From this the candidate will decide if it is possible to continue with the selected compounds.

2. The candidate is to do a literature search on the selected compounds with a special focus on properties, occurrence in wastewater/greywater, and removal from water with biological, chemical and physical treatment processes

3. The candidate is to describe analytical methods common to use on micropollutants with a special focus on HPLC and UV detection.

4. The candidate is to describe adsorption with activated carbon with a special focus on kinetic and isotherm models.

5. The candidate is to develop an analytical method with HPLC and UV detection that can detect and quantify the selected compounds down to µg/L range.

6. The candidate is to conduct batch tests on the selected compounds separate and in mixture, to determine kinetic and isotherm constants. Ultra-pure water (Milli-Q water) and greywater should be used in these tests. The greywater samples will be supplied from PhD candidate Viggo Bjerkelund. How potential competition between the analytes affect adsorption should be evaluated.

7. The candidate will use the results from the experiments to discuss practical implications of activated carbon to remove micropollutants.

Organization and assistance

For this thesis, the main teaching supervisor will be professor Stein Østerhus with co- assistance from PhD candidate Viggo Bjerkelund. Other people at NTNU and Sintef can also be asked for professional advice. Laboratorial help will be provided by the laboratory technicians. The analysis and experiments will be done, as far as possible, by the candidate herself.

Delivery of thesis

The thesis will be delivered in accordance with the regulation set by the Department of Hydraulic and Environmental Engineering, NTNU. The institute requires an electronic copy to be handed in, containing all the text documents, attachments, data, and calculations.

Deadline: 15.01.14

Department of Hydraulic and Environmental Engineering, NTNU

20.08.2013

Stein Østerhus

Professor

Preface and Acknowledgements

This is a Master of Science conducted at the Department of Hydraulic and Environmental Engineering at the Norwegian University of Science and Technology in autumn 2013.

It has been a lot of hard work and long days in the lab, but I have also learned extremely lot.

I wish to thank my supervisor Stein Østerhus at the Department of Hydraulicand Environmental Engineering, Norwegian University of Science and Technology for his assistance. I always felt welcome at his office, and he always took the time for a talk when I needed it.

I would also like to thank PhD candidate Viggo Bjerkelund for invaluable help and assistance with this thesis. When I had problems with the analytical equiptment, he was there to help, both with the machine and the moral.

Also a big thank is given to the technical lab staff Trine Ness and Gøril Thorvaldsen for always having a hand free when I needed help. The whole lab experience would not have been the same without them.

Without the help of these people the implementation of this Master Thesis would have been a lot harder.

Oslo, January 2014

Ingrid Frogner Skår

Abstract

In this Master Thesis, the removal of the micropollutants diethyl phthalate (DEP) and triclocarban (TCC) from greywater by adsorption onto activated carbon was investigated. The commercial activated carbon F400 was selected due to its high microporosity and extensive use on removal of micropollutants from aqueous solutions. Both greywater and milli-Q water were used for all the experiments. This was done to see if the present of dissolved organic carbon in the greywater affected the adsorption efficiency of DEP and TCC. Also, isotherm experiments with the two compounds in mixture were conducted to see the potential competition between them.

The concentrations decay data were interpreted by using kinetic models. Intraparticle diffusion models were used as an attempt to describe the rate limiting step of the adsorption process. The equilibrium adsorption data were interpreted with the linear and non-linear form of the Langmuir and Freundlich model. High removals were obtained for TCC and DEP, both in MQ and GW. An agitation time of 6 hours was needed for the TCC to reach equilibrium, while an agitation time of 24 hours was needed for the DEP to reach equilibrium.

Results revealed that the adsorption decay of DEP and TCC was best fitted with the pseudo second order equation. It obtained the closest correlation coefficients to unity (0.98-1) and the lowest normal standard deviation values (5-7%). The Elovich equation generated the next best fit for the two compounds. The pseudo first order equation seemed to be not suitable in describing the adsorption decay of DEP and TCC onto F400. According to the pseudo second order rate constant, higher rates were obtained in GW than in MQ water for both of the compounds. The difference was considered to be very little. The rate constants of TCC were much higher (0.47-1.1 mg/µgxmin) than the ones obtained for DEP (0.0006-0.0009 mg/µgxmin). This is probably due to the limited water solubility and high hydrophobicity of TCC compared to DEP. Also the initial concentration of TCC (20 µg/L) was much less than the initial concentration of DEP (5 mg/L). For the rate limiting mechanisms it seemed that the sorption of DEP and TCC was a rather complex process where both film diffusion and intraparticle diffusion mechanisms occurred simultaneously. However, the Drumwald-Wagner model showed good fit for the TCC data, which could indicate that intraparticle diffusion is the dominating rate limiting mechanism for TCC sorption.

The results from the equilibrium isotherm data showed that the sorption of TCC was best fitted with the non-linear Langmuir model. This indicates that the sorption of TCC is homogenous and monolayered. The sorption of TCC was considered a bit more favorable in MQ than in GW. No significant difference was observed for TCC alone and TCC in mixture with DEP, which support that TCC possess a great affinity towards the carbon surface. The equilibrium adsorption data of DEP was best fitted to the linear and non-linear Freundlich model. This indicates a more heterogeneous sorption process. The linear approach obtained some better fit than the non-linear model. According to the Freundlich constants, the sorption of DEP was a bit affected by the presence of the dissolved organic carbon in the greywater and by the TCC in the mixture solution. Highest adsorption capacity was achieved for DEP alone in MQ water.

Sammendrag

I denne masteroppgave har det blitt undersøkt om hvorvidt mikroforurensingene diethyl phthalate (DEP) og triclocarban (TCC) kan fjernes fra gråvann ved å benytte seg av adsorpsjon med aktiv kull. Det aktive kullet F400 ble brukt til adsorpsjonen. Dette er et kul med høy mikroporøsitet og som ofte er brukt til å fjerne mikroforurensinger. Alle eksperimentene ble utført med både gråvann og milli-Q vann. Dette for å se om løst organisk stoff i gråvannet kom til å ha noen innvirkning på adsorpsjonen. I tillegg ble det utført forsøk med DEP og TCC sammen i løsning, for å se om det var noen potensiell konkurranse mellom dem.

Minkingen av TCC og DEP i vannløsningen ble tolket ved bruk av kinetikk modeller. Interpartikulære diffusjons modeller ble brukt til å beskrive hvilke mekanismer som begrenset adsorpsjonsprosessen. Resultatene for isoterm forsøkene ble modellert med de ikke- lineære og lineære Langmuir og Freundlich ligningene. Høy fjerning av både TCC og DEP ble oppnådd ved bruk av adsorpsjon, både i gråvann og milli-Q vann. En kontakttid på minst 6 timer var nødvendig for at TCC skulle oppnå likevekt, mens DEP krevde en kontakttid på minst 24 timer for å oppnå likevekt.

Pseudo andregrads ligning passet best til å beskrive adsorpsjonshastighet for både DEP og TCC. Høye korrelasjonskoeffisienter (0.98-1) og lave avvik (5-7%) bekreftet dette. Elovich modellen resulterte i den nest beste tilnærmingen. Den modellen som virket minst passende til å beskrive resultatene var den av pseudo førstegrads orden. I følge kinetikk resultatene så kan man forvente raskere nedgang i gråvann enn i milli-Q vann for både DEP og TCC. Dette er ikke sagt med stor sikkerhet, siden forskjellen mellom de var veldig liten. Hastighets konstant for fjerning av TCC (0.47-1,1 mg/µgxmin) var mye raskere enn hastigheten observert for DEP (0.0006-0.0009 mg/µgxmin . Dette kan skyldes at TCC er mye mindre vannløselig og mer hydrofob sammenlignet med DEP. I tillegg så var start konsentrasjonen av TCC (20 µg/L) veldig mye mindre enn start konsentrasjonen av DEP (5 mg/L). Resultatene fra interpartikulær diffusjon modelleringen indikerte at adsorpsjon av TCC og DEP var en kompleks prosess som involverte både film diffusjon og intrerpartikulær samtidig. Drumwald-Wagner modellen ga gode tilnærminger til TCC resultatene, noe som kan tyde på at interpartikulær er den dominerende begrensende faktoren for adsorpsjon av TCC.

For TCC isotermene så var det den ikke-lineære Langmur modellen som ga best tilnærming til resultatene. Dette kan være en indikasjon på at adsorpsjonen av TCC foregikk forholdsvis homogent, og at det ble dannet et monomolekylært lag på overflaten av kullet. I henhold til Langmuir modellen, så var adsorpsjon potensialet for TCC klassifisert som bedre i milli-Q vann enn i gråvann. Det var ingen stor forskjell mellom TCC alene i løsning og TCC i blanding med DEP. Dette kan tolkes som at TCC har veldig stor tiltrekningskraft til aktiv kull. DEP isotermene var best tilnærmet ved bruk av både den lineær og ikke lineær Freundlich modellen. Dem lineære formen av Freundlich modellen oppnådde litt bedre resultater enn den ikke lineære. Dette indikerer at adsorpsjonen av DEP var en mer heterogen prosess. og at det ble dannet flere lag av molekyler på overflaten til kullet. I henhold til Freundlich konstantene så tyder resultatene på at adsorpsjonen av DEP ble påvirket av andre organiske komponenter i gråvannet og av TCC i den blandete løsningen. Høyest adsorpsjonskapasitet ble oppnådd for DEP alene i milli-Q vann.

Contents

Nomenaclature

Adsorbate: A solute that adsorbs to a solid

Adsorbent: A solid that adsorbs solutes

AOP: Advanced oxidation process

BAF: Bioaccumulation factor

BCF: Bioconcentration factor

BSAF: Biota-sediment accumulation factor

DAD: Diod array detection

DEP: Diethyl phthalate

DOC: Dissolved organic carbon

GW: Greywater

HPLC: High pressure liquid chromatography

HPV: High Production Volume

MQ water: Ultra pure ionized water

MS: Mass spectrometry

OECD: The Organization for Economic Co-operation and Development

RP: Reversed phase

SPE: Solid phase extraction

TCC: Triclocarban

TCS: Triclosan

USEPA: The United States Environmental Protection Agency

1. Introduction

1.1 Background for the Master Thesis

In the last decade it has been an increasing focus towards micro pollutants in drinking water and wastewater. These pollutants are xenobiotic or natural inorganic and organic compounds in small amounts of ng/L –µg/L originating from industry, agriculture, buildings, households etc. Many of these chemicals have been proven to be persistent and bioaccumulative, and possess adverse health effects on humans and wildlife like endocrine disruptor effects, carcinogenesis, and restraining effects on development and reproduction.

Growing populations, urbanization, higher living standard and climate change have led to water shortage in many parts of the world. Traditional centralized water supply and sanitary systems seem incapable of solving the water scarcity problems. Introduction of smaller independent semi-centralized water supply and sanitary units to urban areas, have been proposed as a more sustainable solution than traditional systems. At NTNU, PhD candidate Viggo Bjerkelund is examining such a concept that would reduce the withdrawal from natural water sources with 70 % (compared to traditional systems). This concept uses a partly closed greywater recycling loop for non-potable high body contact applications such as showering, washing purposes and toilet flushing.

In a greywater recycling scheme the same water is recycled over and over again. Therefore, constituents that are poorly removed through the applied treatment processes will accumulate. Especially accumulation of persistent organic trace contaminants is of great concern, since it is known that several groups of micropollutants are present in greywater, most originating from personal care products (PCPs) and household products.

Adsorption onto activated carbon is one of the best available technologies for removing persistent and toxic organic compounds from aqueous solutions. Today, it is one of the most common techniques applied on contaminated medias to get rid of pollutants. It exists several hundred different types of carbon that are carefully designed to suit different purposes and industries (water and air treatment, medicine, food industry etc.), contaminants (humic substances, micropollutants, bacteria etc.), and water qualities (drinking water, waste water, swimming pools, aquariums etc.).

This thesis is a follow up of the preliminary project done by the same candidate, where an investigation of priority micropollutants in greywater from PCPs was conducted. The thesis aims to select two or three compounds from the list of priority compounds that is suitable for analyzing and monitoring in a greywater recycling scheme. An analytical method using high pressure liquid chromatography (HPLC) and UV detection will need to be developed for the picked compounds. The main goal is to find out how well the selected compounds ,separate and in mixture, can be removed with adsorption onto activated carbon by doing kinetic and isotherm experiments in greywater and pure water. The potential competition between the analytes or with other dissolved organic compounds needs to be evaluated. In the end, an assessment on how activated carbon can be used in practical applications to remove micropollutants from greywater will be performed.

1.2 Selection of analytes

In the preliminary specialization project written by the same author (Skår, 2013), an investigation of priority pollutants from PCPs in greywater was conducted. From the priority pollutants found, a list of model pollutants suitable for monitoring in a greywater recycling scheme was proposed. The list is shown in table 1.

The next step was to select two or three compounds from this list that could be the subject for this thesis. The choice fell on triclocarban (TCC), diethyl phthalate (DEP) and 4-MBC. These compounds represented three different PCP groups, had different range of biodegradability and from chemical structure seemed to be analyzable by reversed phase high pressure liquid chromatography (RP-HPLC) and UV detection. The available chromatography equipment at the water lab at NTNU was an important factor in the final selection of analytes. Therefore, a literature search on analytical procedures conducted with RP-HPLC on each of the three compounds was performed. It was also looked into solid phase extraction (SPE) methods, since this is often required when working with environmental samples and small concentrations. The literature searches on HPLC and SPE are put in appendix A and B.

Based on the literature search, it was found that all three compounds were possible to analyze with RP-HPLC, with 4-MBC seeming to be the less suited given the available equipment. Out of the three compounds, diethyl phthalate was the most studied with heaps of literature available. It was thought wise to select two compounds; diethyl phthalate as the "safe" compound and triclocarban as the more unknown, bound breaking compound. Unfortunately, there was no time to analyze 4-MBC.

TABLE 1: Selected model pollutants

Modell pollutant	CAS	Priority	Likely to be found in greywater	Adverse health effects	Classified as environmental toxin	Biodegradable
Galaxolide	1222-05-5	2	Yes	EDC	Yes	Heavily
D5	541-02-6	2	Yes	EDC Carcinogen	Yes	Heavily
Diethyl phthalate (DEP)	84-66-2	3	Yes	EDC Development Carcinogen	Yes	Readily
Diethylhexyl phthalate (DEHP)	117-81-7	3	Yes	EDC Reproduction/Development Carcinogen	Yes	Readily
Triclocarban (TCC)	101-20-2	2	Yes	EDC Reproductive effects	Yes	Heavily
Piperonyl butoxide	51-03-6	2	Yes	Carcinogen	Yes	Moderate
EHMC	5466-77-3	3	Yes	EDC Reproduction	No	Readily
4-MBC	36861-47-9	2	Yes	EDC Reproduction	Yes	Not readily
Nonylphenol	25154-52-3	3	Yes	EDC	Yes	Moderate
Chloroform	67-66-3	3	Yes	Mutagenic Carcinogen	Yes	Heavily (Volatile)

1.3 Greywater characteristics

Greywater characteristics depend on the quality of the water supply, the type of distribution network and the activities in the household, service institution etc. (Eriksson et al., 2002)The production of greywater varies through the day with the highest amounts being produced in the morning and afternoon. The quantity and composition depend on several factors such as water availability, drinking water standard, resident groups, consumption habits, household chemicals, country etc. In general, greywater is less polluted than domestic wastewater due to the absence of toilet water, which contains most of the pathogens, organics and nutrients (nitrogen and phosphorous). However, greywater has a higher chemical content than domestic wastewater due to the presence of chemicals from household and personal care products etc. In some cases the chemical oxygen demand: biological oxygen demand can be as high as 4:1 (Boyjoo et al., 2013).

Greywater is characterized according to its physical and chemical parameters, and content of microorganisms. The physical parameters are made up of:

- Temperature
- Color
- Turbidity
- Suspended solids (SS)
- Electrical conductivity

The chemical parameters include:

- Dissolved organic matter
- Nutrients
- pH
- Heavy metals
- Residual chlorine
- Xenobiotic compounds

Water from kitchen and laundry contains dissolved food, heavy metals and soils. It contributes most to the total turbidity, electrical conductivity and suspended solids in greywater. Also, potential leaching of dissolved elements such as metal ions from old plumping and piping systems adds to the electrical conductivity. Laundry is by far the greatest contributor to heavy metals in greywater. The main sources for nitrogen and phosphorous are kitchen water and detergents (Eriksson et al., 2002). Presence of microorganisms such as protozoa, bacteria and helminthes in greywater is most probably caused by wash out from bodies or contaminated food(Boyjoo et al., 2013). Figure 1 and 2 shows the contribution from urine, faeces, and greywater to common wastewater parameters. Table 2 is an overview for greywater characteristics for different household sources.

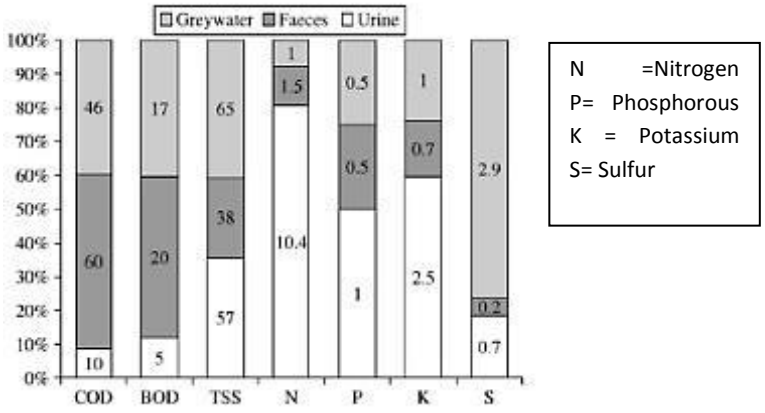

FIGURE 1: Contribution from faeces, urine and greywater to common wastewater parameters, values given in g/p*d (Meinzinger and Oldenburg, 2009)

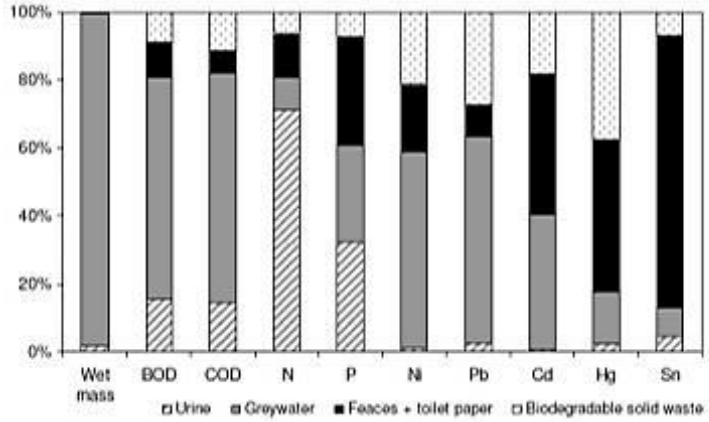

FIGURE 2: Contributions of household waste fractions to total pollutant loads (Donner et al., 2008)

TABLE 2: General characteristics of greywater from different household sources (Donner et al., 2008)

Chemical/physical property	Bathroom[1]	Laundry[2]	Kitchen[3]	Mixed household[4]
Temperature (°C)	18.3 – 31.1	28 – 32	27 – 38	18 – 38
TSS (mg L^{-1})	7 – 207	120 – 280	235 – 720	
Electrical conductivity (µS cm^{-1})	82 – 1890	190 – 1400	No data	360 – 520
pH	6.4 – 8.6	8.1 – 10	6.3 – 7.4	5 – 8.7
BOD_5 (mg L^{-1})	18 – 550	48 – 380	1040 – 1460	41 – 85
BOD_7 (mg L^{-1})	26 – 300	No data	16 – 47	350 – 500
COD (mg L^{-1})	46 – 633	725	936 – 1380	495 – 623
Tot-N (mg L^{-1})	3.2 – 46.4	6 – 21	40 – 74	0.6 – 11
Tot-P (mg L^{-1})	0.11 – 4.2	0.062 – 57	68 – 74	0.6 – 27.3
Alkalinity (mg L^{-1})	5.4 – 13.5	83 –200 ($CaCO_3$)	20 – 340 ($CaCO_3$)	
Chloride (mg L^{-1})	9.0 – 88	9 – 88	No data	3.1 – 33.4
Sulphate (mg L^{-1})	52 – 97	No data	No data	7.9 – 160

2. Description of TCC and DEP

2.1 Triclocarban

2.1.1 Properties

TCC is a trichlorinated binuclear aromatic urea compound with similar characteristics to the more familiar antiseptic triclosan (TCS)(Halden and Paull, 2005). It is used as an antimicrobial compound in PCPs, mostly disinfectants, deodorant, soaps and detergents. TCC has the ability to break down gram-positve bacteria by adsorbing to and destroying the semipermeable nature of the cytoplasmatic membrane, leading to cell death (Ribeiro da Silva et al., 2010). In short, TCC is poorly soluble in water, considerable hydrophobic, and most likely resistant to biodegradation due to its aromatic nature and high chlorine content.

Reported values of water solubility and octanol-water partitioning coefficient for triclocarban vary in literature. The first documented measurement from 1957 states a water solubility of 0.11 mg/L (Snyder and O'Connor, 2013). The EPA High Production Volume Challenge reports a measured water solubility of 0.11 or 11 mg/L , based on a poorly described method, and a logKow of 4.2 and 5.8-6 (TCC Consortium, 2002). EPI Suite estimates a water solubility of 0.65 mg/L and a logKow of 4.9. A more recently study by Snyder el al., done after standardized USEPA guidelines, measured the water solubility and logKow for TCC to be 0.045 mg/L and 3.5, respectively (Snyder et al., 2010). This seems to be the most reliable study of water solubility and logKow for TCC so far in literature.

Important properties of TCC for analysis, is the maximum absorbance wavelength and the pKa value. The maximum absorbance wavelength has been measured to be around 262-265 (see appendix A). Properties of TCC are summarized in table 3. Its chemical structure and formula are shown in figure 3.

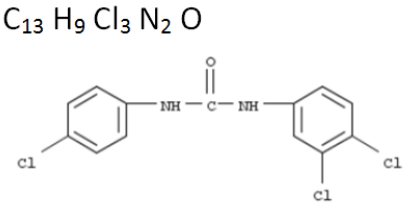

FIGURE 3: TCC chemical structure and formula(Scifinder, 2013)

TABLE 3: TCC properties

Common name (Abbreviation)	CAS No.	Molecular weight g/mol	pKa	Log Kow	Water solubility mg/L	Chlorine content	Maximum absorbance wavelength
Triclocarban (TCC)	101-20-2	315.59	12.7	3.5 4.2 5.8-6 4.9	0.045 0.11 or 11 0.65	36.7 wt %	265

2.1.2 Occurrence and environmental fate

Triclocarban (TCC) was first introduced in 1957 and its usage has continued to increase since then (Snyder et al., 2011). It is classified as and high production volume (HPV) chemical both by the USEPA and OECD (OECD, 2004, USEPA, 2006a, USEPA, 2006b). In the United States, 84% of all antimicrobial bar soaps contain TCC and its content can be as high as 5%. It is estimated that 227-454 tons of TCC are disposed every year, with most of it ending up in the drain. Studies predicts that TCC is most likely to be in the top ranking in occurrence rate and maximum concentration in US water resources among 96 organic micropollutants considered(Halden and Paull, 2005). Concentrations detected in wastewater are in the range of 0.2-50 µg/L.

There are no reported concentrations of TCC in greywater. In general it is expected that concentrations in greywater will be higher than concentrations in wastewater due to the dilution of wastewater with infiltration water and toilet water (Leal, 2010). Table 4 is an overview of reported concentrations in wastewater influents and effluents.

TABLE 4: Concentrations of TCC in wastewater influents and effluents

Wastewater influent	Wastewater effluent	Reference
6 µg/l	-	(Clark et al., 1991)
2 µg/l	-	
6.7 µg/l	0.11 µg /l	(Halden and Paull, 2005)
-	200 ng/l	
-	231 ng/l	
5.812 µg/l		(Nelson et al., 2010)
6.798 µg/l	-	(Kumar et al., 2010)
0.108 µg/l	-	
19.626 µg/l	-	
-	0.33 µg/l	(Klein et al., 2010)
-	0.244 µg/l	
-	0.12 µg/l	
-	0.17 µg/l	
-	0.046 µg/l	
3.3-5900 ng/l	27-980 ng/l	(Blair et al., 2013)
4.57 µg/l	0.62 µg/l	
4.64 µg/l	0.31 µg/l	
42 µg/l	6 µg/l	(Heidler et al., 2006)
6.1 µg/l	0.17 µg/l	
14.5 µg/l	0.54 µg/l	
15 µg/l	5 µg/l	
27 µg/l	2 µg/l	
50 µg/l	12 µg/l	
0.4 µg/l	0.08 µg/l	
16.3 µg/l	4.82 µg/l	
362 ng/l	21 ng/l	(Pedrouzo et al., 2009)
49-350 ng/l	26-130 ng/l	(Trenholm et al., 2008)

During wastewater treatment, a major part of TCC will adsorb to sludge due to its hydrophilic character. Also, further removal of solute TCC in receiving water is expected because of sorption to suspended particles that sediment. High levels of TCC in sediments have been reported downstream WWTPs. In New York, concentrations up to 25 mg/kg were detected in sediment cores (Higgins et al., 2009). In biosolids, Snyder et al. reports of concentrations in the range of 6-43mg/kg and 0.187-441mg/kg (2010). The biosolids are often used as fertilizer in agriculture. This acts as a potential route of entry to surface waters and soils. Halden and Paull calculated that activated sludge treatment plants release a load of 5800 kg of TCC into US water resources each year (2010).

The average concentration of TCC in surface water from 78 locations in the United States was found to be 20 ng/L (TCC Consortium, 2002). In Zawiercie, Poland, TCC was detected in river water in a concentration of 5µg/l (Baranowska and Wojciechowska, 2012). In Texas, concentrations of TCC downstream a WWTP ranged between 0.08 to 0.19 µg/L (Coogan et al., 2007). Some other important sources for TCC into the environment are leakages from sewers and overflow from combined sewers during heavy rainfall. In Maryland, US, TCC was found in six urban streams, none of them which received wastewater effluent, at concentrations of 30ng/L to 5.6µg/L. The source was most likely to be leakages from raw wastewater pipes in the area (Sapkota et al., 2007).

2.1.3 Removal of TCC

Not many studies have been conducted on how to remove TCC from wastewater. Tizaoui et al. studied ozone oxidation of TCC in 70% acetonitrile:30% water solution (Tizaoui et al., 2011). They found that ozone was successful in degrading TCC and that the reaction rates increased with increasing ozone pH, temperature, and concentration, see figure 4 (a), (b) and (c), respectively.

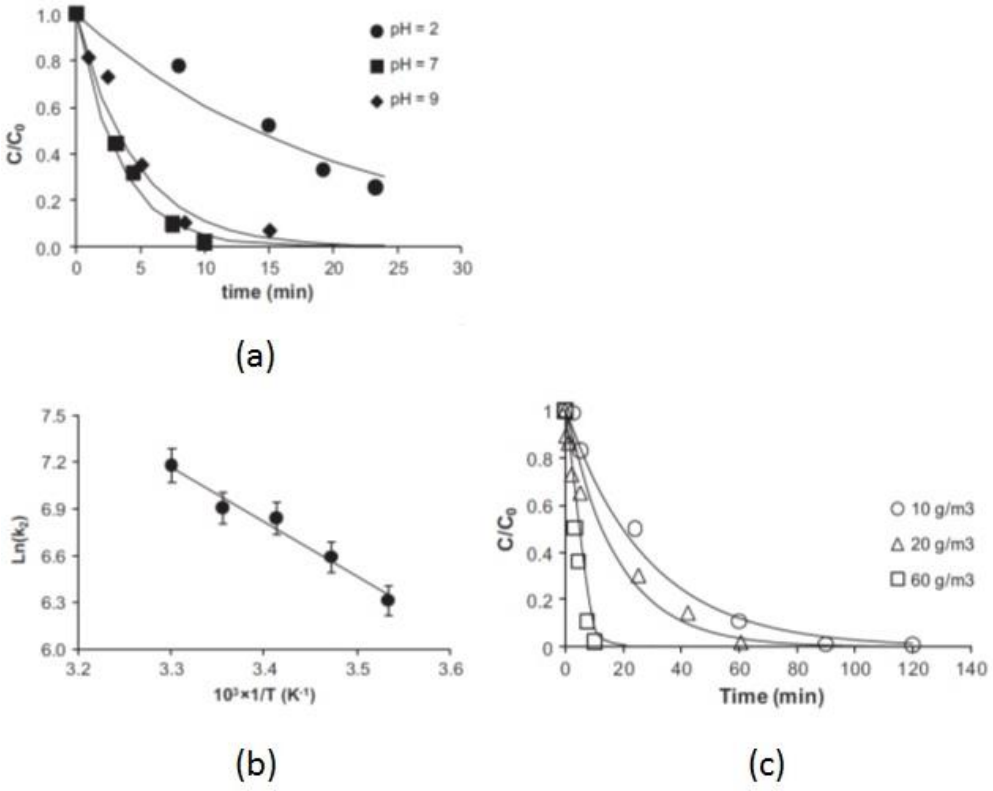

FIGURE 4: Removal of TCC by ozonation (Tizaoui et al., 2011)

2.1.4 Ecotoxicologial concern

Today, scarce information exists on TCC occurrence, fate, persistent, toxicity, bioaccumulation potential, endocrine effects, and potential for antibacterial resistance development (Snyder et al., 2010). In 2009, in the document entitled Initial Risk-Based Prioritization of HPV Chemicals, USEPA listed TCC as a "high priority" HPV chemical for further valuation and risk considerations (2009). Still, little attention and research has been given to the potential risks of TCC exposure to humans and the environment. It can be questioned why so much more resources have been invested in TCS, which is now considered a well monitored chemical in wastewater and environmental context, when the production of TCC is much higher than that of TCS (Howard and Muir, 2010).

TCC can bioaccumulate in both flora and fauna, and aquatic organisms. A study done by Coogan et al., on snails and algae living downstream of WWTPs in Texas, found BAFs up to 1600 and 2700, respectively (2007). Also, in the same study, TCC was found to be more bioaccumulative than TCS. Sediment-dwelling organisms are also subjects for TCC accumulation. A laboratory study on the worm *Lumbriculus varigatus* measured a biota-sediment accumulation factor (BSAF) for TCC and DCC (transformation product of TCC) of 2.2±0.2 and 0.3±0.1 $g_{OC}/g_{lip,}$ which gives and estimated BAF of 2200 for TCC (Higgins et al., 2009). In a study of bioconcentration of organic contaminants in Daphnia resting eggs (plankton with high importance in pelagic food webs), TCC was estimated with the highest internal concentration of the compounds assessed Figure 5 illustrates uptake and elimination kinetics for TCC in Daphnia eggs (Chiaia-Hernandez et al., 2013).

So far, no studies have looked upon TCC's capability of biomagnification in aquatic or terrestrial food chains. To determine if TCC is capable of biomagnifying in food chains, further research is necessary.

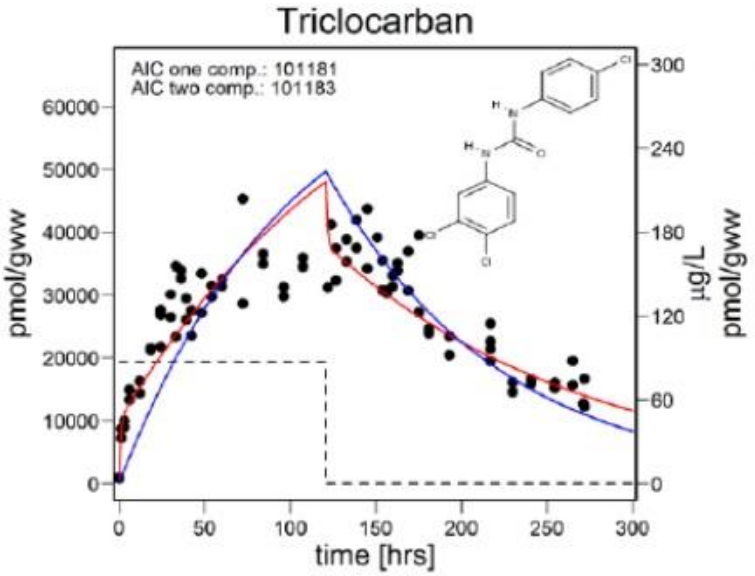

FIGURE 5: Uptake and elimination of TCC in Daphnia eggs (Chiaia-Hernandez et al., 2013)

TCC is not considered to be very toxic to humans and animals, or likely to cause skin dermatitis (Snyder and O'Connor, 2013). However, in recent research TCC have been the subject for acting as an endocrine disruptor. This is of greater concern because TCC can act as an EDC at several times less exposure levels than those seen to cause toxic effects.

In in vitro biological tests TCC has been found to enhance activity of steroid sex hormones in the estrogens and androgens receptors in cells including humans (Duleba et al., 2011). Another concern with TCC is that it is capable of inhibiting the activity of soluble epoxide hydrolase, which is important for metabolism of fatty acids in organisms (Ahn et al., 2012). In a study of freshwater mudsnails exposed to concentrations of 1.6 to 10.5 µg/L of TCC, the production of unshelled embryos was increased. When dietary fed to rats, TCC was found to affect the reproducibility capability and male sex organ (Giudice and Young, 2010, Duleba et al., 2011). Hinther et al. studied the effect of triclocarban on hormone actions and stress in frog and mammalian culture system. They found that TCC at high concentrations (316 µg/L) affected the thyroid hormone-responsive gene transcripts in mammalian cells, whereas a modest effect could be seen in tadpoles at lower concentrations (Hinther et al., 2011).

TCC transformation products also need to be included when assessing the potential impact and toxicity of TCC to aquatic ecosystems. Higgins et al. illustrated the different potential TCC biotransformation pathways, which included metabolic transformation (path A) in humans, microbial transformation (path B), and transformation during chlorination (path C) (2009). This is shown in figure 6. For instance, TCC might be a potential source for dichloroaniline, which is considered as a marine pollutant.

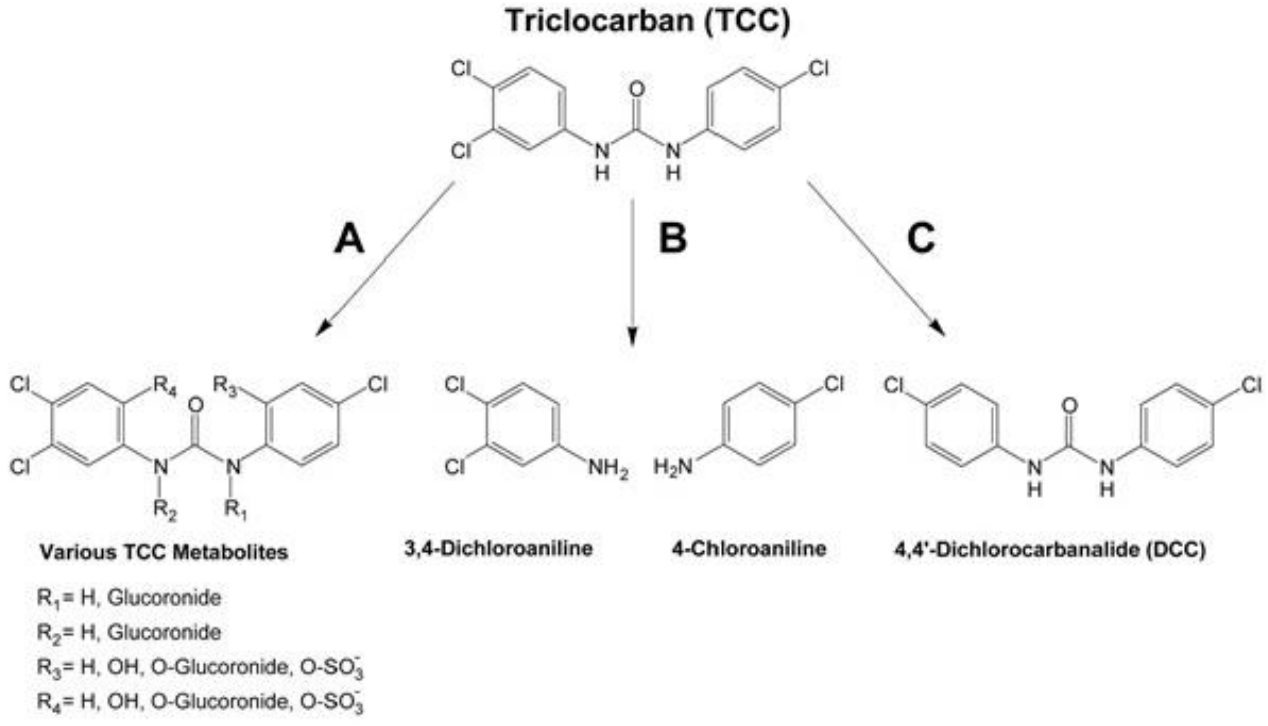

FIGURE 6: TCC transformation pathways and transformation products (Higgins et al., 2009)

2.2 Diehtyl Phthalate

2.2.1 Properties

Diethyl phthalate is one of the short chained pthalic esters. The phthalate esters have a chemical structure as di-alkyl or alkyl aryl esters and contain phthalic acids. The long chained phthalic esters such as DEHP, is commonly applied as plasticizers for cellulosic and some vinyl ester resins. DEP on the other hand, mainly function as a vehicle for fragrances and cosmetic ingredients in PCPs. It is an oily liquid, which is soluble with many of the organic molecules that act as fragrances. Compared to many of the other phthalates, DEP has high water solubility. Therefore, it is often selected as a model pollutant in studies on phthalates. The water solubility given in literature varies some. Alfa Aesar states a water solubility of DEP of 0.4 g/L, while Sigma Aldrich gives a water solubility of DEP of 0.932 g/L (Alfa Aesar, 2013, Sigma Aldrich, 2013). Other values found in literature was 1.1 g/L (Mansouri and Bousselmi, 2012) . DEP is in the middle of the hydrophobicity range with stated values for logKow of 2.65, 2.2, 2.47 and 2.72 (Sigma Aldrich, 2013, Julinova and Slavik, 2012, Api, 2001). The pKa value could not be found. The adsorption maximum wavelength was stated in literature to be between 223-226 nm (see appendix A). The chemical formula and structure of DEP is shown in figure 7. The properties of DEP are summarized in table 5.

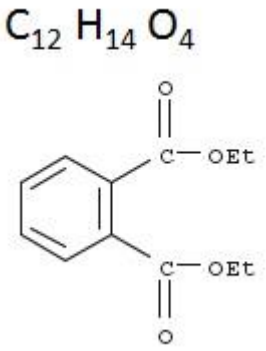

FIGURE 7: DEP chemical formula and structure (Scifinder, 2013)

TABLE 5: DEP properties

Common name (Abbreviation)	CAS No.	Molecular weight g/mol	pKa	Log Kow	Water solubility mg/L	Maximum absorbance wavelength
Diethyl Phthalate (DEP)	84-66-2	224.24 g/mol	-	2.47 [a] 2.65 [d] 2.72 [d]	1.1 g/L 0.4 g/L 0.9 g/L	226

2.2.2 Occurrence and environmental fate

DEP is a common detected micropollutants in environmental samples, and one of the most detected phthalates (Jung et al., 2010). Figure 8 shows the detection frequency of diethyl phthalate in cosmetic products. As shown by the figure, DEP was detected in 40% of the cosmetics investigated, which say something about its extensive use (Koniecki et al., 2011) The phthalates are not chemically bound and thus migration from plastics or other products is likely to happen. It is estimated that 300 metric tons of DEP is released into surface waters in the USA each year(Venkata Mohan et al., 2007). In the Han River in South Korea, phthalates accounted for the highest mass fraction (54.6%) of the micropollutant groups detected. DEP was the second most detected compound after DEHP (Oh et al., 2006).

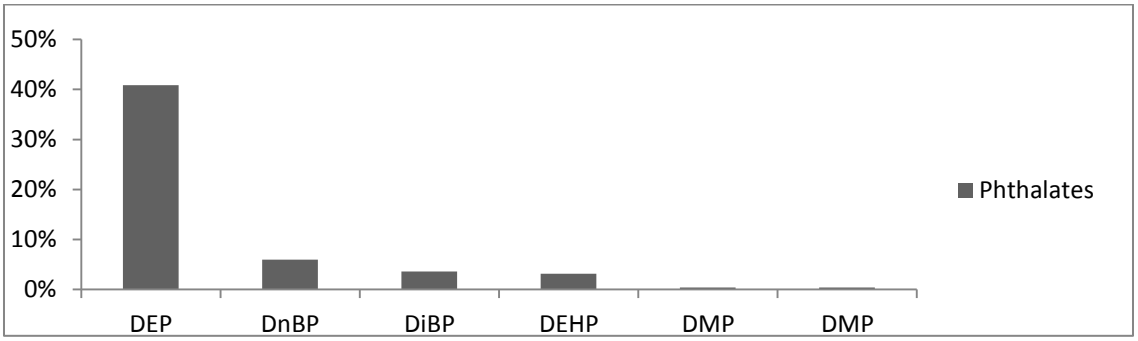

FIGURE 8: Detection frequencies of phthalates (Koniecki et al., 2012)

In an activated sludge wastewater treatment plant in France, DEP was the second major compound of the phthalates detected. Concentrations of DEP were found in all the treatment steps. At the end, a total removal efficiency of 90% was observed for DEP. Because it is a low molecular weight compounds, it is more easily degraded than many of the other phthalates. Bu even if high removal efficiencies are predicted for DEP, it is still present in wastewater effluents in the µg/L range. Some removal of DEP due to sorption to sludge is expected in water treatment. The use of the sludge as bio solids may act as a potential contamination route of DEP into the environment. Also, DEP has a high vapor pressure, and might volatilize to the atmosphere in open air treatment plants (Dargnat et al., 2009). Table 6 lists the found concentration of DEP in wastewater/greywater influent and effluent. In greywater, one article stating the concentration of DEP was found (Eriksson et al., 2003).

TABLE 6: Concentrations of DEP in wastewater influents and effluents

Wastewater influent	Wastewater effluent	Reference
23 µg/L		(Stubin et al., 1996)
4* µg/L		(Eriksson et al., 2003)
7.71 µg/L	0.78 µg/L	(Dargnat et al., 2009)
1506 µg/L	26 µg/L	(Olujimi et al., 2011)
459 µg/L	165 µg/L	
460 µg/L	89 µg/L	
752 µg/L	272 µg/L	
820 µg/L	431 µg/L	
750 µg/L	nd	
2472 µg/L	845 µg/L	

4373 µg/L	210 µg/L	
253 µg/L	nd	
217 µg/L	29 µg/L	
6596 µg/L	100 µg/L	
5281 µg/L	112 µg/L	
2353 µg/L	128 µg/L	
543 µg/L	78 µg/L	
1826 µg/L	50 µg/L	
3353 µg/L	310 µg/L	
7413 µg/L	70 µg/L	
1357 µg/L	146 µg/L	
909 µg/L	117 µg/L	
737 µg/L	nd	
657 µg/L	nd	
2103 µg/L	93 µg/L	
0.77-9.2 ng/L	nd-1.1 ng/L	(Clara et al., 2010)
102 ng/L 59.3 ng/L 389 ng/L		(Tan et al., 2008)
25 µg/L		(Oliver et al., 2005)
4.1-44 µg/L		(Vethaak et al., 2005)
	2.8 µg/L	(Li et al., 2006)
0.15-0.98 µg/L		(Zafra-Gomez et al., 2008)
	29-3206 ng/L	(Sánchez-Avila et al., 2011)

* concentrations in greywater
nd=no detection

2.2.3 Removal of Diethyl Phthalate

Through literature, it has been conducted a lot of studies on the removal of DEP and phthalates from water. DEP is a biodegradable compound and many studies have been done on its biodegradability under aerobically, anaerobically and facultative conditions (Navacharoen and Vangnai, 2011). However, biodegradation often requires long contact time to render the phthalates harmless, and in most cases complete removal is not achieved. Therefore, a lot of studies have looked into the use of adsorption, oxidation, and advanced oxidation processes to remove DEP and phthalates in wastewater (Medellin-Castillo et al., 2013)

Different AOP methods such as TiO_2UV, UV/H_2O_2, O_3/ H_2O_2 and O_3/AC have been tested on the removal of DEP from aqueous solutions (Medellin-Castillo et al., 2013, Mansouri and Bousselmi, 2012). The degradation rate of DEP by TiO_2/UV process was found to reach 78.6% under optimal conditions In general, the technologies of AOPs has been found to significantly increase the removal efficiency of DEP. For ozonation and UV processes, the formation of OH radicals has been found to be the dominaning mechanism of DEP degradation. It has been proven that activated carbon coupled to ozone enhances the formation of OH radicals. In the study by Medellin-Castillo et al., the coupling of O_3/AC was found to achieve the highest removal efficiencies in addition to lowest water toxicity. It was also stated that use of ozonation alone is limited due to the potential formation of more toxic byproducts.

Medellin-Castillo et al. studied the removal of DEP from water solution by adsorption (2013). The activated carbons showed a high adsorption capacity of DEP (up to 858 mg/g). It was found that

adsorption mechanism of DEP on activated carbon is dominated by dispersive interactions between π electrons of its aromatic ring with π electrons present on the carbon surface. It was also discovered that the pH of the solution did not affect the adsorption much.

Ferreira de Oliveria et al. studied the removal of DEP from aqueous solution onto four different activated carbons (2012). The results indicated that adsorption of DEP was favored by the ACs that had a low ratio of microporous surface to external surface. The DEP depended on the mesopores to access the micropores. The Langmuir isotherm model was found to be the most suitable model for the equilibrium adsorption data. It was also found that the presence of basic functional group on the carbon surface favored the dispersion interactions between DEP and the carbon layers. The rate constants were found to increase with temperature, but it seemed higher temperature had no effect on the adsorption capacity.

Another adsorption study done on sorption of DEP onto activated carbon was conducted by Mohan et.al (2007). By utilizing the intraparticle diffusional models it was stated that the sorption of DEP onto carbon involved both film diffusion and intraparticle diffusion. The multlinear intraparticle diffusion model was used as an attempt to describe the different diffusion stages. For the kinetis, the pseudo second order equation was best fitted. The pseudo second order rate constant was found to decrease with increasing initial concentration of DEP. The equilibrium adsorption isotherms were found to follow the Langmuir model and the principals of monolayer adsorption.

2.2.4 Ecotoxicological concern

Although DEP is not considered to be very toxic, it is suspected for being an endocrine disrupting compound and carcinogen. Especially the potential effects on reproducibility have provoked concern. In literature, it has been linked to birth defects, infertility, organ damage and cancer (Venkata Mohan et al., 2007). In an E-screen assay using the MCF-7 breast cancer cell line, DEP and DEHP showed high cell proliferation (Oh et al., 2006) Exposure to low concentrations of DEP over a long period has been reported to damage the heptacellular system (Jung et al., 2010).

DEP is not considered to be very persistent in the environment and is the subject of both photo catalysis and bacterial degradation. However, the frequently detection of DEP in the atmosphere, surface waters, sludge and soils makes it evident that the environment is not able to get rid of the DEP in the same rate as it is released. According to Mankidy et al., the low molecular weight phthalates have higher bioaccumulations potential than the higher molecular weight compounds (2013). The same article pointed out that organisms and humans are exposed to several phthalates simultaneously. In a risk assessment of DEP and phthalates, it is important to consider the potential additive effects from mixture of phthalates with the same biological pathway and same mode of disrupting actions. Bioaccumulation of DEP has been detected in fish. The freshwater bream and the saltwater flounder were found to contain 720-800 ng/g dw and 100-200 ng/g dw, respectively (Dargnat et al., 2009).

DEP has been designated as a toxic pollutant to aquatic ecosystems under the Clean Water Act (Venkata Mohan et al., 2007). The German Water Hazard Classification identified DEP as a WGK2; a substance with hazard to water (Scifinder, 2013). Today, restrictions to the release of phthalates have started to take form. In Europe, a tolerance limit of DEHP has been set to 1.3 µg/L for industrial wastewater. Also, a 30% reduction of phthalates in industrial wastewater is to be achieved by the end of year 2015 (Venkata Mohan et al., 2007)

2.2.5 Transformation products

It was difficult to find information on degradation products of DEP formed during wastewater treatment. It seems not many resources have been put into this subject, yet. By Medlin-Castillo et al., it was stated that the use of ozonation to degrade DEP was limited due to the formation of persistent and toxic byproducts (2013). Oh et al. identified formic acid and hydrogen peroxide as the main degradation products formed during ozonation of DEP (2006). A more thoroughly study on DEP ozonation products, has been conducted by Jung et al (2010). By using HPLC/UV detection, they detected the formation of highly persistent, unknown by-product peaks during ozonation. For ozonation of DEP, two main degradation pathways were identified in the study; a) hydrolysis reaction in the aliphatic chain and b) hydroxylation in the aromatic ring resulting from the attack of OH. Mono ethyl phthalate had the highest peak of the intermediates. Figure 9 shows the two pathways and the potential intermediates of DEP formed during ozonation.

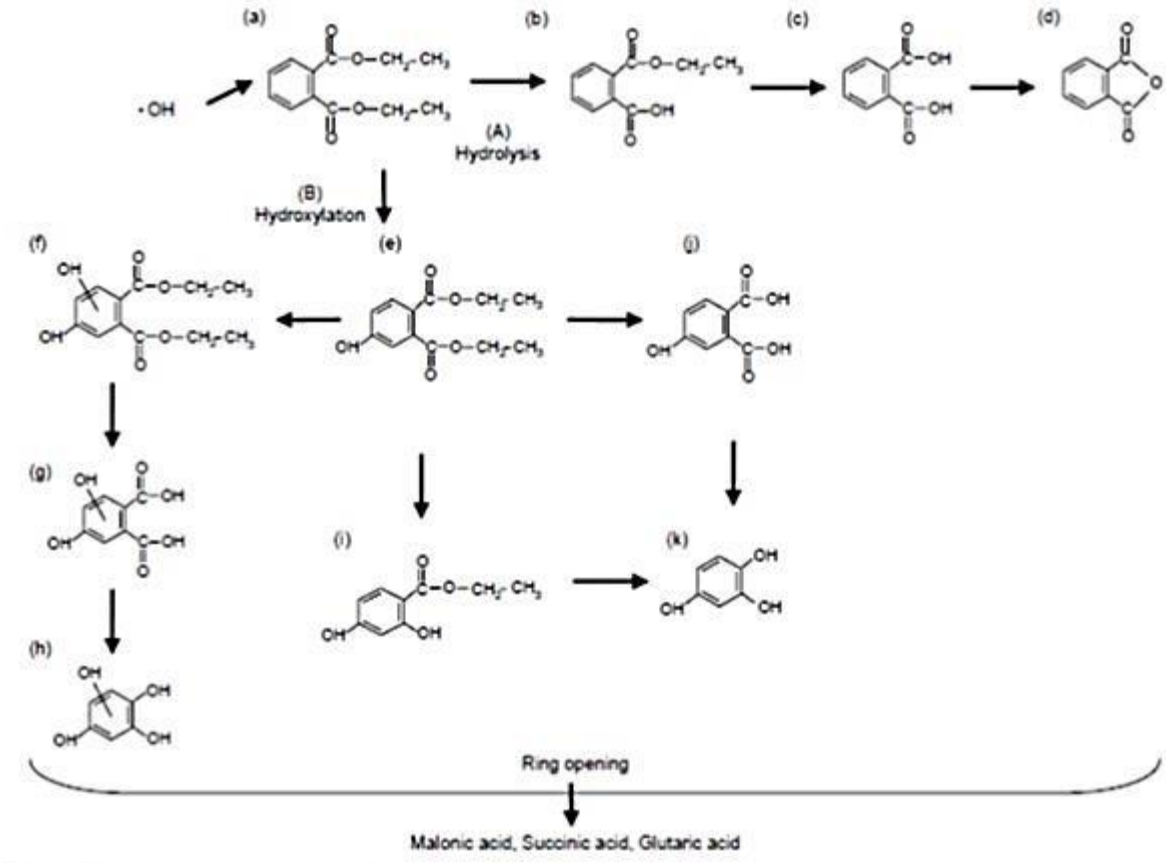

FIGURE 9: Transformation products of DEP during ozonation (Jung et al, 2009)

4. Analytical methods

4.1 Introduction

This chapter aims to give a short overview on the analytical methods and procedures used to detect and quantify micropollutants in water and a more thoroughly description of reversed phase high pressure liquid chromatography, which was used in this thesis.

An analytical technique is used to detect or quantify the concentration of a chemical compound. Today, it exist a huge variety of different techniques from the more simple ones such as gravimetric analysis and titration, to the really advanced ones, such as spectrometry and chromatography, that require highly specialized equipment and hardware. The never ending development and improvements in analytical techniques continue to expand the "analytical window" and lower the detection and quantification limit for many trace contaminants. This has played a crucial role in the acknowledgement and awareness of micropollutants over the last couple of decades (Reinhard and Debroux, 1999).

Selective and sensitive methods are needed to determine low levels of PCPs in water. Analytical methods based on gas chromatography (GC) or liquid chromatography (LC) linked to mass spectrometry (MS) or tandem mass spectrometry (MS^2) are the most common in detection and quantification of trace contaminants in water. Especially when you are dealing with an environmental matrix with many unknown compounds, mass spectrometry is the best option and in some cases essential for identification of trace contaminants. If you are doing experiments in the laboratory with selected compounds, chromatography techniques are often more than enough for quantification. Chromatography techniques alone can also be used to identify compounds in environmental water samples. However, this often requires the conductance of pre-tests in the laboratory to see when the compound is appearing on the chromatogram. Extraction, separation and pre-concentration techniques are often necessary before analytical procedures. Solid-phase-extraction is the most used extraction technique (Pedrouzo et al., 2011)

4.2 Analytical procedures

The general analytical protocol for analysis of trace contaminants in water is shown in figure 10. It consists of several interdependent operations carefully chosen to achieve the most efficient results. The operations needed depends on the concentration and properties of the analyte and quality of the water (Reinhard and Debroux, 1999).

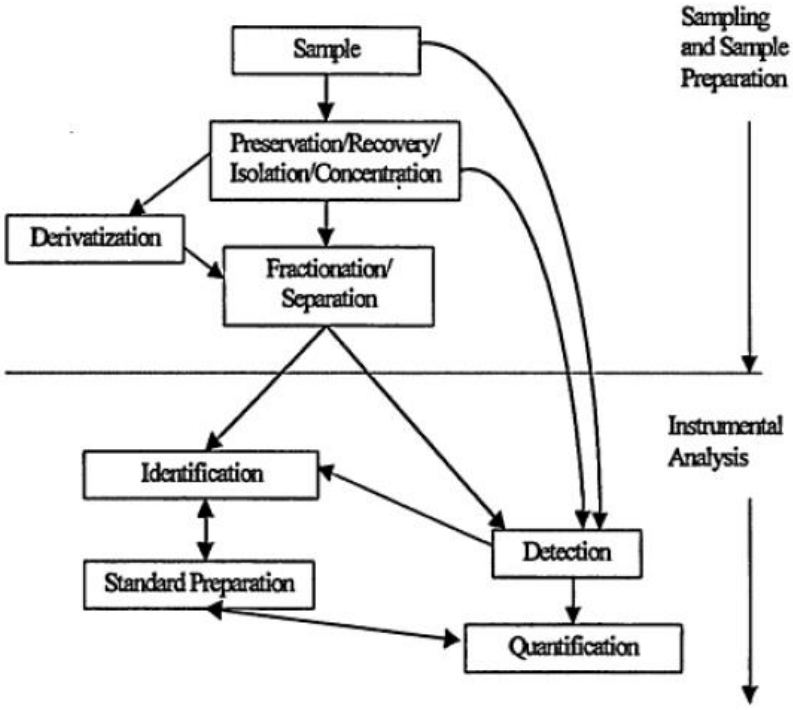

FIGURE 10: General analytical protocol for trace contaminants in water (Reinhard and Debroux, 1999)

4.2.1 Sample preparation

Samples are processed so that they are compatible with the chosen instrumental analysis. It is often necessary to preserve, recover, isolate, and/ or concentrate the analytes before the instrumental analysis. This is referred to as sample preparation and is an important part of developing a method, especially when environmental water samples are investigated. They contain a various number of different compounds that can interfere with the analyte and can have a high concentration of dissolved organic carbon (DOC) (Reinhard and Debroux, 1999).

In preservation, special care needs to be given to biodegradable compounds. Acidification to pH>2, storing at 4°C, removal of microbes by filtration, and exclusion of light are in most cases enough to preserve the samples for a few days. Compounds strongly bound to co-contaminants or to the matrix might need to go through enzymatic hydrolysis before extraction is possible. Extraction has the goal to purify and preconcentrate the analyte, and by this increase the sensitivity of the analyses (Reinhard and Debroux, 1999).

As already mentioned the most used extraction technique for PCPs in water is solid-phase extraction (SPE). SPE extract, clean, and concentrate an analyte by retaining compounds on a sorbent, normally a cartridge or a disk. This can be done in reversed phased mode (polar mobile phase, nonpolar modified solid phase), normal phased mode (nonpolar mobile phase, polar modified solid phase), by ion exchange (electrostatic attractions between charged groups), or by adsorption (interactions of compounds with unmodified materials). By selecting the right sorbent, sample volume, eluent, pH, and extraction scheme, SPE can be used to extract and concentrate compounds with a wide range of polarities and physic-chemical properties. The compounds have to be semi volatile or nonvolatile.

Figure 11 illustrates the three different schemes that are used in SPE to separate compounds of interest from impurities (Supelco, 1998).

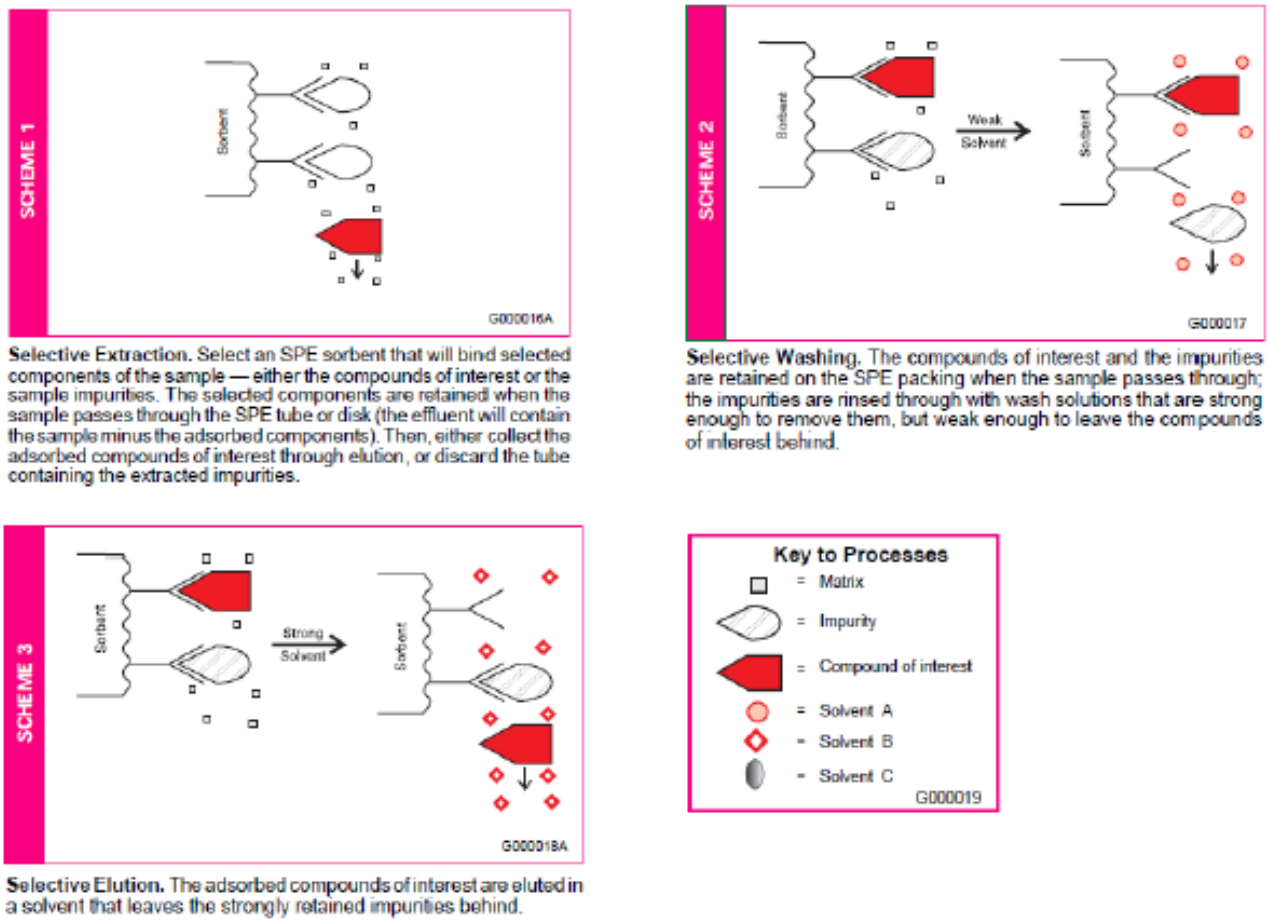

FIGURE 11: Solid Phase Extraction (Supelco, 1998)

After its invention, SPE has been preferred over liquid-liquid extraction (LLE) because it is a more environmental option that requires fewer amounts of solvents and hazardous materials, in additive to being less time-consuming. Other extraction techniques reported for PCPs are:

- Ionic liquid-based single-drop microextraction (IL-SDME)
- Dispersive liquid-liquid microextraction (DLLME)
- Solid-phase microextraction (SPME)
- Ultrasound-assisted emulisification-microextraction (USAEME)
- Stir bar sorptive extraction (SBSE)

Miniaturization is a new trend in analytical chemistry that attempts to reduce the need of organic solvents and with this minimalizing the environmental impact. IL-SDME, DLLME and USAEME are examples of extraction techniques arising from the miniaturization principle. They are becoming more and more popular in the extraction choice for PCPs in water samples (Pedrouzo et al., 2011).

4.2.2 Derivatization, fractionation and separation

Some polar compounds have properties that need to be modified before they can be managed with a given analytical technique. This is referred to as derivatization. Large molecules with thermolabile functional groups (hydroxyl, carboxyl, aminogroups) or small molecules with multiple functional groups are often subject of derivatization. This is done by using an agent that reacts selectively with the functional group to form a stable product that can be further separated from the water matrix or from other analytes by SPE, chromatography, mass spectrometry etc. (Reinhard and Debroux, 1999).

Fractionation and separation mean the use of preparative column chromatography, followed by GC or HPLC. This allows for numerous of compounds to be separated, and is often done as a pre-step before MS operations, where the analytes are identified. New research is focusing on finding MS techniques that are so selective and good that preparative column chromatography is unnecessary. Chromatography is explained more in the following sections (Reinhard and Debroux, 1999).

4.3 Chromatography

The word chromatography refers to the analytical technique where you separate different molecules based on their structure, composition or both. This is done by moving a sample, liquid or gaseous, over a stationary phase, most commonly placed inside a column. The attractive forces and interactions between the molecules, mobile phase and the stationary phase will differ, leading to the separation of molecules (Kupiec, 2004). Figure 12 is a simplified illustration of the separation process in a chromatographic column.

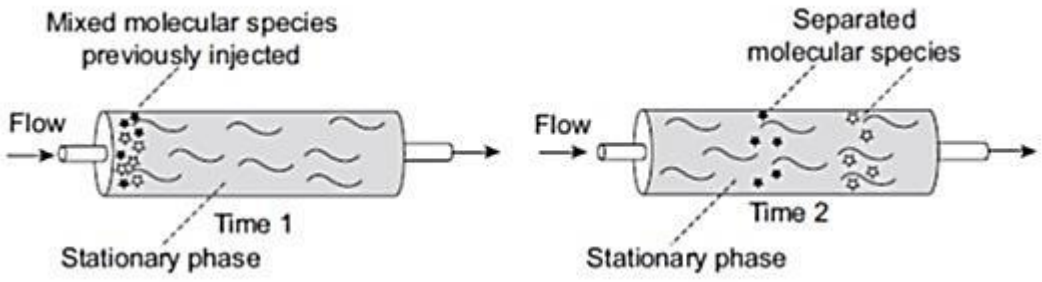

FIGURE 12: Separation process in a chromatographic column (Moldoveanu and David, 2013a)

The discovery of chromatography started in the late 19th century, but the "official" birthday was in 1906 with the article by Michael Tswett describing the fundamental principles and techniques of chromatography. He was able to separate dyes in plant extract by carrying the extract in petroleum through a glass column packed with calcium carbonate powder (Zechmeister, 1948). Tswett discovered that how compounds dissolve in different solvents is an important factor in chromatography. The compounds with strong affinity to the stationary phase or less soluble in the mobile phase will move slower through the column compared to the compounds with weaker affinity and higher solubility. An equilibrium state arises between the affinity to the stationary phase and the solubility in the mobile phase.

The detection of eluted compounds is done by measuring electrical signals they emit, which depend on certain physicochemical properties. Examples on such physicochemical properties, normal to use for detection, are UV-absorption, refractive index, fluorescence, molecular mass and fragmentation in a mass spectrometer. The graphic output of such a signal over time is called a chromatogram. It consists of a baseline set by the mobile phase, with peaks (or patterns) on it. The peaks represent the different compounds of the sample. A typical chromatogram is shown in figure 13. Quantification of a compound can be determined from the peak area (or peak height).

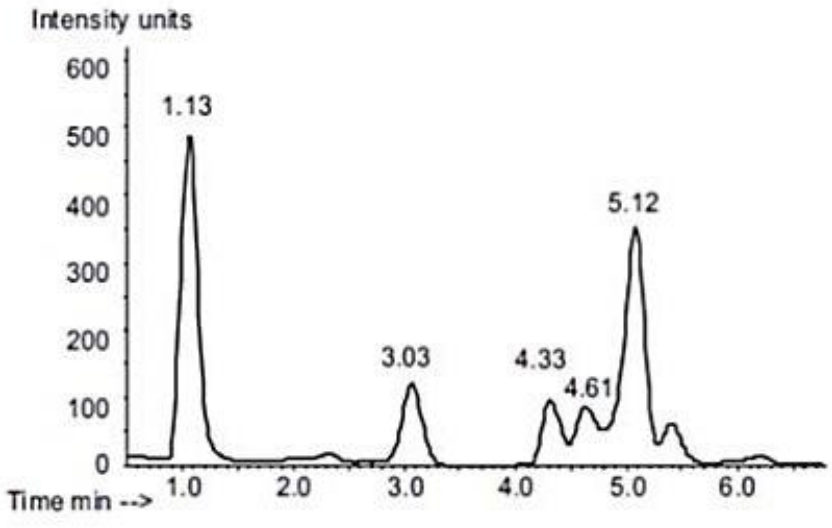

FIGURE 13: Typical chromatograom (Moldoveanu and David, 2013a)

Chromatography can be used to separate and purify the intermediates and products in various syntheses, and to identify and quantify different compounds in environmental matrixes (Faust, 1997). Preparative chromatography is to isolate and purify while analytical chromatograph is to gather information on the analytes and sample composition. Same chromatographic technique can be used for both purposes.

All the different chromatographic techniques have a stationary phase (column) and a mobile phase (eluent, gas etc), and rely on adsorption, partition, ion exchange or molecular exclusion. Adsorption chromatography consists of a solid stationary phase and a liquid or gaseous mobile phase. It was the first chromatography technique on the market and is based on the principals of Tswetts. The time the different solutes use to travel through the column is given by equilibrium between adsorption onto the surface of the solid and solubility in the solvent (eluent) (Faust, 1997).

In partition chromatography, the stationary phase is a thin film of non-volatile liquid held on the surface of an inert solid. The compounds are carried over the film by liquid or gas. The less soluble analytes are carried by the stationary phase reaching the end of the column last. The principle of partition chromatography is shown in figure 14.

Chromatography techniques based on ion exchange has an ionically charged solid (resin) as stationary phase. The resin consists of either anions or cations with ions of the opposite charge electrostatically bound to it. The mobile phase in ion exchange chromatography is always a liquid. When a sample passes through the column, charged compounds with stronger affinity to the resin replace the electrostatic bound ions. The stronger the charge of the analyte, the longer it takes to elute it (Faust, 1997). The principle of ion exchange chromatography is shown in figure 15.

Separation in molecular exclusion chromatography is based upon particle size and does not involve any equilibrium state between the solute and stationary phase such as in the other mentioned techniques. In molecular exclusion the stationary phase consists of a gel material with carefully designed and selected pore size. The smaller particles are permeated in the gel and slowed down while the large molecules pass through unhindered (Kupiec, 2004). The principle of separation chromatography is shown in figure 16.

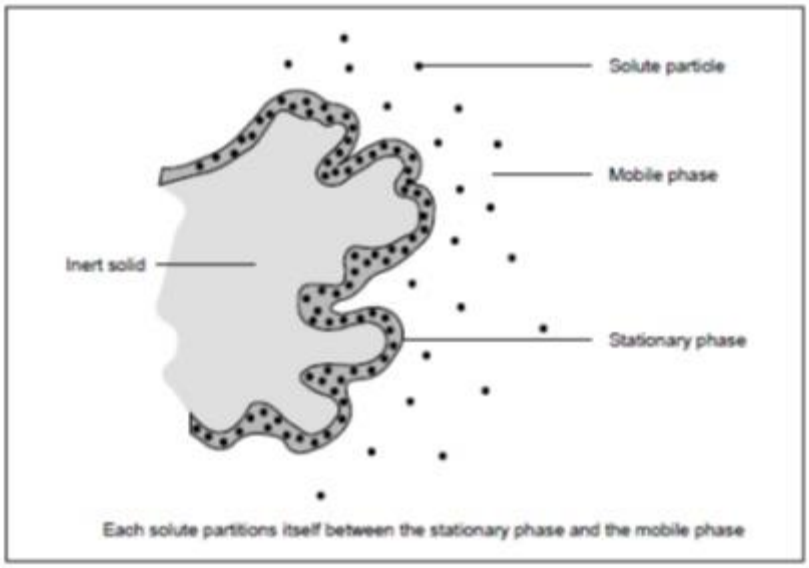

FIGURE 14: Partition chromatography (Faust, 1997)

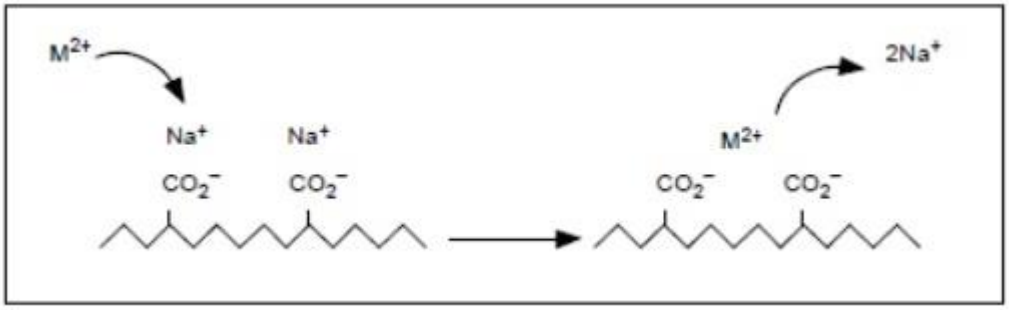

FIGURE 15: Ion exhange chromatography (Faust, 1997)

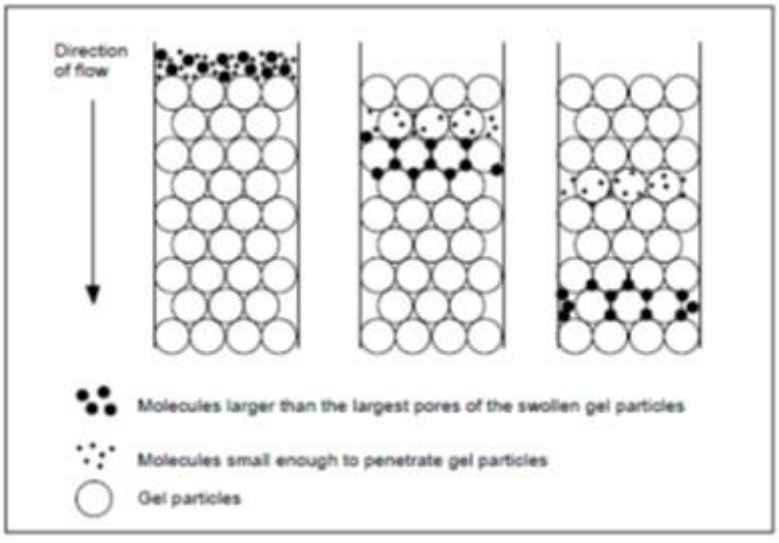

FIGURE 16: Molecular exclusion chromatography (Faust, 1997)

Examples on chromatography techniques, which will not be discussed further, are paper chromatography and thin layer chromatography.

Gas chromatography is a common technique to use on volatile trace contaminants such as siloxanes and musk fragrances (Pedrouzo et al., 2011). As the name implies, this technique uses gas as mobile phase. The stationary phase can either be a solid, gas-solid adsorption chromatography, or a non-volatile liquid, gas-liquid chromatography, which is the most common one. The sample is injected into the column through a heated chamber, which vaporize the sample if needed. The temperature of the oven is kept constant (isocratic) or, if a good separation proves to be difficult, gradually increased (gradient). The mobile phase is an inert gas such as nitrogen or helium. The detection is done by thermal conductivity or flame ionization. Identification of known substances is done based on retention time. Flame ionization detection (FID) is 1000 times as sensitive as thermal conductivity detection, and is more common to use one organic micropollutants. A principal sketch of gas chromatography is shown in figure 17. (Faust, 1997)

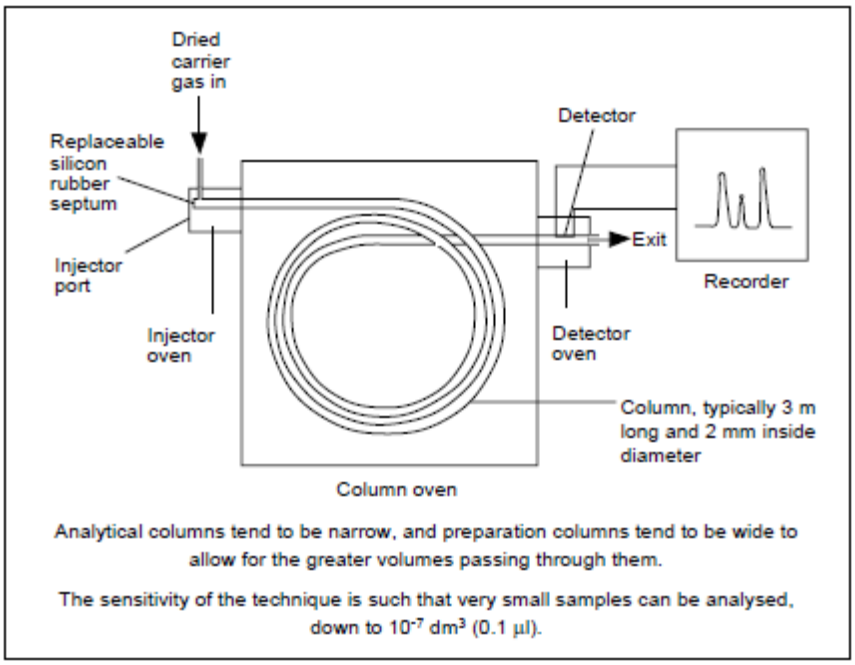

FIGURE 17: Principals of gas chromatography (Faust, 1997)

Liquid chromatography techniques are built on the same basic principles as gas chromatography except it uses liquid as mobile phase. Also, liquid chromatography offers a greater variety of solvating options, hence more scope for selectivity optimization, compared to gas chromatography. Most PCP compounds are non-volatile, thermally stabile, and persistent, and are therefore suitable for liquid chromatography techniques. The selectivity in HPLC towards a certain component is determined by the separation mode, the stationary phase structure, and the mobile phase composition (Poole, 2003).

The type of distribution process is often used to classify the different LC techniques, see figure 18. The main distribution processes are (Poole, 2003):

- Interfacial adsorption, the basis of liquid-solid chromatography (LSC)
- Restricted permeability of porous solids, the basis of size-exclusion chromatography (SEC)

- Partition between the mobile and stationary phase, the basis of liquid-liquid chromatography (LLC) and bonded-phase chromatography (BPC)
- Electrostatic interactions between solute ions and immobilized ionic groups on the stationary surface, the basis of ion-exchange chromatography (IEC)
- Structure specific binding of biopolymers to molecular immobilized ligands on the stationary surface, the basis of affinity chromatography (AC)

In HPLC, high pressure is applied to force the solvent through the column. The advantage with HPLC compared to gravity driven liquid chromatography is that smaller particles can be used for the stationary phase. This increases the effectiveness of separation because the solute can equilibrate more rapidly between the two phases (Faust, 1997).

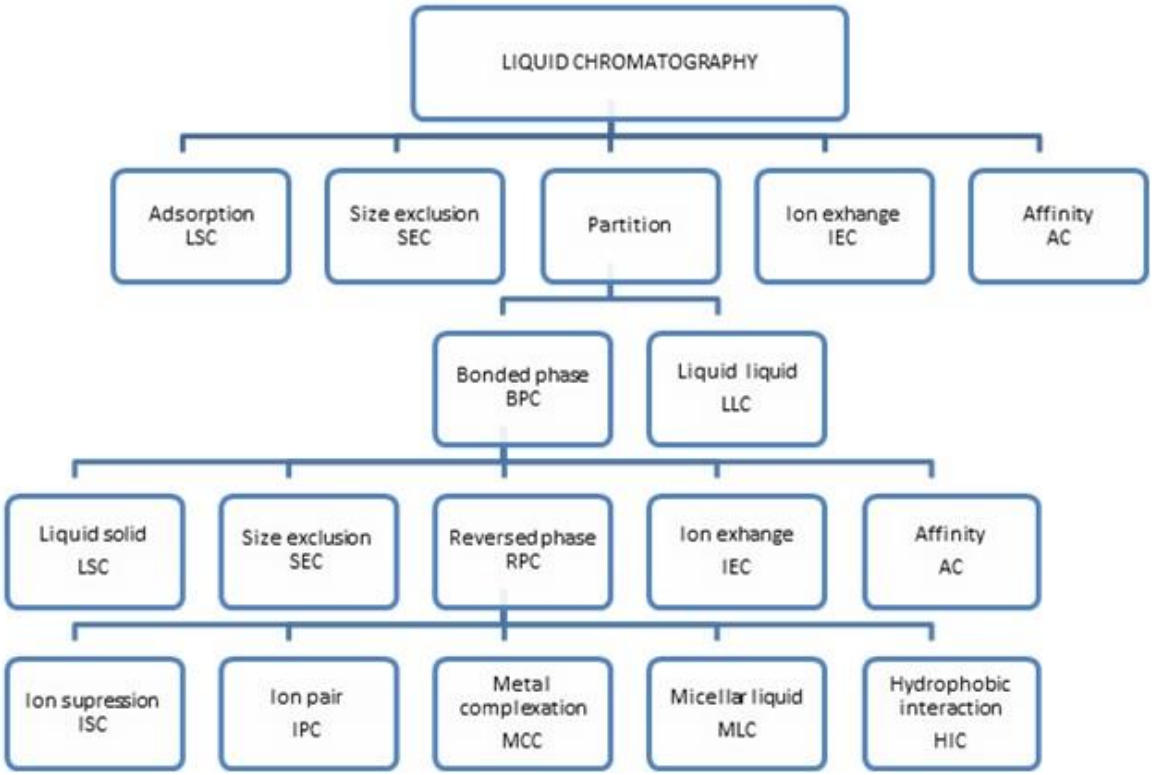

FIGURE 18: Famiiliy tree of liquid chromatography (Poole, 2003)

4.4 Reversed- phase high pressure liquid chromatography

4.4.1 Definition

This subchapter focuses on the use of RP-HPLC with UV-Vis diode array detector (UV-Vis DAD) to detect and quantify micropollutants in aqueous samples.

RP-HPLC is the most popular separation technique in liquid chromatography due to its versatility in separation of a variety of neutral, polar, and ionic samples of a wide range of molecular weights. (Poole, 2003). RP-HPLC consists of a non-polar stationary phase and an aqueous, moderately polar mobile phase; the opposite of normal-phase chromatography (Malviya et al., 2010). The separation is done on the basis of hydrophobicity. How the analyte reacts with the immobilized carbon groups attached to the stationary phase depends on the hydrophobicity of the analyte.

In RP-HPLC, modifications and addition of additives to the mobile phase yield different separation modes. By controlling the pH and exploiting secondary chemical equilibria of the mobile phase, weak acids and bases can be separated using ion suppression chromatography (ISC). In ion pair chromatography (IPC) permanently ionized compounds are separated by using mobile phase additives with opposite charge to the analyte. Metal complexation chromatography (MLC) is used to separate metal ions by adding ligands to the mobile phase that form neutral complexes with the metal ions. In micellar liquid chromatography (MLC) the distribution of solutes between the mobile and stationary phase is modified by addition of a surfactant. At last, biopolymers can be separated by using an aqueous buffered mobile phase and hydrophobic interaction chromatography (HIC) (Poole, 2003).

4.4.2 Components

The main components in a HPLC system are the mobile phase and reservoir, the high-pressure pump, the injector, the column (stationary phase), the detector, and the data collection/ integrator system. This is illustrated in figure 19.

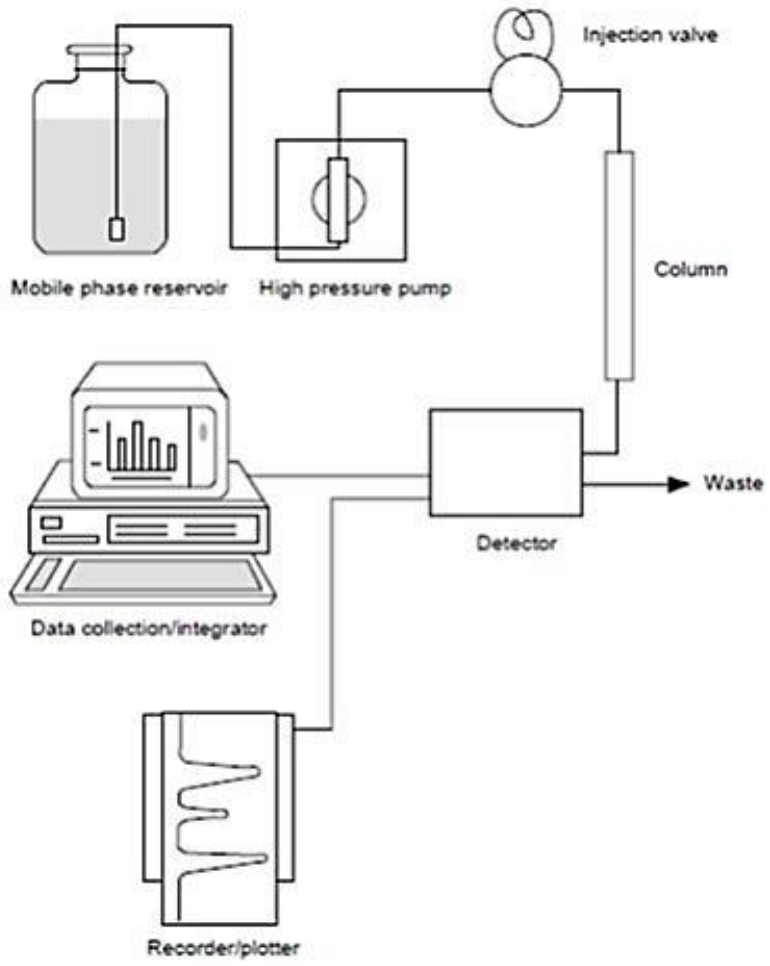

FIGURE 19: HPLC system (Faust, 1997)

Mobile phase

The properties of the mobile phase are important for the separation, the detection, and the HPLC performance. The mobile phase must be able to dissolve the sample without reacting with it chemically. Important solvent characteristics for the separation are solubility, polarity, surface tension, dipole moment, etc. Viscosity is an important parameter affecting the HPLC performance. Low viscosity minimizes the column backpressure extending the life of the column. Solvent properties that are important for the detection of analytes are UV-absorbance (e.g. when UV-Vis and UV-DAD detectors are used), volatility (e.g. when ELS detection is used), and ionization capability (e.g. when MS detector is used) (Moldoveanu and David, 2013d).

In RP-HPLC, the key features of the mobile phase are that it is polar and aqueous. In almost all cases, it consists of water mixed with one or several organic solvents. The presence of water plays an important role in the separation process due to properties such as high cohesive energy, hydrogen-bond acidity, and dipolarity. Retention increases with analyte size, and decreases with higher polarity of the solutes and ions. Water molecules tend to favor self-interactions over reactions with different solvents and solute molecules. Water is commonly referred to as the weak solvent in RP-HPLC. An increase in the volume fraction of the organic solvent reduces the polarity of the mobile phase and hence the retention time (Poole, 2003).

Waters preference for self-interactions limits the number of organic solvents that are miscible with water. For RP-HPLC with UV detection, the solvents that count for almost all applications are methanol, acetonitrile, 2-propanol, and tetrahydrofuran (Poole, 2003). They are soluble in water and have low UV-cutoff. Some of their physical properties are shown in table 7. Acetonitrile is a stronger eluent compared to methanol (Moldoveanu and David, 2013d).

TABLE 7: Solvent properties (Moldoveanu and David, 2013d)

Solvent	Boiling point (°C)	Viscosity (cP)	Refractive index	UV cutoff (nm)	Dielectric constant	Surface tension (dyne/cm)
Water	100	1	1.333	<190	80.4	73
Methanol	65	0.55	1.328	205	33.6	22.6
Acetonitrile	82	0.36	1.355	190	37.5	19.1
2-Propanol	82	2.40	1.377	205	18.3	21.8
Tetrahydrofuran	66	0.55	1.407	212	7.58	26.4

The separation process can either be done by isocratic elution or gradient elution. In isocratic elution, the mobile phase composition is held constant, while in gradient elution the mobile strength is changing as a function of time. If possible, isocratic methods are preferred because of simplicity and reproducibility (Poole, 2003). However, if the samples contain a various number of compounds with a wide retention range, gradient elution may be necessary to achieve good separation and reduce the total runtime. Gradient elution is also often applied as cleaning and/or regeneration process of the chromatographic column between runs. In fact, most separations performed by RP-HPLC are done by gradient elution(Agilent, 2011, Moldoveanu and David, 2013d). The gradient elution can be down in linear mode, nonlinear mode, or stepwise. Common for them all, is the need of a re-equilibrating step at the end of each run. The different gradient elution methods are shown in figure 20.

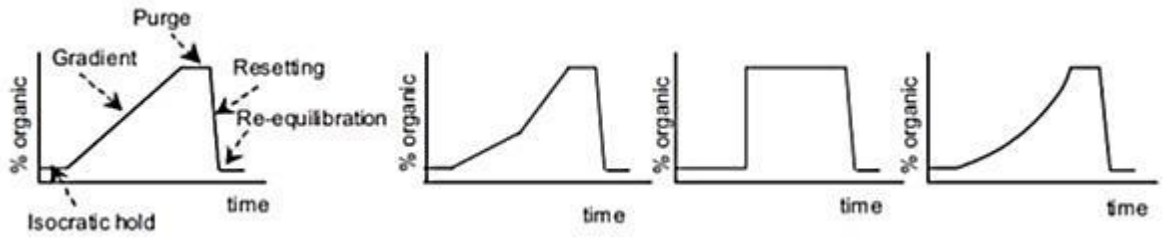

FIGURE 20: Different gradient elution schemes (Moldoveanu and David, 2013d)

It is common to add buffers or other additives to the mobile phase as a part of the method optimization. Water is the typical carrier for buffers, acids, bases or salts. The structure of organic compounds that have acidic, basic, or amphoteric character is very depended on the pH. A pH change during the separation process could affect the retention time of such an analyte significantly. Typical buffers to control the pH are potassium formate and potassium acetate. Buffers to control pH can also be used similar to gradient elution, where pH is changed as a function of time to achieve a specific separation (Moldoveanu and David, 2013d).

Column and stationary phase

Columns used in HPLC are made from cylinders of stainless steel, polymers, or, more rarely, glass, containing porous microparticles. For separation of small molecules and inert macromolecules, the dominating packing materials are prepared from porous inorganic oxides (especially silica), polymers and graphitic carbon. The choice of physical dimensions of the column is particular related to the sample load. The load is preferred to be low, but this is often limited by the detector sensitivity, which gives a minimum amount of injection volume. A classification of HPLC columns based on their dimensions and purposes are shown in table 8.

TABLE 8: Classification of HPLC columns based on their dimensions and purposes (Moldoveanu and David, 2013c)

Type	Diameter (mm)	Length (mm)	Typical flow rate (mL/min)	Void volume (mL)	Sample loading
Preparative	>25	300, larger	>20	>50	>25mg
Semi-preparative	10	250, larger	5-10	>5	10-20 mg
Conventional	3, 4.6	50, 100, 150, 250	0.5-2	>1	50-200 µg
Narrowbore	2, 2.1	50, 100, 150, 250	0.2-0.5	0.2	20-100 µg
Microbore	1, 1.7	50, 100	0.05-0.1	<0.1	<5 µg
Micro LC-capillary	<0.5	50, 100	1-10 µL/min	10-20 µL	1 µg
Nano LC-capillary	<0.1	50	<1 µL/min	0.1-1 µL	<0.1 µg

Today, porous silica is the most important and used adsorbent for liquid-solid phase chromatography and chemically bonded phases. They are mechanical strong, resistant to compaction under high pressures, and have an extremely large surface available for adsorption. Porous silica consists of silica (SiO2) particles. The particle surfaces are covered by a network of reactive groups (silanol ≡Si-OH). It is possible to chemically attach desired organic groups to these reactive groups by covalent binding. This is referred to as the bonded phase (Moldoveanu and David, 2013c). The different silica materials are characterized by their particle morphology and surface structure. In general, most silica materials are mesoporous with an average poresize between 5 and 15 nm, and surface areas between 150-600 m^2/g (Poole, 2003). A close up photography of silica particles is shown in figure 21. The particle size of a typical HPLC column is normally in the range of 1.8-5 µm. Columns with small particle size have higher plate number N, but also higher backpressure. The backpressure increases linearly with the column length (Agilent, 2011).

It exist a huge variety of bonded phases with significant differences in selectivity (Poole, 2003). . In RP-HPLC, the silica particles are chemically treated to be non-polar or hydrophobic. The most common bonded phase used for RP-HPLC is C18 (octyldecylsilane). Other common linear alkylsilane phases are C8 and C4. (Agilent, 2011). The main problems with the use of silicas in chromatography are the high solubility in alkaline solution (pH>8), the limited stability of siloxane bonded phases in acid solution (pH<2), and the strong activity with basic compounds, which can result in peak distortion.

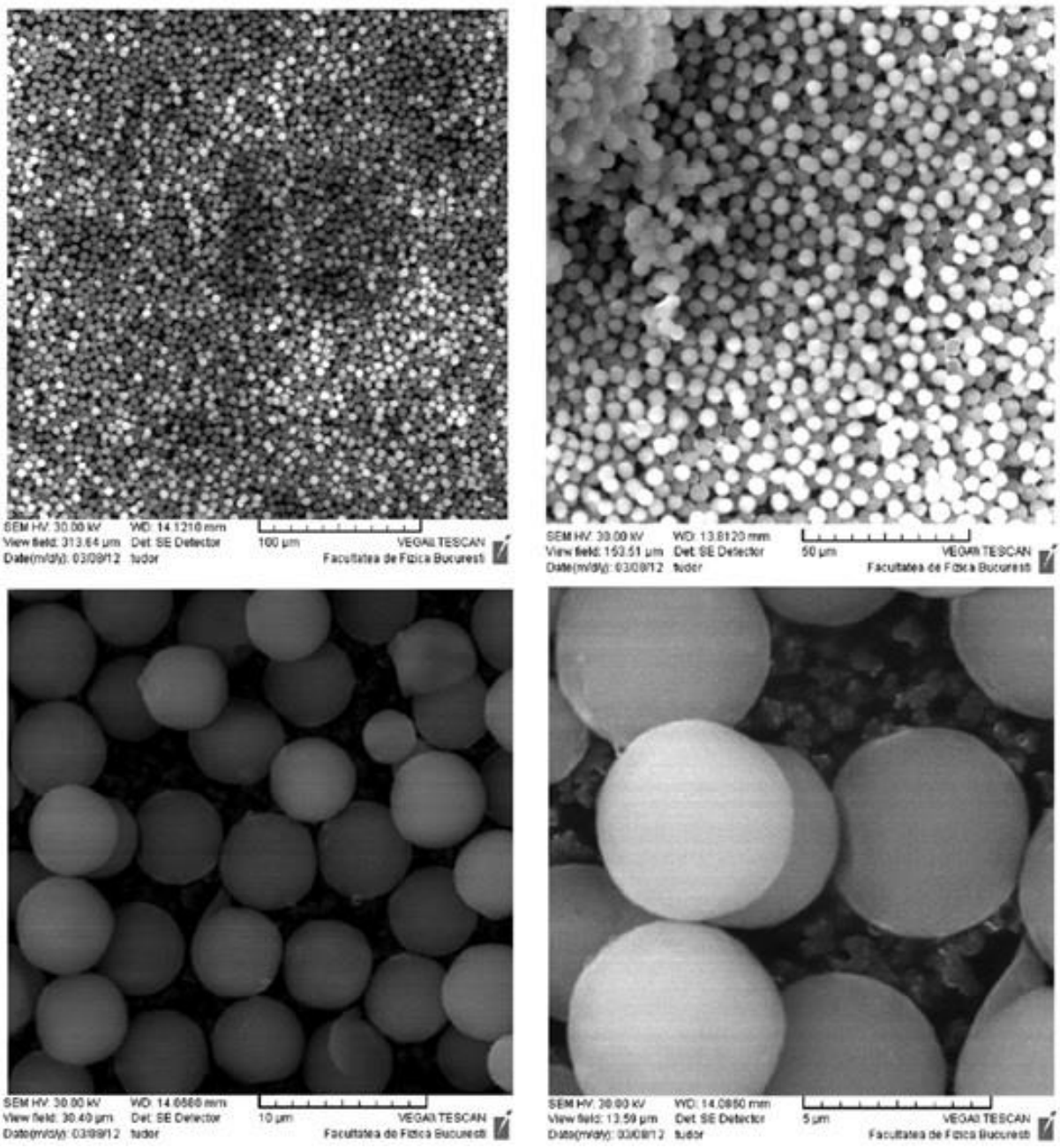

FIGURE 21: Silica particles (Moldoveanu and David, 2013c)

UV-Vis diode array detection (UV-Vis DAD)

The UV-Vis detector is the most used detector in liquid chromatography (Poole, 2003). Diode array detectors (DAD) are UV-Vis detectors capable of measuring absorbance over the whole spectrum range. The UV-Vis detector sends a beam of light from a UV light source, which is then separated into its component wavelengths. Before going into the sample, each monochromatic beam is split by a splitter into two identical beams with equal intensity. One is going into the sample cell and to the detector, while the other is sent to the reference detector. The baseline is created from the intensity of the reference beam, defined as I_0. The intensity I_1 is measured from the sample cell. If the sample compound absorbs light, I_1 is less than I_0. Absorption is usually presented as transmittance or absorbance, defined by the following equations:

$$T = \frac{I_1}{I_0} \qquad \textbf{EQUATION 4-1}$$

$$A = \log(\frac{I_0}{I_1}) \qquad \textbf{EQUATION 4-2}$$

Most organic compounds adsorb some light in the UV spectra, but different compounds can have very different absorption maxima and absorbance intensities. The maximum absorbance wavelength refers to the wavelength where the compound absorbs most light, also known as λ_{max}. Wavelength for maximum absorbance can be found by measuring the absorbance of a compound over the whole UV spectrum, normally between 190-600 nm. Figure x shows the maximum adsorption wavelength for TCC.

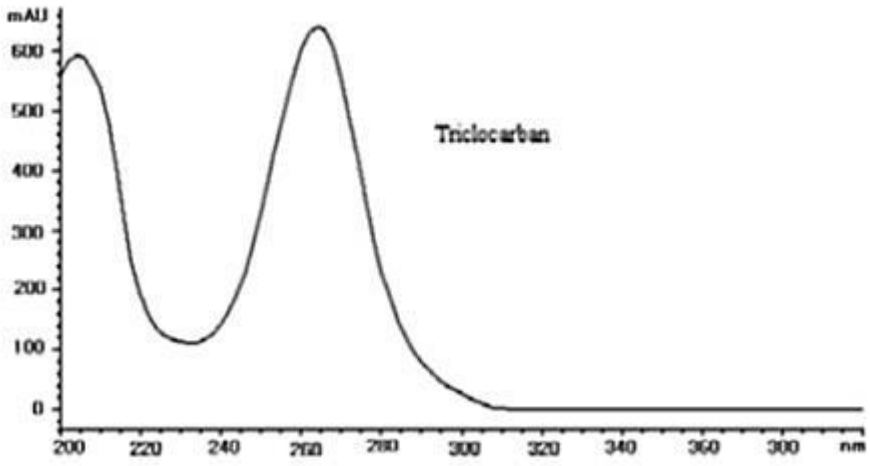

FIGURE 22: Maximum adsorption wavelength TCC (Liu and Wu, 2012)

The absorbance of a compound is proportional to its molar concentration as stated by the Lambert-Beer law:

$$A_\lambda = \varepsilon_\lambda [X] l \qquad \textbf{EQUATION 4-3}$$

where ε_λ is the molar absorption coefficient at the wavelength λ, [X] is the molar concentration, and l is the length of light path through the sample cell. The parameter ε_λ can be used to predict the size of the chromophore (light adsorbing functions) and the probability that light of a given wavelength will be adsorbed by the chromophore. Depending on the nature of the analyte, UV-Vis can be used to

detect concentrations down to 0.1-1 ng/L. When using UV detection it is important to select a solvent with low UV cut off so it don't interfere with the absorption range of the analyte (Moldoveanu and David, 2013a).

4.4.3 Parameters that characterize the RP-HPLC analysis

General

Parameters used to describe the separation of the HPLC method are either related to physical characteristics of the HPLC system or to the separation itself by inspecting the chromatogram. Limit of detection (LOD), limit of quantification (LOQ), linearity of calibration curves, repeatability, accuracy, selectivity, and recovery of the sample processing are all parameters used to characterize the effectiveness of the HPLC method. It is important to properly conduct and control the HPLC method to achieve the optimum settings with regards to the mentioned parameters above (Moldoveanu and David, 2013b).

Flow rate

Flow rate is a physical parameter of the HPLC system, which describes how fast the mobile phase flows through the column. It can be used to calculate the consumption of mobile phase in a certain time period. The linear flow rate u is the velocity of a point in the fluid, while the volumetric flow rate U is the volume of fluid per unit time (mL/min). In the column, the linear flow rate u depends on the porosity of the column material indicated as ε*. The relation between linear flow rate and volumetric flow rate is given by the area of the column as follows:

$$U = \frac{1}{4}\pi\varepsilon^* d^2$$ **EQUATION 4-4**

where d is the internal diameter of the column (mm). The volumetric flow rate is set and controlled by the pump (Moldoveanu and David, 2013b).

Retention time (t_R) and dead time (t_0)

The retention time t_R is the time it takes for a compound to elute from the sample. It is given by the time from injection to the time to the maximum apex of the peak belonging to the compound. The necessary length of the chromatographic run is given by the retention time of the last peak in the chromatogram.

The dead time t_0, also known as void time or hold up time, is the time it takes for a nonretained molecule to travel through the column. It only depends on the flowrate and column characteristics (length, diameter, and porosity). The time a compound X is retained on the column is given by the difference between t_R and t_0, which is referred to as the reduced retention time t'_R (Moldoveanu and David, 2013b):

$$t'_R(X) = t_R(X) - t_0$$ **EQUATION 4-5**

Retention volume

The retention volume V_R for a compound X is defined as the volume of mobile phase used from the time of injection until the corresponding t_R (X) is reached. V_R and t_R is related by the following equation:

$$V_R(X) = Ut_R(X) \quad \text{EQUATION 4-6}$$

The column dead volume V_0 is the volume in the column that is not occupied by the stationary phase particles and inside their pores. It corresponds to the dead time t_0. As for the reduced retention time, the reduced retention volume V'_R for a compound X is given as:

$$V'_R(X) = V_R(X) - V_0 \quad \text{EQUATION 4-7}$$

V_0 is related to the stationary phase packing. An approximate value of dead volume V_0 can be found by using the equation:

$$V_0 = \varepsilon^*(\frac{\pi}{4})d^2L \quad \text{EQUATION 4-8}$$

where ε* is the porosity of the column packing material and L is the length of the column. For a column with 5 µm particles, ε* is about 0.7(Moldoveanu and David, 2013b).

Retention factor (Capacity factor)

The retention factor k is a measure of the period of time that the analyte resides in the stationary phase compared to the time it resides in the mobile phase. It is given by the reduced retention time t'_R divided by the dead time t_0 or the reduced retention volume V'_R divided by dead volume V_0 (Moldoveanu and David, 2013b):

$$k = \frac{t_R - t_0}{t_0} \quad \text{EQUATION 4-9}$$

$$k = \frac{V_R - V_0}{V_0} \quad \text{EQUATION 4-10}$$

The k value should be between 1 and 10. A low k value indicates poor retention and the risk of early eluting peaks running into nonretained components or matrix components, which make quantification difficult to obtain. Also, at low k values, the peaks are often influenced by extra column effects and broadening. If the k value is too high, the separation time may be too excessive and the detection limit higher due to broader peaks (Agilent, 2011).

Ideal peak shape and efficiency of column

The band of an analyte in the flow of the HPLC system right after an injection is extremely narrow (almost plug flow). With time, as a result of different diffusion mechanisms and other mechanisms, the band is broadened into a chromatographic peak. By only considering ordinary diffusion by Ficks law, the peak shape can be described by a Gaussian bell curve of a given width, see figure 23 (a).

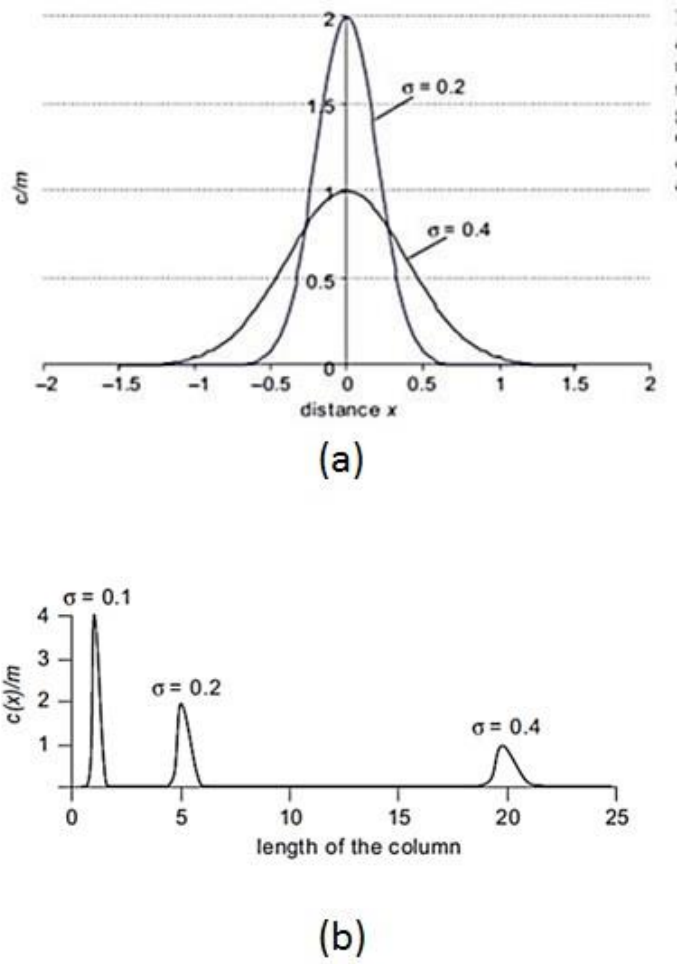

FIGURE 23: Ideal peak shape and effect of column length (Moldoveanu and David, 2013b)

The normal probability density function describing a Gaussian bell curve is given as:

$$c(x,t)/m = \frac{1}{\sqrt{2\pi\sigma^2}}\exp(-x^2/2\sigma^2) \qquad \textbf{EQUATION 4-11}$$

where c is the concentration given as a function of the longitudinal diffusion in the direction of x and time t, m is the whole amount of material, and σ^2 is the variance. The variance σ^2 equals to 2Dt where D is the diffusion constant (cm^2/s). The standard deviation is represented by σ, and describes the width of the Gaussian bell curve. As seen in figure 23 (a), a larger σ leads to a wider peak. The σ for an analyte peak is increasing over the length of the column, as seen in figure 23 (b). The σ as a function of time (σ_t) is written as:

$$\sigma_t = \frac{\sigma t_R}{t_0 u} \qquad \textbf{EQUATION 4-12}$$

The peak width is an important parameter in chromatography describing the effeciency of the column. Peak width is given as the width at inflection point W_i, the width at half height W_h, and the width at the baseline W_b. The different widths, retention time t_R, and peak height are shown in figure 24. It is most common to use W_h or W_b as a measure of peak broadening. The peak width W_b is the

distance between the points of intersection of baseline with the tangents to the curve at inflexion points. It equals to two times W_i.

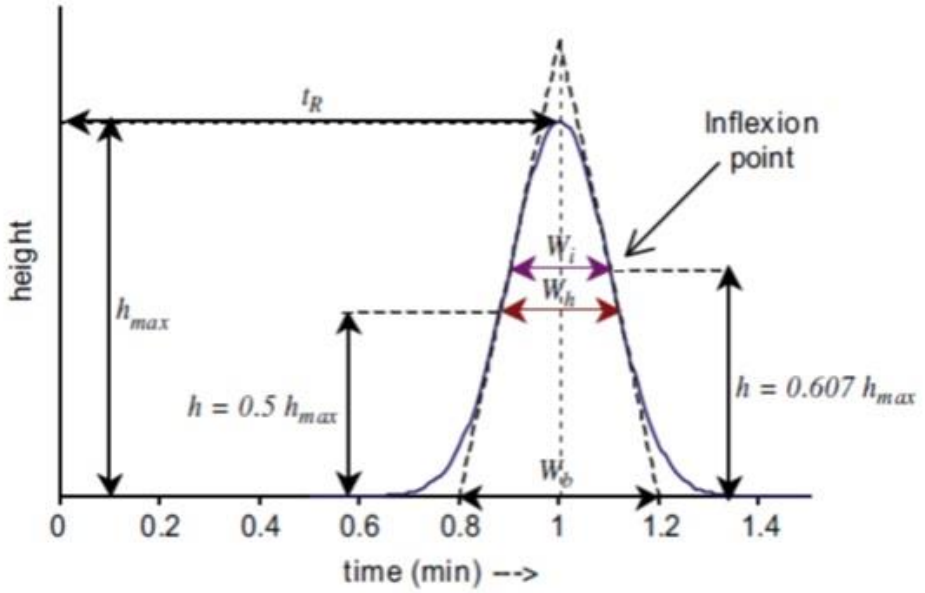

FIGURE 24: Different peak widths (Moldoveanu and David, 2013b)

From the widths, the σ_t can be calculated by using the relations:

$$\sigma_t = (8ln2)^{-1/2} W_h \quad \text{EQUATION 4-13}$$

$$\sigma_t = 0.25 W_b \quad \text{EQUATION 4-14}$$

The most used parameter of column performance and efficiency is the theoretical plate number N. The theoretical plate number N is defined as:

$$N = L/H \quad \text{EQUATION 4-15}$$

where L is the length of the column and H is the height equivalent to a theoretical plate number defined as:

$$H = \sigma^2/L \quad \text{EQUATION 4-16}$$

By substituting equation 4-15 into equation 4-16 the following expression for N is obtained:

$$N = L^2/\sigma^2 \quad \text{EQUATION 4-17}$$

From equation 4-12, 4-13 and 4-15, equation 4-16 can be rewritten to:

$$N = 16{t_R}^2/{W_b}^2 \quad \text{EQUATION 4-18}$$

$$N = 5.55{t_R}^2/{W_h}^2 \quad \text{EQUATION 4-19}$$

The theoretical plate number N is proportional to the column length L and inversely proportional to the theoretical height H. The higher plate number, the more efficient is the column. A high N value indicates a narrow peak at a given retention time. It is influenced by physical properties of the columns stationary phase such as structure of the particles, particle diameterand homogeneity of

particles. Typical range of N value for a HPLC column is between 20,000 and 150,000 (Moldoveanu and David, 2013b, Agilent, 2011).

Selectivity or separation factor (α)

Separation factor α describes the ratio of time or distance between the maxima of two peaks. It is given as the ratio of the two peaks retention factor k_2 and k_1:

$$\alpha = \frac{k_2}{k_1} \qquad \text{EQUATION 4-20}$$

The closer α is to 1, the closer is the peaks retention time and the risk of them colliding. Typical, a value of α>1.2 is necessary to obtain a good separation. However, even if the selectivity is high, the separation can still be poor due to excessive peak broadening. The selectivity of a method can be improved by adjusting the temperature, changing the mobile phase constituents or changing the stationary phase (Agilent, 2011, Moldoveanu and David, 2013b)

Resolution (R_s)

The resolution factor is a measure on the columns ability to separate the peaks of interest. It comprehends all the mentioned factors; efficiency, selectivity, and retention, and is expressed as:

$$R_S = \frac{\sqrt{N}}{4}\frac{(\alpha - 1)}{\alpha}\frac{k}{(k+1)} \qquad \text{EQUATION 4-21}$$

The higher R_S, the easier it is to achieve good separation between two peaks. Figure 25 shows how the selectivity, efficiency, and retention affect the resolution factor (Agilent, 2011).

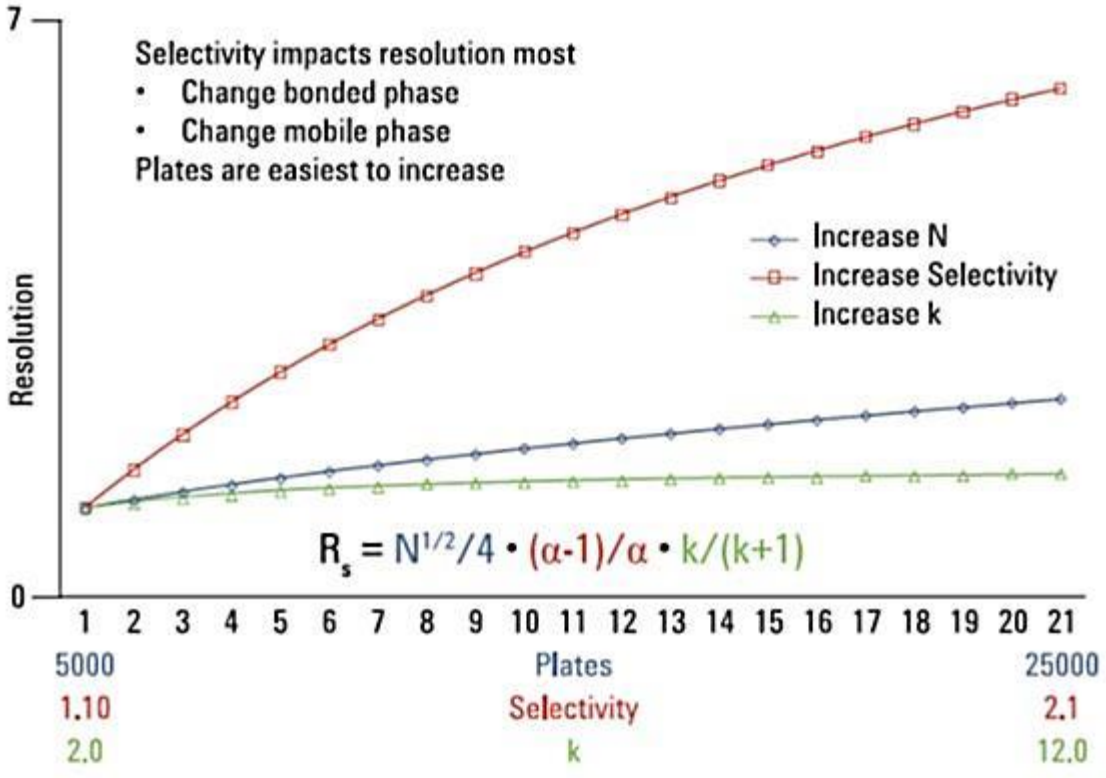

FIGURE 25: Resolution factor, effect of selectivity, efficiency, and retention (Agilent, 2011)

Pressure

A higher flow rate is desirable due to shorter elution time. However, the flow rate in a HPLC system cannot be increased unlimited due to the increase of pressure drop over the column Δpmax, also reffered to as backpressure. The pressure drop across the column is given by the difference between the pressure at the inlet and that at the outlet of column. The factors that affect the system pressure are the solvent viscosity (η), the flow rate (u), the column length (L) and radius (r), and the particle diameter (d_p) of the column packing material. The pressure equation is given by the following equation:

$$\Delta p = \frac{\eta u L}{K^0 \pi r^2 d_p} \qquad \textbf{EQUATION 4-22}$$

where K^0 is the column permeability. A limiting backpressure for the HPLC system is normally set to be between 200-400 bars. The efficiency of the column is given by the column dimensions and particle diameter, hence affecting the backpressure. It is desirable to achieve the best separation as function of efficiency and flow rate without exceeding the limiting backpressure (Agilent, 2011, Moldoveanu and David, 2013d)

Peak asymmetry

In liquid chromatography, the peak shape is rarely a perfect Gaussian curve, which was created on the basis of longitudinal diffusion. In fact the, the longitudinal diffusion is only a small contributor to the total peak broadening. Other factors affecting peak broadening are:

- Eddy diffusion
- Lateral movement caused by convection of material
- Mass transfer processes
- Contribution from the stagnant mobile phase in a porous material

The characterization of peak asymmetry is often done by the asymmetry parameter As. The asymmetry of a compound X is measured by drawing a vertical line at peak maximum and two parallel lines at the rear and front side of peak maximum at 10% peak height, see figure x. The ratio between the rear and the front cut distances defines the asymmetry, which is given by the following expression:

$$As(X) = \frac{r}{f} \qquad \textbf{EQUATION 4-23}$$

where r and f represent the rear and front distances, respectively, from the vertical line at peak maximum to the parallel line drawn at front and rear. The closer As is to 1, the more symmetric is the peak shape. An As>1 is referred to as peak tailing, while an As<1 is referred to as peak fronting. One common cause to peak tailing or fronting is too high injection volume. The stationary phase can then become saturated or complete covered with the sample, thus, affecting the separation process. Peak tailing may also be caused by active sites on the stationary phase where more than one interaction of an analyte can take place. This can for example be the present of silanol groups on a C18 based column. It is less common to have peak fronting. Peak fronting can be caused by more than one solute interacting with the stationary phase (Moldoveanu and David, 2013b). The problem

of peak distortion due to large injection volumes can be overcome by including an extraction step. This to concentrate the analyte so that smaller injection volumes can be used (Agilent, 2011).

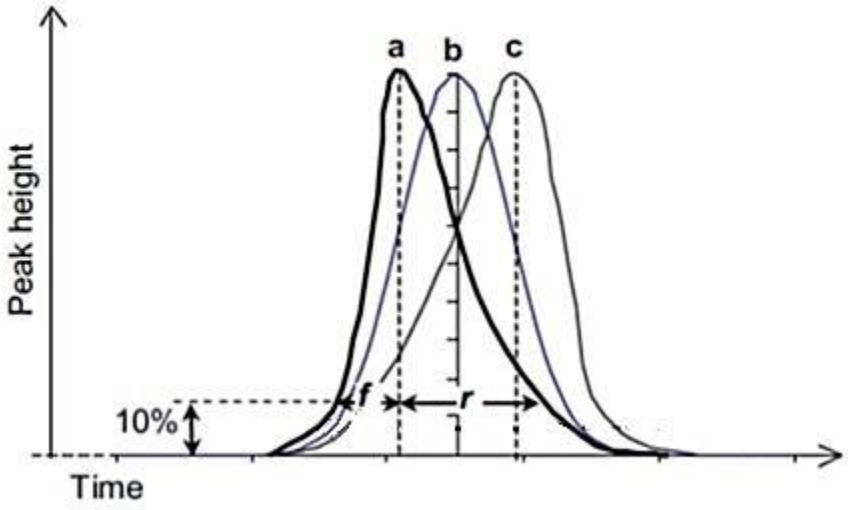

FIGURE 26: Peak shapes, a= tailing shape, b=gaussian shape, c=fronting shape (Moldoveanu and David 2013b)

Peak tailing or fronting will most likely cause errors in the quantification and accuracy of the analysis. Peak distortion depends on the stationary phase, the compound and the physical parameters of the HPLC system (Moldoveanu and David, 2013b).

5. Adsorption with activated carbon

5.1 Adsorption in general

Adsorption is the process where molecules in gas or liquid adsorb to the internal surface of a solid. It must not be confused with absorption where the substances only adhere to the external surface of the solid. In adsorption the pollutants diffuse into the adsorbent pores and attach to the internal structure of the adsorbent. This happens in four consecutive steps (Reinert, 2013, Qiu et al., 2009):

1. Bulk diffusion where the contaminate diffuses from the bulk phase to the liquid surrounding the adsorbent particle, see figure 27 (a)
2. Film diffusion where the contaminate diffuses through the liquid film surrounding the adsorbent particles, see figure 27 (b)
3. Internal or intra-particle diffusion where the contaminate diffuses in the liquid contained in the pores and/or along the pore walls, see figure 27 (c)
4. Mass action, which is the adsorption and desorption between the contaminate and active site, see figure 27 (d)

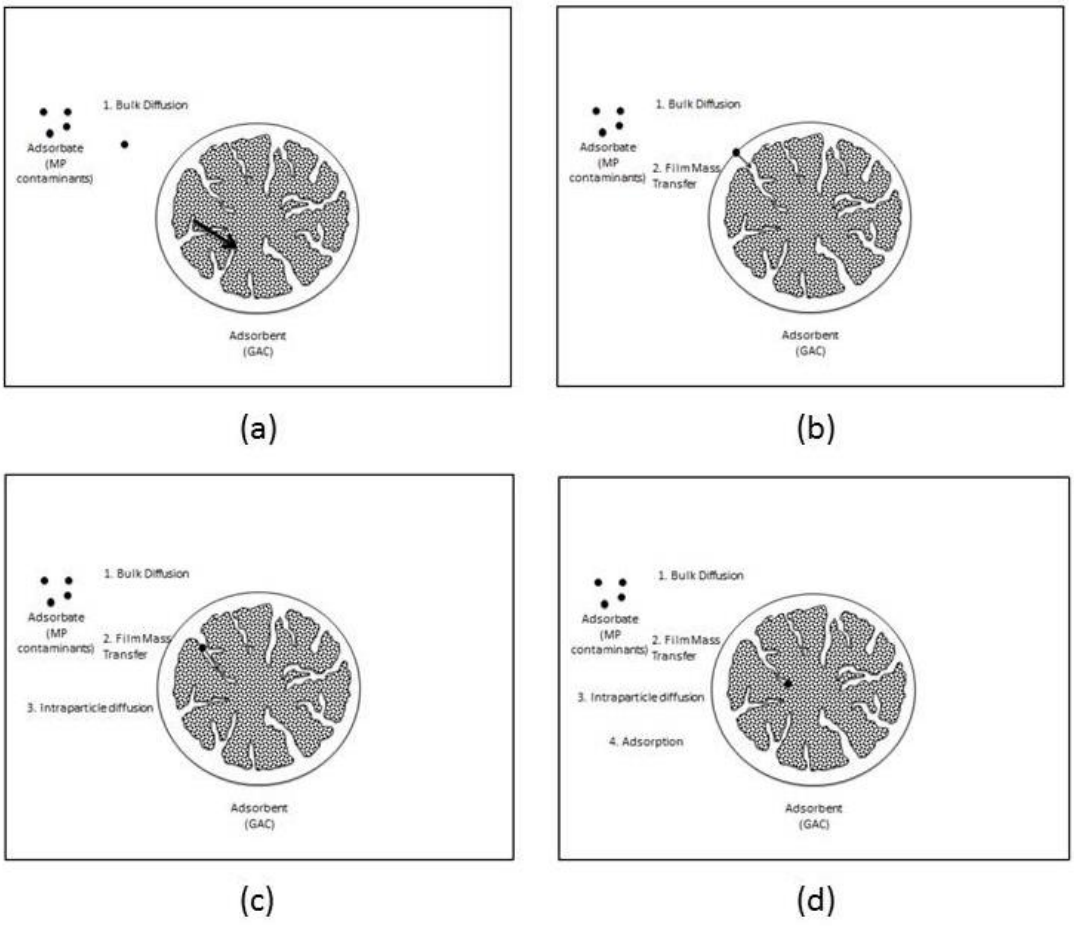

FIGURE 27: Adsorption processes (Reinert, 2013)

Adsorption is primarily a surface phenomenon that occurs in the interface due to an excess of free energy. As the solid adsorbs solute molecules, the Gibbs energy decreases (if p=constant) or the Helmholtz energy decreases (if V =constant)(Virkutyte et al., 2010).The dissolved compound is concentrated on the interface between the solid and the bulk phase. The decrease of concentration in the liquid/gas phase is eventually slowed down by decreased mobility of the substance and lack of adsorption sites on the solid. At the end, equilibrium between the concentration of solute in the liquid/gas and the concentration of adsorbate on the adsorbent is established.

Adsorption is done physically (Van der Waals forces, hydrogen binding, hydrophobic binding), chemically (chemisorption) or by ion-exchange with functional groups on the carbon surface. Chemisorption is the process where molecules chemically react with the carbon surface to form strong chemical bonds (Cameron Carbon, 2006).

Today adsorption is one of the most common techniques applied on contaminated medias to get rid of pollutants. It exists several hundred different types of carbon that are carefully designed to suit different purposes and industries (water and air treatment, medicine, food industry etc.), contaminants (humic substances, micropollutants, bacteria etc.), and water qualities (drinking water, waste water, swimming pools, aquariums etc.). Activated carbon, molecular sieves, polymeric adsorbents, and clays are common adsorbents. This section focuses on the use of activated carbon as adsorbent and different kinetic and isotherm models used to describe the adsorption process.

5.2 Factors effecting adsorption

The main factors affecting the adsorption process are (Grassi et al., 2012):

- Surface area
- Properties and concentration of adsorbate
- Solution pH
- Temperature
- Interfering substances
- Properties and dose of adsorbent

Surface area has a huge influence on adsorption. Since adsorption is a surface phenomenon, the degree of adsorption is proportional to the surface area that is available for adsorption.

Solute properties that influence adsorption are charge, size, hydrophobicity and presence of certain functional groups. The extent of adsorption decreases with increased solubility of the solute in the solvent. Within a chemical group of organic compounds, the water solubility of the compounds decreases with increasing chain length (e.g. number of carbon atoms) (Weber Jr, 1974). Higher molecular weight compounds are preferentially adsorbed over low molecular weight species. Also, it has been found that adsorption increases with decreasing solute charge (Cameron Carbon, 2006).

Solution pH can affect adsorption by changing the chemical nature of the adsorbent functional groups.

Temperature is a parameter affecting the adsorption process. Adsorption reactions are mostly known to be exothermic. The degree of adsorption normally increases with decreasing temperature.

Interfering substances can decrease the extent of adsorption by outdistancing of adsorption sites or by blocking the entrance to the micropores. But they can also enhance the adsorption process by reacting with the target compound increasing its adsorption abilities

Adsorbent properties that influence adsorption are mainly given by the chemical composition and present of functional groups on the adsorbent surface.

5.3 Activated carbon

5.3.1 Manufacturing

The main elements in activated carbons are carbon (84-99% w/w) and oxygen (<1%-16% w/w) (De Ridder, 2012). Activated carbons are made by physical or chemical processes of a wide variety of materials such as wood, coal (anthracite, bituminous, and lignite), coconut shells, peat, petroleum based residues, synthetic polymeric materials, liquid and gaseous hydrocarbons, organic wastes etc. The raw material used should have a low inorganic matter, high carbon content, low ash content, easy activation, and low cost. Activation of carbon is done by controlled oxidation of the carbon atoms under high temperatures. In physical processes, the increase in porosity is done by adding steam and CO_2, resulting in partial gasification of the carbon. In chemical processes, the carbon is heated and compounds like H_3PO_4 and $ZnCl_2$ are added. This leads to an increase in porosity because of charring and aromatization of the carbon skeleton (De Ridder, 2012). After activation the activated carbon normally has an internal surface area between 700-1200 m^2/g. It is due to this highly porous structure and large surface area that activated carbons are able to take up molecules and ions from the bulk phase (Cameron Carbon, 2006).

5.3.2 Carbon structure

Despite the extensive use in purification of air and water, the precise atomic structure of activated carbon is still unknown. One theory, which many confide to, is a modified graphite-like structure with interior vacancies. The formation of interior vacancies is due to the presence of microcrystallites, which are formed during the carbonization process, and impurities present in the raw material. Thus, pores are the result of faults in the crystalline structure. However, a weakness of this theory is the hardness of activated carbon that disagrees with the layered structure of graphite (Cameron Carbon, 2006). In fact, it has been found that activated carbons is resistant to graphitization, meaning it cannot be transformed into crystalline graphite, even at temperatures above 3000°C.

In later research, with new microscopic imaging techniques, findings indicate a fullerene-related structure. This means that the activated carbon, in addition to hexagons, consists of curved fragments of pentagons or other non-hexagonal rings, see figure 28. The present of pentagon rings or other non-hexagonal rings would explain the hardness, microporosity and non-graphitizing resistance of activated carbon (Harris et al., 2008):

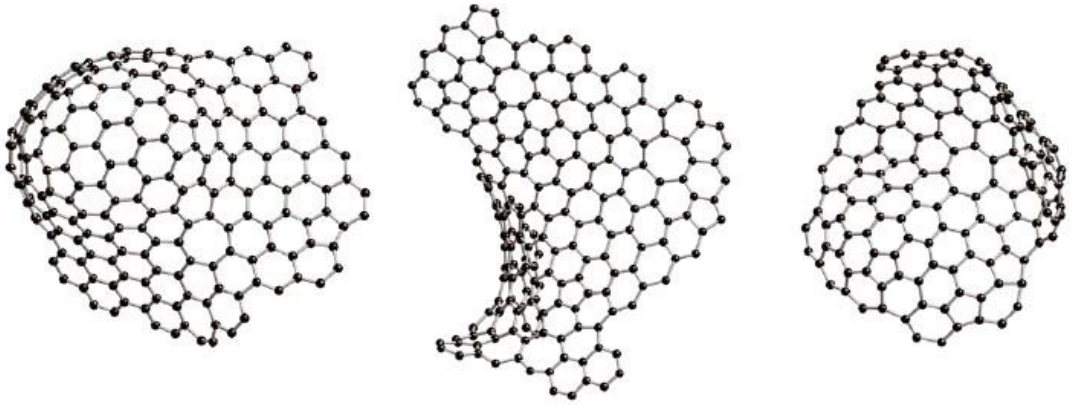

FIGURE 28: Illustration of carbon structure (Harries et al, 2008)

5.3.3 Pore size

A normal division of pore diameters is micro pores (≤2 nm), mesopores (2-50 nm) and macro pores (> 50 nm) (Virkutyte et al., 2010). All activated carbons contain all of the pore sizes but the ratios between them vary depending on the raw material used. It is the micro pores that contributes most to the internal surface area and therefor is the effective means of adsorption. The mesopores and makropores act mainly as access points and channels to and between the micropores. In some cases, when dealing with very large molecules, makropores plays an important role in adsorption. Figure 29 shows a microscopic photo of a coconut shell carbon. The photo illustrates the heterogeneity in pore sizes.

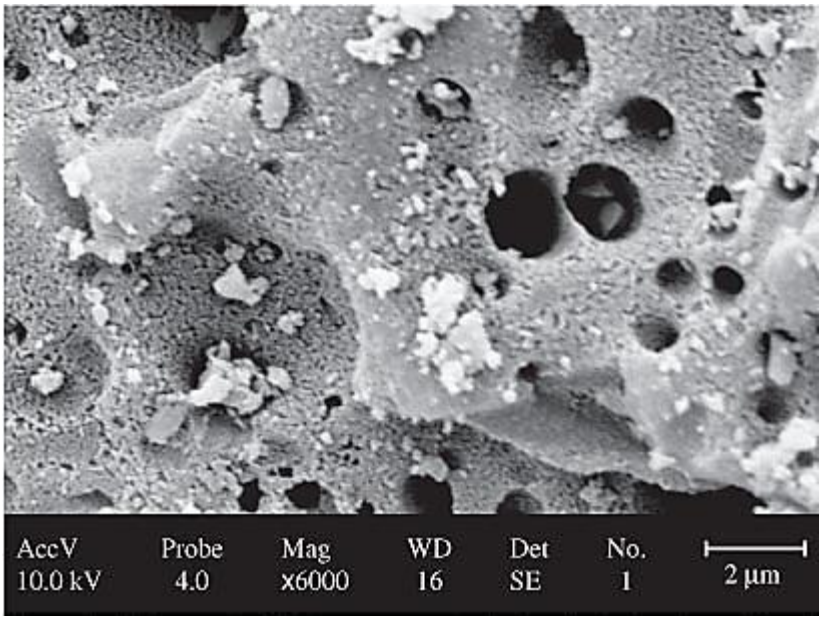

FIGURE 29: Microscopic photo of a cocunut shell carbon (Matta et al., 2008)

Pore size is a significant parameter affecting the adsorption process. It is important to select a carbon with a pore size comparable to the pollutant. For example, a fine-pored coconut shell carbon is efficient in adsorbing low-weight molecular compounds, such as micropollutants, while a wood based carbon with larger pore size is more efficient in adsorbing larger molecules, such has humic. The right selection of pore size makes sure the attractive forces together with the opposite wall effect will be at a maximum. A thumb rule is to select a carbon with pore size 1.3-2 times larger than the target compound diameter. This prevent larger molecules from blocking the entry to the micropores (De Ridder, 2012). Figure 30 is a simplified sketch of pore structure in activated carbon.

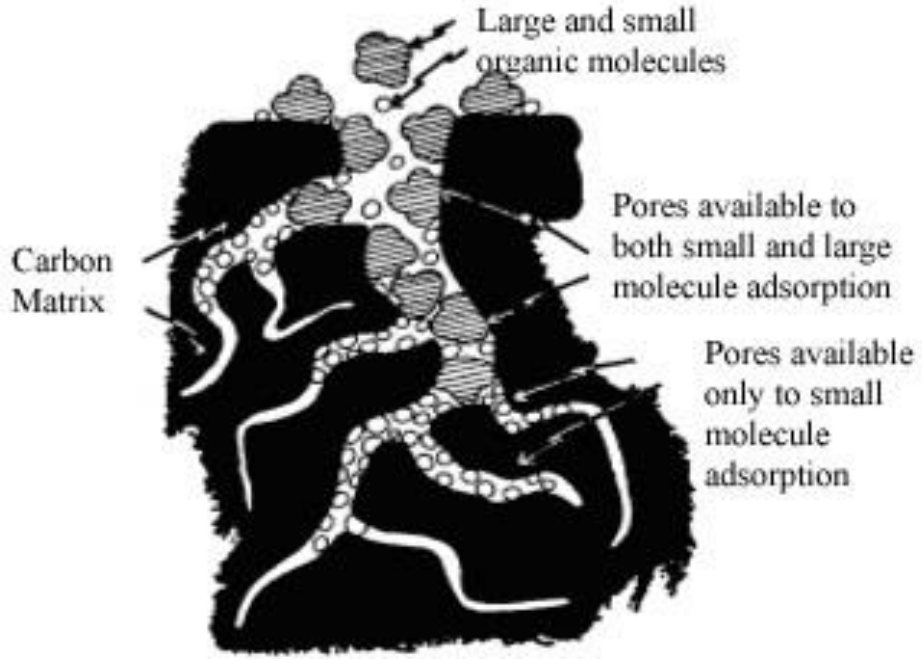

FIGURE 30: Principal scetch pore structre (Dvorak and Skipton, 2013)

Iodine number is used to describe the amount of pores at sizes of 10 to 20 Angstroms (1 to 2 nm). It is given in milligram adsorbed iodine per gram of GAC. The iodine number reflects the area on the GAC that is available for adsorption of low molecular weight organics (DeSilva, 2000).

5.3.4 Surface area

The internal surface area of activated carbon is most common found by the BET method. It utilizes a molecule of known dimension, usually nitrogen, and the low-pressure range of the adsorption isotherm e.g. monolayer adsorption. The specific surface area is given as area occupied by nitrogen per gram of carbon (cm^2/g) (Cameron Carbon, 2006).

5.3.5 Functional groups

Activated carbon has a heterogeneous surface. At the edges of the carbon layers, different chemical functional groups can be present. Carbons have different selectively towards different compounds and this depends mostly on the chemical composition and concentration of the surface functional groups. The main functional groups are the ones created during oxidation, which contain oxygen, such as carboxylic acids, ether, lactones, and phenolic hydroxyls. Other functional groups containing nitrogen, sulfur, phosphorus and halogens can be created by changing the conditions around the

carbon surface treatment (temperature, activation agents, time, precursors and templates) (Virkutyte et al., 2010). Typical carbon functional groups are shown in figure 32.

The carbon surface has an electrostatic charge, which is set by the type and number of functional groups. This can influence solute adsorption. Many of the oxygen-containing functional groups have acidic nature such as phenol and carboxyl. High acidity makes the carbon more hydrophilic, which decreases the adsorption of hydrophobic compounds. The surface charge can be manipulated by increasing or decreasing the pH, leading to dissociating or protonating of the functional groups(De Ridder, 2012). The pH_{PZC} is a parameter used to describe the surface charge of an adsorbent as a function of pH. It is the defined as the pH where the solid surface has a net neutral charge e.g. a "point of zero charge" (PZC). At pH less than the PZC the solid surface will have a negative charge and at pH larger than the PZC the solid surface will have a positive charge as illustrated in figure 31 (Railsbakc, 2006).

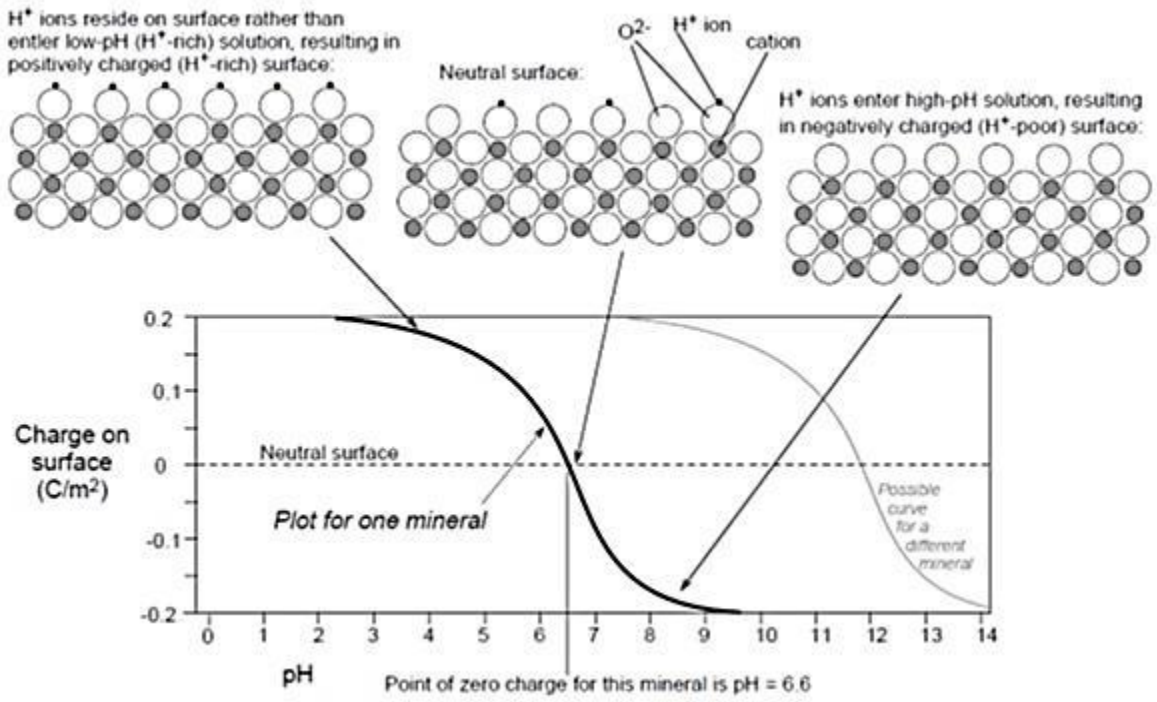

FIGURE 31: Illustration of pKa (Railsbakc, 2006)

Some carbons can have ion exchange abilities due to the present of cationic an anionic functional groups on the carbon surface (Virkutyte et al., 2010).

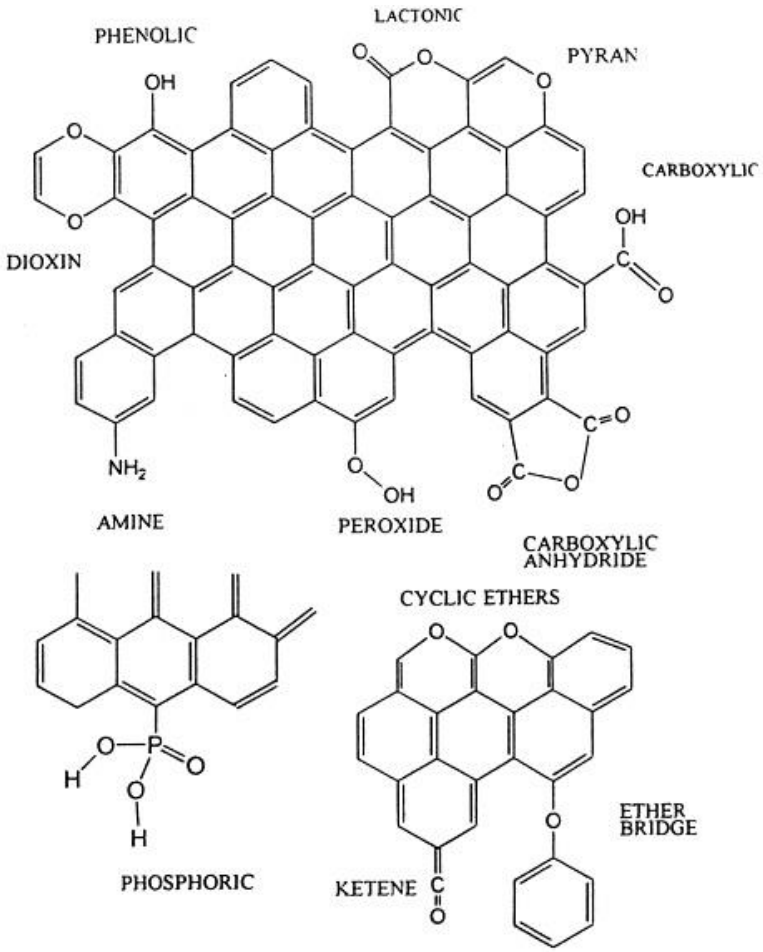

FIGURE 32: Typical carbon functional groups (Brennan et al., 2001)

5.3.6 Particle size

Particle size is an important parameter to consider when optimizing the performance of a filtration system. Smaller particle size increases the adsorption rate (increased internal surface area compared to external surface area) but it also increases the pressure drop over the filtration bed leading to less filter run time. Particle size is used to roughly distinguish the two main types of carbons. Powder activated carbon (PAC) is made up of crushed carbon particles (<0.276 mm) and is most typical used in waste-and drinking water treatment that require periodical removal of pollutants. It is not suitable in column or filters due to the fast buildup of head-loss and short filter run time. Granular activated carbon (GAC) has relatively larger particles than PAC and is usually incorporated into water treatment plants that require continuously removal of substances and pollutants.

Mesh sizes is often used to describe the particle size distribution of GACs. For example a 20x40 carbon is made up of particles where about 85% will pass through a U.S Standard Mesh Size No.20 (0.85mm) but about 95% is retained on a U.S Standard Mesh Size No.40 (0.42 mm) (Thomas, 2010).

5.4 Competitive adsorption

Environmental water samples contain a numerous set of different compounds, organics and inorganics. Competitive or preferential adsorption is the phenomenon where some compounds are preferred over others, taking up the adsorption sites. This is important to consider when predicting the removal efficiency for a selected contaminant. Competition between solutes is affected by both the solute and adsorbent properties. Solute properties that influence adsorption are charge, size, hydrophobicity and presence of certain functional groups. As already mentioned, the selectivity of an activated carbon is mainly decided by its chemical composition and concentration of functional groups (De Ridder, 2012). Hydrophobic adsorbents have higher removal efficiencies than hydrophilic adsorbents. A high concentration of oxygen-containing functional groups decreases the carbons hydrophobicity and increases the preferential adsorption of water molecules over organic compounds. Higher molecular weight compounds are preferentially adsorbed over low molecular weight species. Also, it has been found that adsorption increases with decreasing charge of the compound because polar compounds will have larger affinity for water (Cameron Carbon, 2006). Competition can be minimized by using carbons with small pore size, large enough to admit the micropollutants of interest but small enough to block out the higher molecular weight compounds. The pH and temperature can be optimized with regard to competition. By increasing the selectivity of a carbon towards a certain compound, competition with compounds with similar action modes can be avoided.

5.5 Kinetic models

The kinetic performance of a certain adsorbent is important to know before using it in real-life treatment processes. By doing kinetic analysis, the solute uptake rate and complete residence time for adsorption reaction can be found. The kinetics can be used to determine the performance of fixed-beds, column size, and the scale of an adsorption treatment system.

It has been developed many mathematical models that aim to describe adsorption data. This is most commonly done by looking at adsorption on the basis of diffusion or chemical reactions, i.e., adsorption diffusion models or adsorption reaction models. Adsorption diffusion models are based on the diffusion steps; film diffusion, intra-particle diffusion and mass action, while adsorption reaction models look at adsorption as a chemical process without considering the diffusion mechanisms.

The kinetic models and diffusional models attempt to describe the expected amounts of solute adsorbed at a given time t. This is referred to as the adsorption capacity. The adsorption capacity at a certain time t is given by the following equation:

$$q_t = \frac{(C_i - C_t)V}{M} \qquad \text{EQUATION 5-1}$$

where q_t is the adsorption capacity (µg adsorbed solute/mg adsorbent) at time t, Ci and Ct is the concentration at initial time (t=0) and time t, respectively, V is the volume of solution (L), and M is the mass of adsorbent added (mg).

By using equation 5-1, the adsorption capacity at equilibrium q_e, is given as:

$$q_e = \frac{(C_i - C_e)V}{M}$$ EQUATION 5-2

5.5.1 Adsorption reaction models

Adsorption reaction models are a simple way to describe the kinetic process of adsorption for many compounds. However, they are unsuitable for organics where adsorption is mainly a process of physical adsorption and not chemical. This applies especially for non-polar polymeric adsorbents.

Pseudo-first-order rate equation

Lagergren's Pseudo-first-order rate equation was developed in 1898 and is believed to be the first kinetic model that describes adsorption rate based on the sorption capacity of the solid. It is used to describe the kinetic process of liquid-solid phase adsorption. The Pseudo-first-order rate equation is given as:

$$\frac{dq_t}{dt} = k_{p1}(q_e - q_t)$$ EQUATION 5-3

where k_{p1} (min^{-1}) is the rate constant of pseudo-first-order reaction, q_e and q_i (µg/mg) are the adsorption capacities at equilibrium and time t (min), respectively. Intergrating equation 5-1with the boundary conditions of q_t=0 at t=0 and q_t=q_t at t=t gives (Qiu et al., 2009):

$$ln(q_e - q_i) = lnq_e - k_{p1}t$$ EQUATION 5-4

If the reaction follows pseudo-first-order rate equation the plot of ln(q_e-q_i) against t should yield a straight line. Commonly, for micropollutants, the pseudo-first order rate equation is only applicable at describing the first 30 min of the adsorption process (de Oliveira et al., 2012).

Pseudo-second-order rate equaiton

The pseudo-second-order rate equation was developed by Ho in 1995. He investigated the adsorption of copper ions onto peat, which was assumed caused by chemical bonding between the divalent copper ion and polar functional groups on the peat surface. The reaction was represented with the two following equations (Ho and McKay, 1999):

$$2P^- + Cu^{2+} \leftrightarrow CuP_2$$ EQUATION 5-5

$$2HP + Cu^{2+} \leftrightarrow CuP_2 + 2H^+$$ EQUATION 5-6

where P^- and HP represent polar sites on the peat surface. The adsorption rate depends on the amount of copper ions on the surface of peat at time t and the amount adsorbed at equilibrium. If the adsorption follows seond-order, the rate expression should yield:

$$\frac{d(P)_t}{dt} = k_{p2}[(P)_0 - (P)_t]^2$$ EQUATION 5-7

$$\frac{d(HP)_t}{dt} = k_{p2}[(HP)_0 - (HP)_t]^2$$ EQUATION 5-8

where $(P)_0$ and $(HP)_0$ are the number of active sites available at equilibrium and $(P)_t$ and $(HP)_t$ are the number of active sites occupied on the peat at time t. The k_{p2} (mg/µg·min) is the second-order rate constant. Further, assuming that the sorption capacity is proportional to the available number of active sites, equation 5-5 and 5-6 can be rewritten to the pseudo-second order rate equation:

$$\frac{dq_t}{dt} = k_{p2}(q_e - q_i)^{\,2}$$ EQUATION 5-9

With the boundary conditions of q_t=0 at t=0 and q_t=q_t at t=t, equation 5-7 is integrated into the following expression:

EQUATION 5-10

$$\frac{t}{q_t} = \frac{1}{k_2 \times {q_e}^2} + \frac{t}{q_e}$$

If the adsorption reaction follows the pseudo-second-order rate equation the plot of t/q_e against t should yield a straight line. The pseudo-second-order-rate equation has been successfully used on adsorption of metal ions, herbicides, oils, and organic substances in liquids (Qiu et al., 2009).

Elovich equation

The elovich equation is another common method successfully used to describe the kinetics of adsorption processes. It is based on the principals of chemisorption and is written as follows (Hameed et al., 2008):

$$q_t = \left(\frac{1}{b}\right)\ln(ab) + \left(\frac{1}{b}\right)lnt$$ EQUATION 5-11

where a and b are the rate constants found from the slope and intercept of q_t versus lnt (NB! When plotting the elovich equation it is important that the time is given in hours. Otherwise the intercept with the y axis becomes negative and the equation is of no use)

5.5.2 Adsorption diffusion models

Film diffusion, intraparticle diffusion, and mass action are always present in a liquid/solid adsorption. However, mass action is a very rapid process that can be neglected for kinetic study. This means that the controlling factor for an adsorption process is liquid film diffusion, intrapartical diffusion, or both. This is often referred to as the rate limiting step (Qiu et al., 2009). Therefore, adsorption diffusion models mainly focus on describing these two processes. In this thesis, no characterization of the

activated carbon was conducted. Therefore, only the intraparticle diffusion models that did not require such data were used to give an indication of the rate limiting step. A short description of the liquid film diffusion model is still given.

Liquid film diffusion model

For solid particles, the rate of solute accumulation depends on the volume of the particle (V_p) and the average concentration of adsorbed solute ($\bar{q}$) at time t. The difference between the concentration of solute in the interface of liquid/particle and the concentration of solute in the liquid far from the particle is referred to as the concentration driving force, (C-Ci). The solute mass transfer through the liquid film is proportional to the concentration driving force and surface area of particle (A_s). This gives us the mass transfer equation as follows, which is often referred to as the linear **driving force rate law of film diffusion**:

$$\frac{\partial \bar{q}}{\partial t} = k_f S_0 (C - C_i) \qquad \text{EQUATION 5-12}$$

where k_f is the film mass transfer coefficient and S_0 is A_s divided by V_p.

This was further developed by Boyd et al. to the film diffusion mass transfer rate equation as follows (1947):

$$\ln\left(1 - \frac{q_t}{q_e}\right) = -R^1 t \qquad \text{EQUATION 5-13}$$

$$R^1 = \frac{3{D_e}^1}{r_0 \Delta r_0 k'} \qquad \text{EQUATION 5-14}$$

where R^1 (min^{-1}) represents the liquid film diffusion constant, ${D_e}^1$ (cm^2/min) is liquid film diffusion coefficient, r_0 (cm) the radius of a spherical adsorbent particle and Δr_0 is the thickness of the film (cm). The plot of ln(1-qt/qe) versus t should yield a straight line through origin with a slope of R^1.

Intraparticle diffusion model

Intraparticle diffusion models are based on the assumption that film diffusion is negligible. One of the most used intraparticle diffusion models is the **Weber-Morris model**. He discovered that in many cases, solute adsorption is proportional with $t^{1/2}$ rather than with contact time t. The Weber-Morris equation is written as (Qiu et al., 2009):

$$q_t = k_{int} t^{1/2} \qquad \text{EQUATION 5-15}$$

where k_{int} represents the intraparticle diffusion rate constant (mg/g $min^{1/2}$). If the process follows the intraparticle diffusion model, q_t versus $t^{1/2}$ should yield a straight line passing through the origin. However, if this is not the case, the sorption removal is a more complex process, involving both film diffusion and intraparticle diffusion simultaneously.

A multilinear approach can be used to evaluate the Weber-Morris equation. The intraparticle diffusion plot is divided into different stages by considering the shape of the curve. External adsorption may cause a first, sharper region on the curve. After external adsorption a second more

gradual adsorption stage occurs where intraparticle diffusion often is the rate limiting mechanism. At the last regions, referred to as the equilibrium stages, the diffusion process is slowed down due the very low concentration of solute in the aqueous solution and the q_t stagnates. The multilinear Weber Morris equation can be written as:

$$q_t = k_{int,i}\, t^{1/2} + C_i \qquad \text{EQUATION 5-16}$$

where i refers to the different stages and C_i is the interception of stage i. The intercept of stage i, provides an indication of the thickness of the boundary layer. The boundary layer effect increases with larger i (Hameed et al., 2008, de Oliveira et al., 2012).

Another intraparticle diffusion model is the **Drumwald-Wagner model**. It is written as (Qiu et al., 2009):

$$\log(1 - F^2) = -\frac{K}{2.303} t \qquad \text{EQUATION 5-17}$$

where F is q_t^2/q_e^2 and K is the rate constant. A plot of $\log(1-F^2)$ versus t should yield a straight line through the origin if intraparticle diffusion is the rate limiting step.

5.6 Isotherm models

An isotherm is a measure on the equilibrium relationships between a solute and an adsorbent. It describes how the solute reacts with the adsorbent, the retention or mobility of a solute from the liquid media to a solid, at a constant pH and temperature (Foo and Hameed, 2010).

Some of the most used isotherm models are the linear least-squares methods such as the linear Langmuir and Freundlich model. Recently, the weaknesses of such linearized methods have been pointed out like a vast amount of different outcomes depending on the way the equation is linearized, large error variance, the normality assumptions of standard least squares method leading to a bias of data etc. Thus, over the last years, the use of non-linearized models together with a number of error analysis techniques has increased (Foo and Hameed, 2010).

Adsorption isotherms are formulated on the basis of three fundamentals approaches; kinetic approach, thermodynamic approach or theory approach. The last mentioned aims to generate characteristics curves out of theoretical assumptions (Foo and Hameed, 2010). An isotherm experiment is commonly done by batch tests. Several containers are added the same volume of sample with an initial concentration of solute and different amounts of adsorbent (or opposite). They are then left to react under constant pH and temperature. After equilibrium is reached, the solute equilibrium concentration for each container is found.

5.6.1 Langmuir isotherm model

The Langmuir isotherm was originally developed for gas-solid-phase adsorption, but it has been and still are widely used to model liquid-solid-phase adsorption, especially onto bio-solid adsorbents. It is based upon the two main assumptions:

- The adsorption is homogenous

- The adsorption is monolayer

Homogenous adsorption means that all the adsorption sites possess equal affinity for the adsorbate. In the Langmuir isotherm, once a molecule occupies a site, no further adsorption can take place. Monolayer adsorption refers to the assumption that each adsorption site only can take up one molecule; hence the adsorption layer is only one molecule in thickness. Furthermore, the Langmuir isotherm assumes no interaction and hindrance between the adsorbed molecules, even at adjacent sites. The rapid decrease of intermolecular attractive forces is explained by the rise of distance.

The non-linear form of the Langmuir isotherm is given by the equation:

$$q_e = \frac{Q_0 K_L C_e}{1 + K_L C_e} \qquad \textbf{EQUATION 5-18}$$

where Q_0 is the maximum sorption capacity (mg/g) related to the monolayer area occupied by the sorbate and K_L is the Langmuir constant, which is a measure of the intensity of sorption (L/mg). The constants in the non-linear form of the Langmuir isotherm can be found by using regression techniques and the solver function in excel.

One linearized form of the Langmuir isotherm is given by the equation:

$$\frac{1}{q_e} = \frac{1}{Q_0} + \frac{1}{K_L Q_0} \times \frac{1}{C_e} \qquad \textbf{EQUATION 5-19}$$

If the reaction follows this linear form of Langmuir isotherm, a plot of 1/qe against 1/Ce should yield a straight line.

A separation factor for Langmuir isotherm (R_L) has been developed. It is written as:

$$R_L = \frac{1}{1 + K_L C_0} \qquad \textbf{EQUATION 5-20}$$

The R_L value is a measure on how favorable the adsorption is; unfavorable (R_L>1), linear (R_L=1), favorable (0<R_L<1) or irreversible (R_L=0) (Foo and Hameed, 2010).

5.6.2 Freundlich isotherm model

In contrast to the Langmuir isotherm model, the Freundlich isotherm model is not constricted to the formation of monolayer and can be applied to multilayer adsorption. It describes heterogeneous adsorption, where active sites have different affinities and is non-uniformly distributed over the surface. The Freundlich isotherm says that sites with the strongest bond energy are occupied first, and hereby, the adsorption energy decreases exponentially towards equilibrium. The amount adsorbed solute is the summation of adsorption on all sites. This explains why the ratio of the adsorbate onto a set mass of adsorbent is not a constant at different solute concentrations. The Freundlich isotherm is widely applied to organic compounds or highly interactive species on activated carbon and molecular sieves.

The Freundlich equation in its non-linear form is written as:

$$q_e = K_F C_e{}^{1/n}$$ EQUATION 5-21

where K_F ((mg/g)/(L/mg)$^{1/n}$) and n (dimensionless) are measures on adsorption capacity and intensity, respectively. The constants for the non-linear form of the Freundlich isotherm can be found by using regression techniques and the solver function in excel.

The linear form of the Freundlich equation is written as:

$$logq_e = logK_F + \frac{1}{n} logC_e$$ EQUATION 5-22

A plot pf $logq_e$ versus $logC_e$ should yield a straight line if the adsorption follows the Freundlich model. The adsorption intensity or surface heterogeneity is shown by the slope value, which ranges between 0 and 1. The closer the slope is to 0, the more heterogeneous the surface is. A 1/n below 1 indicates chemisorption processes while a value larger than 1 is an indication of more complicated and cooperative adsorption processes (Foo and Hameed, 2010).

5.6.3 Validation of kinetic and isotherm models

The models were evaluated according to the correlation coefficient R^2. This value is automatic calculated by excel when generating linear trend lines. The closer R^2 is to unity, the better is the fit of the model to the experimental data. For non-linear regression isotherm models, the correlation coefficient can be calculated as follows:

$$R^2 = 1 - RSS/TSS$$ EQUATION 5-23

where RSS is the residual sum of squares and TSS the total sum of squares. They are given by the following equations:

$$RSS = (q_{e,exp} - q_{e,calc})^2$$ EQUATION 5-24

$$TSS = (q_{e,exp} - \bar{q}_{e,exp})^2$$ EQUATION 5-25

where $q_{e,exp}$ and $q_{e,calc}$ are the experimental and calculated adsorption capacities, respectively, and $\bar{q}_{e,exp}$ is the average experimental adsorption capacity.

In addition to R^2, the normalized standard deviation Δq_e can be used to validate the suitability of the kinetic models. The normalized standard deviation equation is written as:

$$\Delta q_e(\%) = 100 \sqrt{\frac{\sum[(q_{e,exp} - q_{e,cal})/q_{e,exp}]^2}{(N-1)}}$$ EQUATION 5-26

where N is the number of data points. A low Δq_e indicates low deviation of the model (Hameed et al., 2008).

5.7 Breakthrough curve

Isotherms give an indication of how well an impurity may be removed using activated carbon, but it cannot give definitive scale-up data for a granular carbon operative. In a packed granular carbon bed, the solute concentration changes as it moves through the bed, which is not the case in an isotherm test procedure. The adsorption pattern through the bed is referred to as the breakthrough curve. A typical breakthrough curve for a fixed-bed adsorber is shown in figure 33. It is most commonly obtained from a pilot column test, as shown in figure 34, as the plot of the relative concentration (C/C_0) measured at a fixed point in the column, usually near the outlet, against time or volume of water treated. The breakthrough curve is used to predict and design full scale systems and estimate operating costs.

The breakthrough curve has a typical S shape. In the initial stages of operation, the solute is adsorbed most rapidly and effective by the first layers of fresh activated carbon. The small concentrations of contaminant that escapes the first layers of adsorbent are then adsorbed in the following subsequent strata. The adsorption zone or mass transfer zone refers to the layers where the main adsorption takes place. As the contaminated water continues to flow into the column, the top layers of carbon become saturated with the solute and minimal of further adsorption can occure. Thus, the adsorption zone and C_0 concentration front moves downward the column to layers with fresh carbon. As the adsorption zone gets closer to the column outlet, more and more solute escape into the effluent. At breakpoint the column is in equilibrium with the influent water. Beyond this point little removal of solute will occur and a steep increase in the breakthrough curve happens.

The shape of the breakthrough curve will have varying degree of steepness and position of breakpoint. The longer time to breakpoint and the steeper S shape, the more effective is the adsorption. Factors that affect the shape of the curve are depth of column and flowrate, in addition to all of the parameters discussed earlier for adsorption (pH, temperature, contaminant and adsorbent properties, concentration etc.) In general, time to breakpoint is decreased by:

- Increased particle size
- Increased initial concentration of solute
- Increased pH
- Increased flowrate
- Decreased bed depth

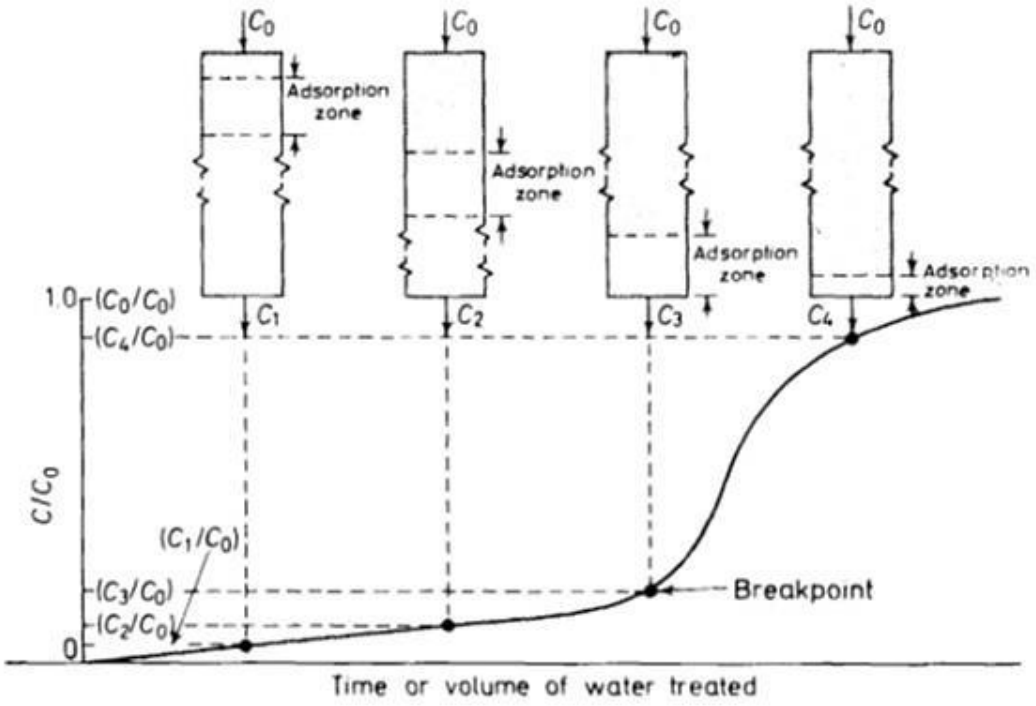

FIGURE 33: Breakthrough curve fixed adsorbent bed (Weber jr, 1974)

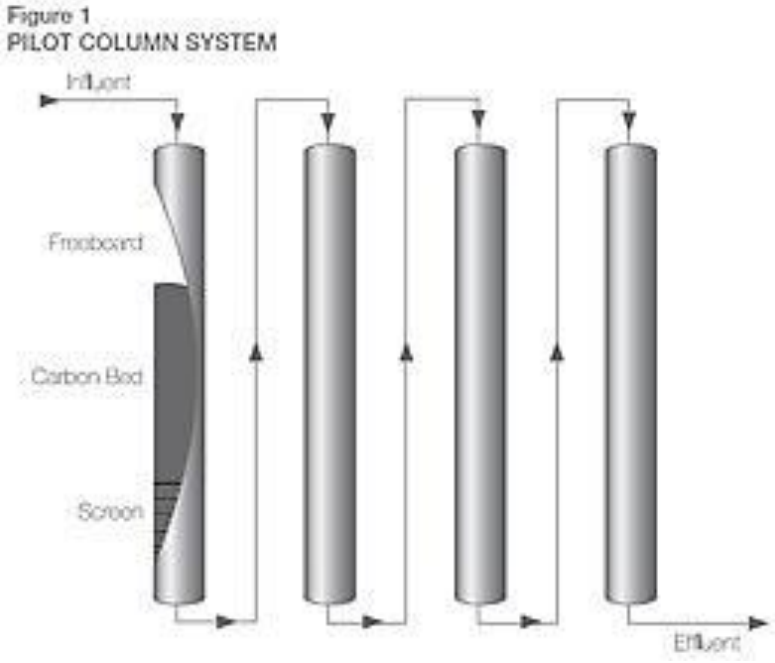

FIGURE 34: Column test (Norit, 2001)

5.8 The use of activated carbon in water treatment

In **batch systems** a certain amount of carbon is mixed continuously with a specific volume of water until the wanted removal is achieved. It can be done with GAC or more common, PAC. The use of larger GAC particles requires longer contact time and larger basin/tank volumes, but is easier to collect and regenerate than PAC. Batch systems are most commonly used for smaller water volumes or if only periodically removal of the contaminants is needed. For batch systems, the required amount of carbon and contact time to reach wanted removal efficiencies are given by the isotherm curves.

In a **fixed bed system** the GAC particles are held on place in a stationary, packed bed. The adsorbent is continuously in contact with fresh solution of adsorbate. It normally consists of one or more columns, often cylindrical steel vessels, packed with GAC particles, which are held on place with screens at the bottom and top. The columns can be connected in series or parallel mode. The advantage with column-type systems with continuous flow over batch-type systems are that the adsorption rates only depend on the solute concentration. The solute concentration in contact with a given layer of carbon changes slowly, utilizing the full adsorption capacity of the carbon. A fixed bed system can be operated in down flow mode, either driven by pressure or gravity, or pressure-driven up flow mode, also known as expanded-bed systems. The advantages with expanded beds are less head-loss, air-binding, and plugging with suspended matter. In down flow driven columns, the system must be periodically backwashed (about 50% expansion of the bed) to flush out the accumulation of suspended solid (Cooney, 1998, Weber Jr, 1974).

The prediction and design of fixed bed systems are done on basis of the breakthrough curve. The bed depth service time (BDST) model for designing adsorption columns, braces to establish the shape of the breakthrough curve and its velocity through the bed. When the break-through concentration of contaminant reaches a set maximum level (C_s) the adsorption operation is stopped. The saturated carbon is then replaced or regenerated before next cycle. Often the system is operated with two identical columns in series. When column 1 reaches the selected break-through concentration, it is taken off-line, and column 2 is connected to the feed stream (Cooney, 1998, Weber Jr, 1974).

Normal operating and design parameters for fixed bed systems are (Cooney, 1998):

- 15-35 min residence time
- Hydraulic loading of 7-12 $m^3/hr/m^2$ for down flow operated systems
- Hydraulic loading of 10-24 $m^3/hr/m^2$ for up flow operated systems
- Carbon depths from 3-12 m
- Pressure drop across the column<0.23 bar/m
- Extra bed depth of 10-50% (if backwashing is used)

In steady state moving bed adsorption the adsorbent solid is moving downward through the column while the liquid is flowing upward, shown in figure 35. The advantage with moving bed systems is that the carbon is continuously regenerated when it is saturated. It is widely used in wastewater treatment (Kumar et al., 2004).

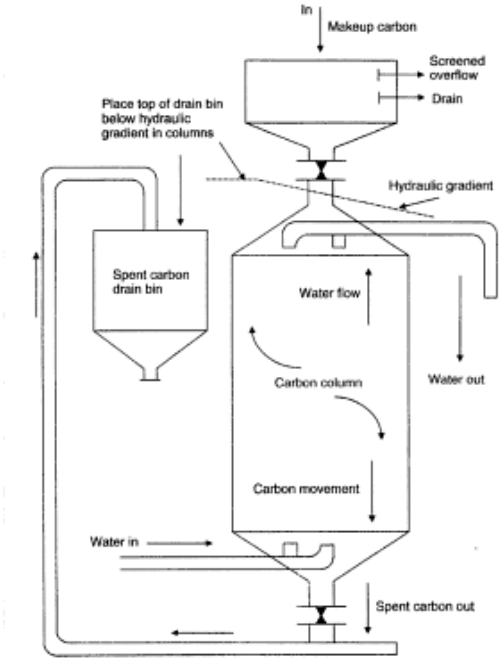

Figure 5.8 Schematic of a pulsed flow adsorber (adapted and redrawn from Faust and Aly, 1987).

FIGURE 35: Steady state moving bed adsorption (Kumar et al., 2004)

Cost of adsorbent and difficulties with regeneration are the two biggest barrier with the application of activated carbon in water treatment (Foo and Hameed, 2010). Rates of liquid/solid adsorption onto granular activated carbon increase with decreasing particle size. However, it is difficult to achieve efficient operations with small particle size because of the fast build- up of pressure. It is therefore desired to find the best optimization point between particle size and efficient operation (Weber Jr, 1974).

6. Method

6.1 Materials

6.1.1 Chemicals and reagents

Triclocarban (3,3,4'-Trichlorocarbanilide;CAS 101-20-2; 99% purity) and diethyl phthalate (diethyl phthalate; CAS 84-66-2;99% purity) were purchased from Sigma-Aldrich (St. Louis, MO, USA). Acetonitrile (CAS 75-05-8) for mobile phase and stock solution was bought from VWR and was of HPLC grade (water content<0.002%) Water used for mobile phase and other purposes was of Milli-Q quality. Adjustments of pH were performed with 0.1 M and 1M hydrochloric acid (HCl).

6.1.2 Activated carbon

The activated carbon Filtrasorb 400 (F400) was chosen for this study. This adsorbent is often cited in literature and is considered as a reference material in the adsorption of solutes in aqueous solutions. It has been widely applied on removal of micropollutants (Rivera-Utrilla and Sánchez-Polo, 2002, Morlay and Joly, 2009). It is made from bituminous coal by physical stem activation. In general, F400 is a highly microporous activated carbon with a large distribution of poresize from ultramicropores up to mesopores. It has a low content of oxygen containing functional groups, and thus a high pH_{PZC} of about 10.3. The properties of F400 are summarized in table 9, which is based on the report by Molay et al. (2009) and Karanfil and Kilduff (1999), and by the description from the manufacture CalgonCarbon (2012). The activated carbon was washed in MQ water and dried over night at 140°C before each experiment.

TABLE 9: Properties of activated carbon F400

Effective particle size mm	Iodine number mg/g(min)	S_{BET} m^2/g	V_p cm^3/g	V_{micro} cm^3/g	Oxygen content % weight	Tot- acidic groups µeq/m^2	Tot- basic groups µeq/m^2	pH_{ZPC}
0.55-0.75	1000	1012	0.57	0.37	<1	0.24	0.40	10.3

6.2 Stock solution, working solutions and calibration curves

6.2.1 Triclocarban

The preparing of TCC stock solution showed to be more difficult than first thought. The TCC powder was difficult to operate with, sticking to the equipment. Because of the very low water solubility (0.04 mg/L), it had to be dissolved in 100 % methanol or acetonitrile before added to water. Acetonitrile was chosen among these two, because by eye it seemed better in dissolving TCC. In the methanol stock solution, formation of thin white treads of TCC could be seen.

A strong stock solution of concentration 1 g TCC/L acetonitrile was made by adding 100 mg TCC to a 100 mL volumetric flask. This was done in the following way:

1. 100 mg (±0.0001) TCC was measured in a plastic cup on a milligram lab scale
2. The TCC powder was transferred to a 50 mL bottle with screw cap by bending the sides of the cup to create a narrow V shape and then rinsing it with acetonitrile using a beaker until no TCC was left on the cup. This required about 40 mL of acetonitrile.
3. The bottle with about 40 mL was then sequentially shaken, heated under hot water, and put on ultrasound for 5 min until a minimum of TCC particles could be seen
4. The content in the bottle was then transferred to the 100 mL volumetric flask by a glass funnel.
5. To make sure no TCC were left in the bottle, the volumetric flask was filled with the remaining acetonitrile by adding small amounts to the bottle, shaking, and then to the flask. This was done as many times as possible until 100 mL was reached.
6. The stock solution was encapsulated with paraffin and stored in a dark ventilation cabinet. It was not stored in the fridge because this was found to cause precipitation of TCC.

From the strong stock solution, two weaker working solutions of concentration 10mg/L and 5mg/L in acetonitrile were made. Those were used to prepare the samples for the calibration curve and for the experiments. A standard solution concentration of 20 µg/L was chosen for the adsorption experiments.

The calibration curve for TCC was made by spiking milli-Q water with the working solution of TCC to wanted concentrations. 11 solutions in the concentration range of 0.05-20 µg/L were prepared. The maximum concentration of 20 µg/L was chosen because of the difficulty of dissolving TCC in water. It was thought wise to choose a concentration that was not too close to the solubility limit. The pH of the milli-Q and TCC samples was 6.5. This was measured with a pH meter, which before each test run was calibrated with buffer pH7 and buffer pH4. No pH adjustments were done to the milli-Q samples.

6.2.2 Diethyl phthalate

DEP has much higher water solubility (0.4-1 mg/L) than TCC and could be directly dissolved in water. The stock solution of DEP was prepared in milli-Q water in a concentration of 200 mg/L. This was done by pipetting 0,179 mL of 99% DEP to a 1000 mL volumetric flask and then filling it with milli-Q water. Before shaking, the DEP was visible in the water as a transparent bobble. After shaking and heating under hot water, no bobbles could be seen and the DEP was completely dissolved. The stock solution was encapsulated with paraffin and stored in a dark ventilation closet.

The stock solution of DEP was also used as working solution. Milli-Q water was spike with the stock solution to wanted concentrations. The calibration curve was made with 15 solutions with concentrations from 0.001-5 mg/L.

A DEP concentration of 5 mg/L was chosen for the adsorption experiments. This was selected based on the influent concentrations of DEP found in literature (section x). The highest documented influent concentration of DEP was as high as 7.4 mg/L. The pH of DEP in milli-Q water was 6.5. It was not adjusted.

6.3 Sample preparation

The greywater samples were collected from the pilot plant driven by PhD candidate Viggo Bjerkelund at NTNU. Table 10 gives an overview of the greywater and its characteristics. Some of these characteristics were only tested ones and may have varied slightly from time to time depending on the greywater used.

TABLE 10: Characteristics greywater

pH	TDS mg/L	COD mg/L	DOC mg/L	Tot-P mg/L	Tot-N mg/L	Conductivity µS/cm
≈8.1	289 mg/L	17.7 mg/L	5-6	3.79 mg/L	3.34 mg/L	399

TDS= Total dissolved solids, COD=Chemical oxygen demand, DOC= Dissolved organic carbon
Tot-P= Total phosphorous, Tot-N= Total nitrogen

The greywater samples were collected continuously during the experiment period. The greywater were filtered through 1.2 µm glass-fiber filter (GF/F) and the pH was adjusted to pH 6.5 (same as milli-Q) by addition of about 1.1 mL of 1M HCl to 1000 mL greywater. The samples were stored in the fridge at 4°C until the experiments were conducted. They were not stored for longer than two days at a time.

The greywater and MQ water samples were spiked with TCC and DEP right before each experiment. For the isotherm experiments, which required large volume of water, two 2000 mL volumetric flasks were prepared and then mixed together in a 4000 mL beaker. This to make sure the initial concentration was the same for all the isotherms. When preparing the samples containing TCC, the volumetric flasks were filled half full with greywater/MQ water and heated under hot water before the TCC was added. This was done to increase the solubility of TCC in the moment of adding and avoid precipitation before it was completely disturbed in the water phase. The flasks were then left to cool before the rest of the greywater/milli-Q water was added. This was done to avoid volumetric error due to water expansion at higher temperatures.

To protect the HPLC machine column from particles in the greywater it is important to filter the samples before they are analyzed, preferably with a filter with pore size less than 0.45 µm. However, it was discovered that the TCC reacted with both the cellulose filter (0.45 µm) and the Teflon filter (0.2 µm), especially the first one mentioned. Therefore, the greywater samples containing TCC were filtered through 0.7 µm GF filter before added to the analysis vials. Although this was not optimal, it was considered safe because the machine was equipped with a pre-guard column protecting it from potential particles. The DEP did not react with either the cellulose filter or the Teflon filter. Teflon filter was used on the greywater samples containing only DEP. The samples with both DEP and TCC were filtered through GF filter. The filter tests conducted on TCC are shown in appendix C.

6.4 Equipment

6.4.1 Analytical equipment

The analytes were separated and detected with and Agilent 1200 HPCL system, which consisted of a degasser (G1322A), a quaternary pump (G1311A), a thermostated, column compartment (G1316A), an autosampler (G1329A) and a diode array detector (DAD G1315D). The separation was performed using a Zorbax Eclipse XDB C18 reversed phase analytical column (150mmx4.6mm i.d., 5 µm particle size). A pre-column was used to guard the column.

1.1.1 Other equipment

The analyses of dissolved organic carbon (DOC) were done by the laboratory personal at NTNU. IT was done on a Tekmar fusion total organic carbon analyzer.

6.5 Analytical procedure

6.5.1 Triclocarban

The separation of TCC was carried out by the following HPLC settings:

- Injection volume was 900 µL
- Flowrate at 1.5 mL/min
- Mobile phase composition of water (A) and acetonitrile (B) at ratio 20:80
- Temperature of column oven at 25°C
- Detection wavelength at 265 nm

The peak attained for these settings in MQ water are shown in figure 36 The retention time (t_r) was about 5.2 min. The runtime was set to 10 min. The total time it took to run each sample was 30 min including the pre-run time, injection, and equilibration post-time.

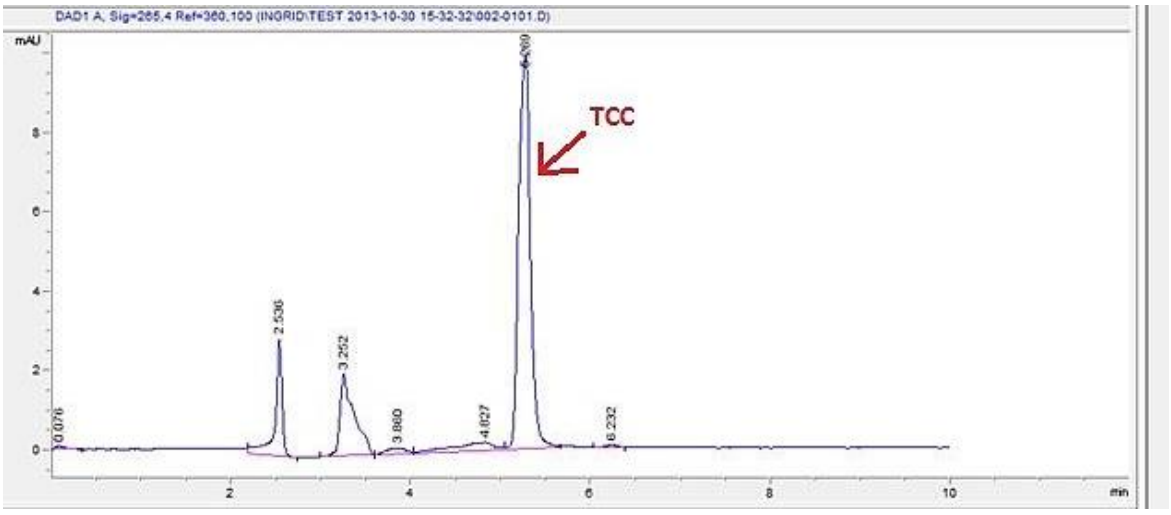

FIGURE 36: TCC peak obtained with the selected method

6.5.2 Diethyl phthalate

The separation of DEP was carried out by the following HPLC settings:

- Injection volume was 450 µL
- Flowrate at 1.5 mL/min
- Mobile phase composition of water (A) and acetonitrile (B) at ratio 40:60
- Temperature of column oven at 25°C
- Detection wavelength at 226 nm

The peak attained for these settings in MQ water are shown in figure 37. The retention time (t_r) was about 5.1 min. The runtime was set to 10 min. The total time it took to run each sample was 20 min including the pre-run time, injection, and equilibration post-time.

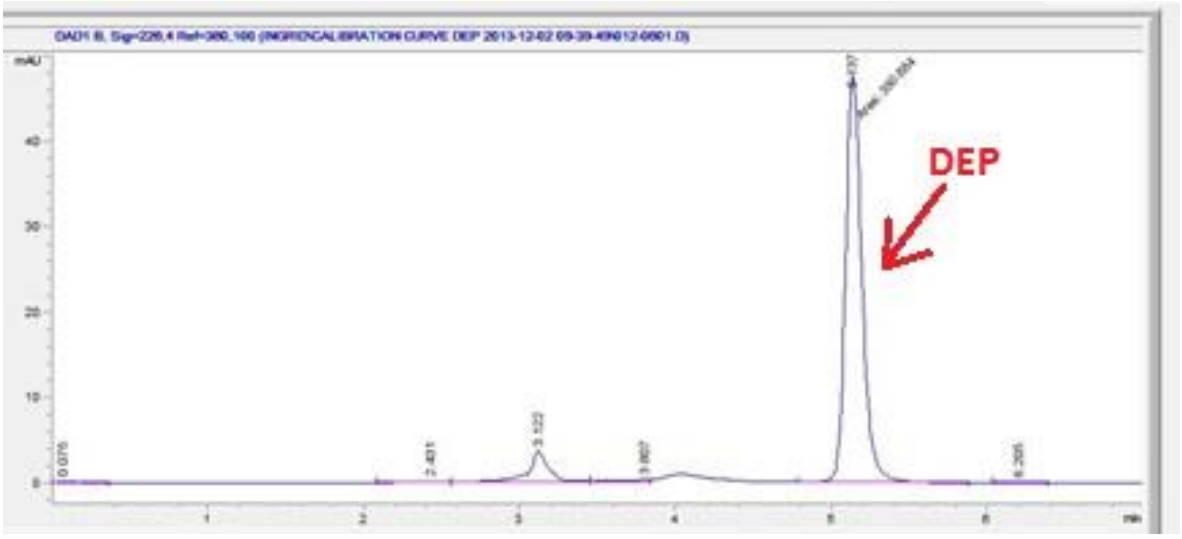

FIGURE 37: DEP peak obtained with the selected method

6.5.3 Mixture of TCC and DEP

For the samples containing both TCC and DEP, the detections were run separate. All of the samples were first tested for TCC using the settings in 6.5.1. After this, the samples were run over again and tested for DEP using the settings in section 6.5.2. It was sufficient to use the same vials for both TCC and DEP, since one vial contains 2 mL of solution. The total time it took to analyze each sample for both TCC and DEP was about 50 min.

6.5.4 Cleaning procedure

The washing procedure consisted of an external needle wash vial of acetonitrile and water at ratio 80:20. The needle was washed between each sample injection. The needle wash vial was exchanged between each total sample run. At the end of each sample run, the system was cleansed with 100% acetonitrile for 10-20 min. The speed was increased to heighten the pressure and by this forcing potential impurities out of the system. The pump vial was cleaned regularly (about every second analysis) with MQ water containing 10% 2-propnal (v/v).

6.6 Adsorption kinetic experiment

The kinetic experiment was carried out by initial concentrations of TCC and DEP of 20 µg/L and 5 mg/L, respectively. No adsorption kinetic experiment was conducted for the mixture solution because of the limited amount of time at the end. Both greywater and MQ water was used for each kinetic experiment. The DOC adsorption kinetic experiments were only done for the DEP greywater solutions due to the present of acetonitrile in the solutions spiked with TCC, which could not go into the TOC analyzer. It was also done a DOC adsorption experiment in greywater Reference samples were run for each test.

The following procedure was use: wanted weight of washed activated carbon was added to 1000 and 500 mL (or 250 mL) bottles with screw cap containing 900 mL or 500 mL (or 250 mL) solution. The first adsorption experiment was performed with a volume of 250 mL but because of the total volume of solution that needed to be withdrawn, the volume was increased to 900 mL for the greywater TCC experiments and 500 mL for the greywater and MQ DEP experiments. To make sure all the weighed carbon got into the bottles, the adding was done by first pipetting some solution onto the carbon in the plastic weighing cup, as seen in figure 38, and then rinsing it down into the bottles. After the adding, the bottles were put on an orbital shaker, similar to the one seen in figure 39, set at 175 rpm. The pH of the samples was 6.5 and the temperature was ambient.

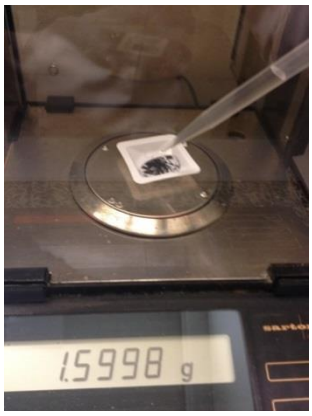

FIGURE 38: Weighing of carbon

FIGURE 39: Orbital shaker (Grant, 2013)

Samples were taken from the bottle at suitable time intervals. Closer time intervals were selected in the beginning of the time frame. 5 mL was withdrawn from the solution for each DEP and TCC sample, and 20 mL (10 mL to dilute to 1:5) was withdrawn from the solution for each DOC sample. Before analysis, the TCC and DOC samples were filtered through a 0.7 GF filter and the samples containing DEP were filtered through a 0.2 Teflon filter. Tables over sample time intervals are shown in appendix D. The time intervals varied some from experiment to experiment.

The pseudo first and second order rate equations as described in section 5.5.1 were used to model the adsorption kinetics. Intraparticle diffusion models as described in section 5.5.2 were used to explain the adsorption mechanisms and the rate limiting steps. All the experimental data obtained for the adsorption kinetic experiments are shown in appendix F. The points that seemed out of the trend were not included in the modelling. They are marked with red in the appendix. All calculations are presented in the excels sheet in appendix H.

Table 11 is an overview of the different kinetic experiments conducted

TABLE 11: Kinetic experiments conducted

	Compound	Water used	Weight carbon g	Volume solution mL
Experiment 1	TCC	GW and MQ	0.1	250
Experiment 2	TCC	GW and MQ	0.252 (equals 0.07g/250 mL)	900
Experiment 3	TCC	GW and MQ	0.18 (equals 0.05g/250 mL)	900
Experiment 4	DEP, DOC (GW)	GW and MQ	0.2 (equals to 0.1g/250 mL)	500

6.7 Adsorption isotherm experiment

For the isotherm experiments, an initial concentration of TCC and DEP of 20 µg/L and 5 mg/L, respectively, were chosen. Same concentrations were used for the mixture isotherm experiment. Both greywater and MQ water was used for each experiment. Reference samples were run for each set. The isotherm experiments were conducted as a batch test. 9-10 bottles with screw cap were filled with 250 mL (or 500 mL) solution and added different amounts of carbon (0.0007-0.1g). A volume of 500 mL was used on the smallest ratio of carbon and solution. This because it was difficult to measures the smallest carbon weights accurately when 250 mL volume was used. After addition of carbon, the bottles were mechanical stirred at 175 rpm until equilibrium was reached. The pH of greywater was adjusted to 6.5 and the temperature was ambient. Based on the kinetic results, a time of 10 hours was chosen for the TCC isotherms and a time of 27 hours was chosen for the DEP and mixture isotherms. TCC were filtered through a 0.7 GF filter and the samples containing only DEP were filtered through a 0.2 Teflon filter before analysis.

As for the kinetic experiments, DOC isotherm test was only conducted for greywater containing only DEP.

Table12 is an overview over the different isotherm experiments done.

TABLE 12: Isotherm experiments conducted

	Compound	Water used	Range carbon weight mg	Volume solution mL
Experiment 1	TCC	GW and MQ	2-100	6x250, 4x500
Experiment 2	DEP, DOC(GW)	GW and MQ	2-100	250
Experiment 3	TCC, DEP	GW and MQ	1-100	250

The amounts of matter adsorbed at time of equilibrium, was calculated according to equation 5-2. Langmuir and Freundlich isotherm models (linear and non-linear) were used to model the isotherm data and to find the adsorption parameters. The data was evaluated with regard to R^2 and normalized standard deviation Δq as decribed in section 5.6.3. The different isotherm models are explained in section 5.6. All calculations are given in the excel sheet in appendix H.

7. Results and discussion

7.1 Analytical method

7.1.1 Development of method

Selection of settings

The optimization of the TCC and DEP method were done by varying the composition of the mobile phase, the flow rate, and the injection volume to wanted retention times and peak characteristics were achieved. The selected methods were the ones that best fulfilled the following points:

- The TCC and DEP peaks did not collide with other compounds in the greywater
- The peak width was as narrow as possible
- The peak showed minimal of tailing effect
- The peak symmetry was as high as possible
- The lowest detectable concentration was 99% of initial concentration
- The injection volume was selected as low as the detection limit allowed

In general, the following relations between the parameters mentioned above and the detected peaks were observed:

- Increase in flow rate
  - Decrease of retention time and selectivity α for both compounds
  - Decrease of peak width for both compounds
  - Decrease of tailing factor and increased symmetry for both compounds
  - Decrease of area detected for TCC
- Increase in percentage acetonitrile
  - Decrease of retention time and selectivity α for both compounds
  - Decrease of peak width TCC
  - Decrease of area detected for TCC
- Increase in injection volume
  - Decrease of peak symmetry
  - Increase of tailing effect
  - Increase of total run time
  - Increase of area detected

The concentration range used for TCC was much smaller than the concentration range used for DEP. Therefore, a maximum injection volume of 900 µL was needed for TCC while a 450 µL could be used for DEP. A tailing effect on the TCC peak was observed for many of the different settings tested. This was probably due to the high injection volume. An increase in flow rate improved the problem, but still some tailing could be seen on the peaks, especially for the low concentrations. The influence of flow rate on the TCC peak area, peak width and symmetry is shown in figure 40. Acetonitrile was chosen as solvent for the mobile phase due to its low UV cut-off and high strength, which was needed for the TCC.

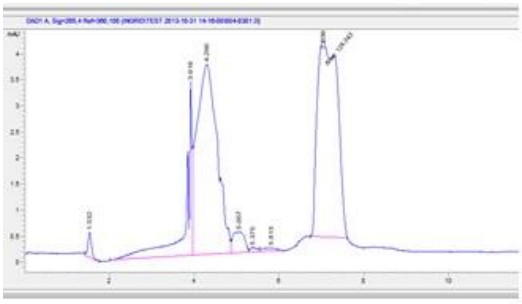

Acetontrile:water: 80:20
Flowrate: 1.0 mL/min
Area: 124.3
Peak width: 0.551
Symmetry : 0.435

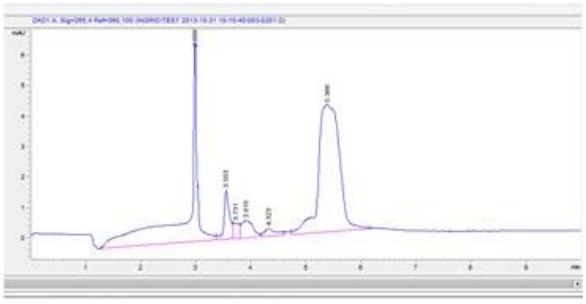

Acetontrile:water: 80:20
Flowrate: 1.3 mL/min
Area: 112.8
Peak width: 0.371
Symmetry : 0.732

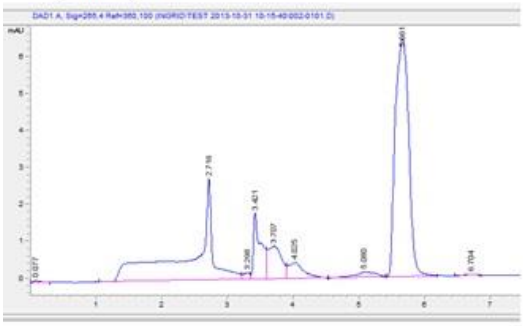

Acetontrile:water: 80:20
Flowrate: 1.4 mL/min
Area: 92.2
Peak width: 0.241
Symmetry : 1.056

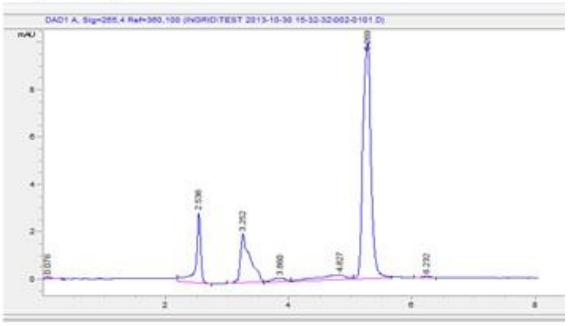

Acetontrile:water: 80:20
Flowrate: 1.5 mL/min
Area: 90.3
Peak width: 0.148
Symmetry : 1.066

FIGURE 40: Influence of flow rate on TCC peak

The retention time of DEP was shorter compared to the retention time of TCC. Since DEP is one of the short chained phthalate esters and have fewer carbon atoms than TCC, it is likely to be a more polar compound. As seen from the logKow values, it is also a less hydrophobic compound than TCC. This results in greater affinity to the mobile phase and shorter retention time. Therefore, the percentage of acetonitrile in the mobile phase was lowered to 60% for the detection of DEP. This resulted in a retention time of 5 min, similar to the retention time of TCC when 80% acetonitrile was used. The effects of mobile phase composition on DEP retention time and peak characteristics are shown in figure 41. As seen by the figure, the area is not much affected by the increase in percentage of acetonitrile. In general, it was harder to obtain a narrow peak for DEP than it was for TCC, even though the injection volume of DEP was half the size as the one used for TCC.

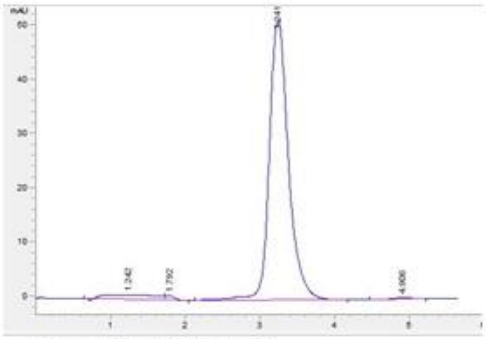

Acetontrile:Water 65:35
Flow rate: 2 mL/min
Area: 920
Peak symmetry: 0.81
Retention time: 324

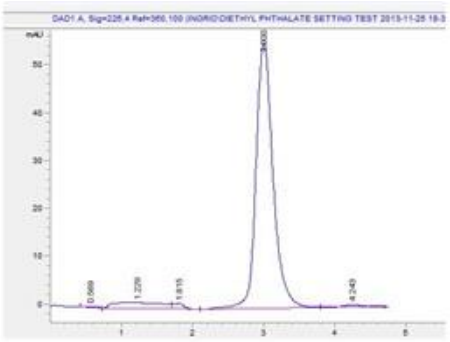

Acetontrile:Water 70:30
Flow rate: 2 mL/min
Area: 930
Peak symmetry: 0.81
Retention time: 3

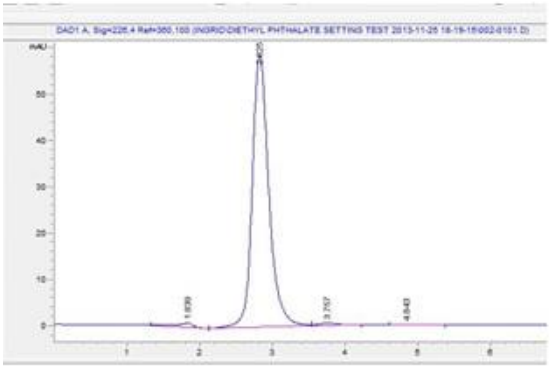

Acetontrile:Water 75:25
Flow rate: 2 mL/min
Area: 940
Peak symmetry: 0.78
Retention time: 2.8

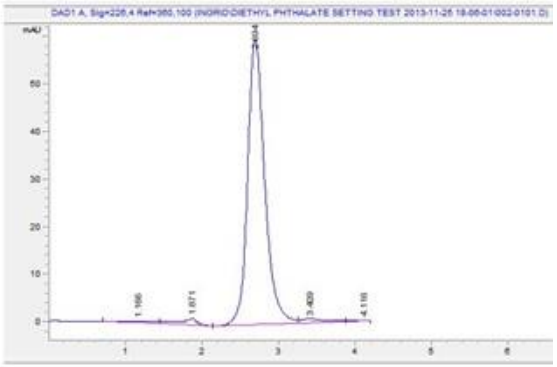

Acetontrile:Water 80:20
Flow rate: 2 mL/min
Area: 935
Peak symmetry: 0.45
Retention time: 2.7

FIGURE 41: Influence of mobile phase composition on DEP retention time

Importance of cleaning procedure

During the work with this thesis, it was experienced how important it is with a proper cleaning procedure and regularly maintenance of the HPLC system. After about two weeks of experiments, the HPLC autosampler got contaminated with TCC, which lead to a constant carry-over of TCC, even when blank samples were injected. It was probably caused by improper needle wash or wear on some of the autosampler parts or both. The problem was solved by changing the most exposed autosampler parts such as the needle and the needle seat (where injection is flushed trough). After this, more consideration was given to the cleaning procedure. The strength of the needle wash was increased and the system was flushed with 100 % acetonitrile under higher pressure (by increasing flowrate) than used before the contamination happened.

7.1.2 Calibration curve

The calibration curves obtained for TCC and DEP with the selected methods are shown in figure 42 and 43, respectively. The linear trend lines and their following equations are given in the figures (framed in blue). The trend lines have high R^2 values (≈1), which means the standard concentrations prepared correlated very well with the areas detected. The DEP line was forced through zero to avoid negative values for DEP concentration of areas under 1.17. This is not optimal, which is discussed later on. The equation that was forced through zero is framed in red. The intersection of the TCC line with the y-axis was very low and was considered to be insignificant.

The concentration of TCC and DEP according to the calibration curves, are given by the following equations:

$$C_{TCC} = \frac{A + 0.0435}{4.7507}$$ **EQUATION 7-1**

$$C_{DEP} = \frac{A}{518.01}$$ **EQUATION 7-2**

where A is the peak area (mAu) detected.

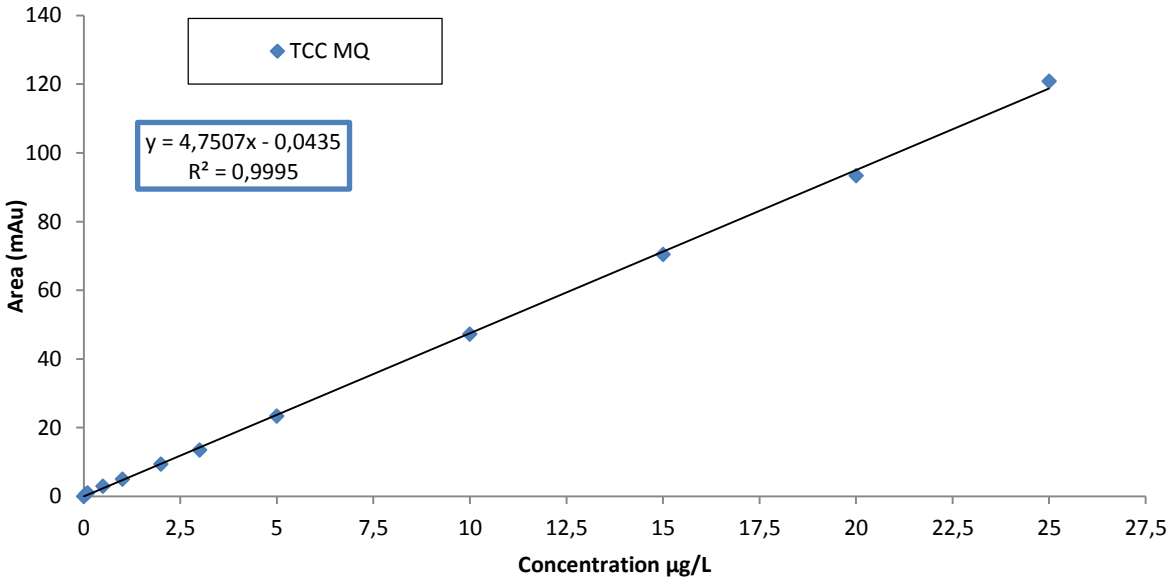

FIGURE 42: TCC calibration curve

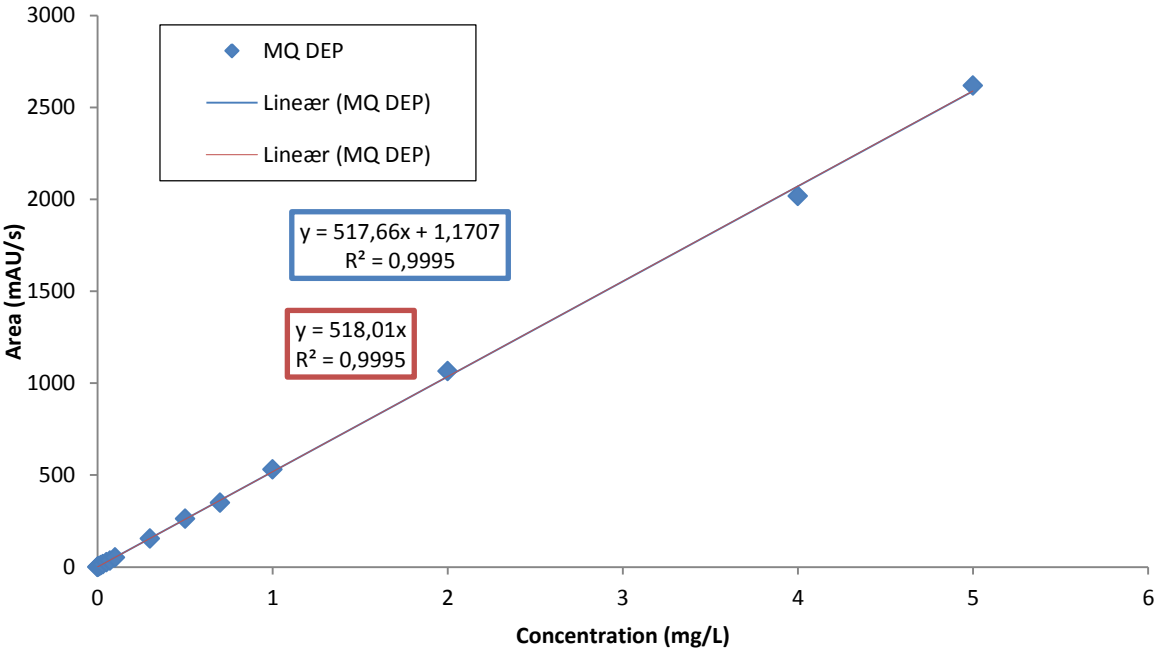

FIGURE 43: DEP calibration curve

7.1.3 Discussion of the analytical methods

The DEP calibration curve intersected with the y axis at 1.17, see figure 43. This might be an indication of background noise or interferences from the baseline, disturbance from other compounds or slightly errors in the concentrations prepared. Since the correlation factor was very close to unity, the interception was most likely caused by background noise or interference from other compounds. The wavelength of diethyl phthalate was set at 226 nm. The detection of low DEP concentration could have been interfered by the acetonitrile cut-off at 190 nm. At low concentrations of DEP, the baseline was crooked, as shown in figure 44. However, acetonitrile and the same detection wavelength were used by others literature. The disturbance may also have been caused by interfering compounds in the water, but this is strange since the UV cut-off of pure water is <190nm. A last possibility is that the HPLC system still had a small contamination of TCC stuck somewhere, even after the change of parts, which created noise on the baseline. One solution to the problem could have been to increase the injection volume of DEP and by this increasing the detection areas. Negative aspects to this solution, are the increased run time and consumption of acetonitrile. Also, worse peak shape is expected for higher injection volumes.

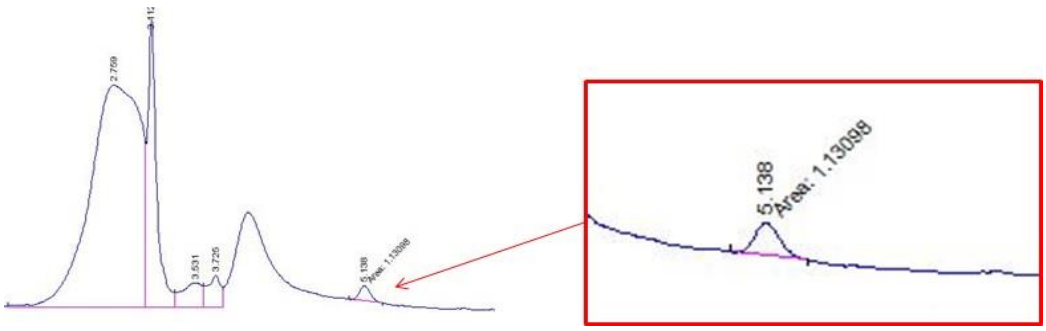

FIGURE 44: Crooked baseline of DEP detection in MQ water

The final peaks obtained in GW for the chosen methods are shown in figure 45 and 46. The retention factor k and selectivity α were obtained by assuming a dead volume time (t_0) of 1 min. The selectivity α was evaluated for the smallest amounts of TCC and DEP, since a potential interference will cause biggest error to the smallest areas. As seen in figure 46, the selectivity for TCC was less than 1.2. This might have caused errors to the lowest detected concentration of TCC in the adsorption experiments. The tailing effect on TCC is also illustrated on the figure. As already mentioned, this is most likely caused by the high injection volume. The selectivity of DEP in GW seems to be fine, with sufficient distance to the closest peaks.

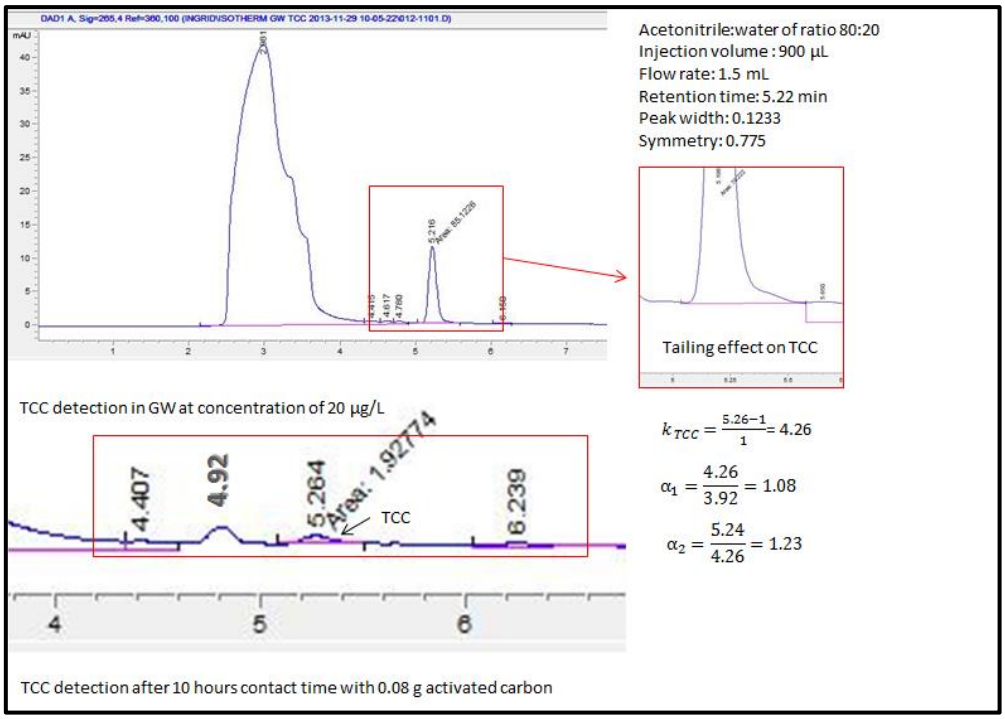

FIGURE 45: TCC peak obtained in GW

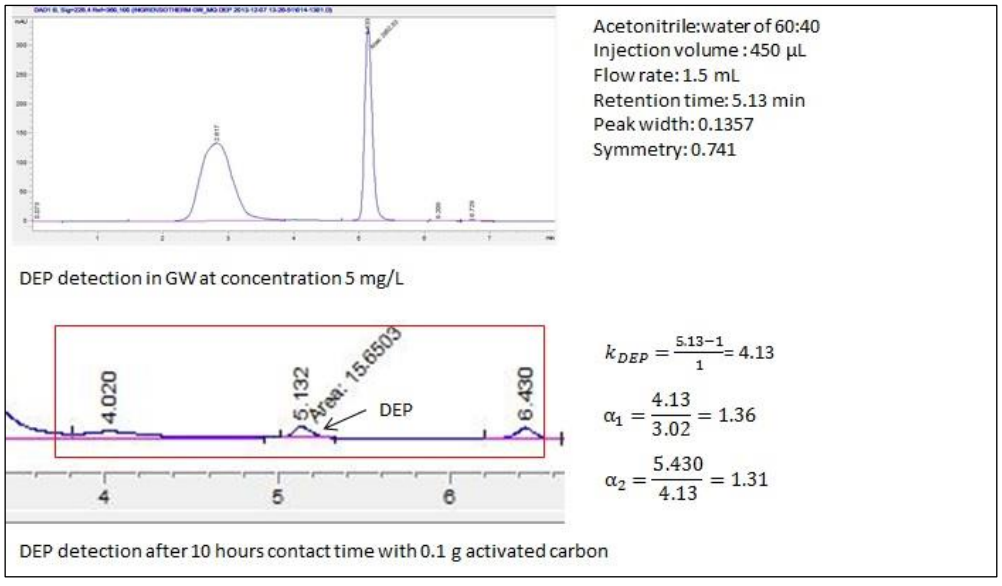

FIGURE 46: DEP peak obtained in GW

Because the compounds had different affinity to the stationary phase, the DEP and TCC in mixture caused no disturbance to the detection, as shown in figure 47. In fact, the figure shows that a method detecting the compounds simultaneously could have been developed. Then, new calibration curves would have to be created but the total run time and consumption of acetonitrile may have been decreased for the mixture experiments.

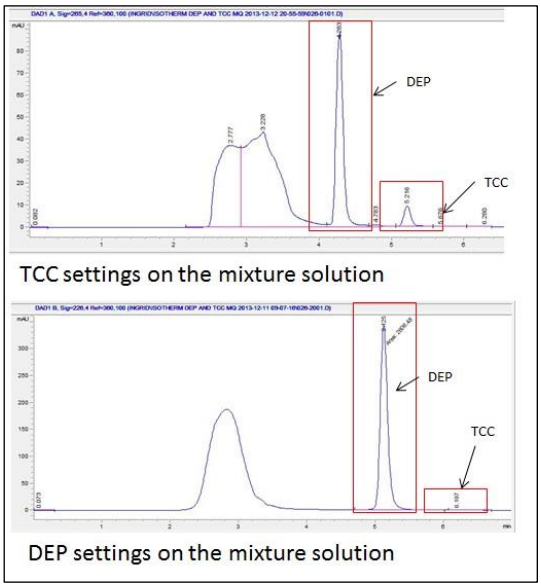

FIGURE 47: TCC and DEP peaks in the mixture solution

As discussed above, the drawbacks with the selected methods were potential disturbance in the low concentration range, and problems with tailing effect and asymmetry, which were most likely caused by the high injection volumes. Almost all of the methods described in literature had some kind of solid phase extraction before the analytical detection, and thus, injection volumes of only 10-20 µL. For future study on DEP and TCC, development of a suitable extraction and concentration method should be considered. This to decrease the injection volume, the consumption of organic solvents and to attain better peak shapes. However, it must be noted that the development of an SPE method is a complex procedure that also require time and resources. Another improvement to the methods could be to look into buffer addition and pH control of the mobile phase. No pH control was conducted during this work, and this might be something that could improve the efficiency of the column. At last, other columns with better selectivity towards DEP and TCC is something that should be investigated. Although, the C18 column has been regularly used by others to quantify and detect DEP and TCC.

Despite all of the mentioned, the methods selected were successful in detection of DEP and TCC in GW and could be used for the set purpose; to determine adsorption kinetics and isotherms for the two compounds.

7.2 Adsorption kinetic experiments

7.2.1 Triclocarban

Adsorption curves

The adsorption decay of TCC in MQ and GW for different amounts of activated carbon are shown in figure 48. The figure shows that after about 2 hours the adsorption rate of TCC slows down. After 6 hours, almost no further removal of TCC is seen, which means that the adsorption has reached equilibrium state. From the figure it seems the equilibrium time is not affected by the carbon dose. Also, it looks like a bit higher removal of TCC is obtained in GW compared to MQ (the curves of GW are below the curves of MQ). However, this may have been caused by some of the TCC reacting with compounds or solids in the GW, which decreased the initial concentration of TCC. This was the case for many of the experiments, where the initial concentration of TCC for the greywater reference sample was lower than the aimed concentration of 20 µg/L, see table 13. This could explain why the GW adsorption curves lies under the MQ adsorption curves, because lower equilibrium concentration is expected for lower initial concentration

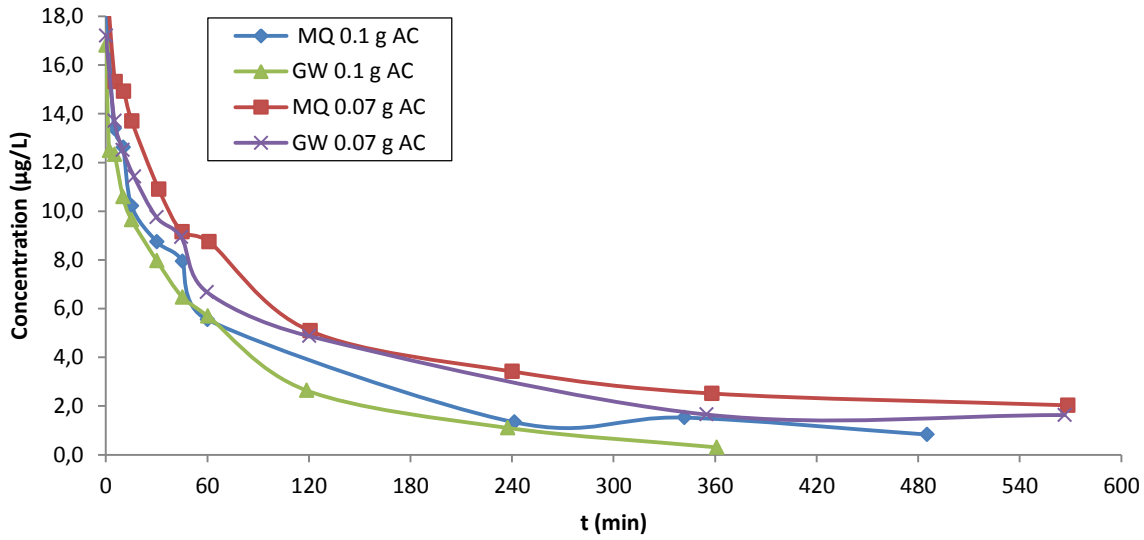

FIGURE 48: Adsorption decay of TCC in MQ and GW

TABLE 13: Achieved initial concentrations of TCC for adsorption kinetic experiments

Experiment	Ci, TCC µg/L
MQ TCC (0.1 g AC)	19.04
GW TCC (0.1 g AC)	16.81
MQ TCC(0.07 g AC)	19.84
GW TCC (0.07 g AC)	17,21

Adsorption kinetics

The kinetic results of TCC adsorption onto F400 are summarized in table 14. The plots of the pseudo equations and the elovich equation are shown in figure 49, 50 and 51, respectively. The pseudo first order equation showed the worst fit with the lowest R^2 values and the highest Δq of 35.1%. It showed suitable for the first 60 minutes of adsorption, which agrees with theory. Both the pseudo second order equation and elovich equation satisfactorily fitted the experimental data with high R^2 values (>0.97) and low Δq of 5.2% and 4.15%, respectively. The pseudo second order equation generated the best fit with estimated equilibrium adsorption capacities close to the experimental equilibrium adsorption capacities. Figure 52 is a plot of the experimental data (seen as points) versus the values obtained with the pseudo second order rate constants and elovich rate constants as a function of time (shown as stippled lines). The figure verifies that pseudo second order equation is the best fit for TCC adsorption onto carbon F400. The elovich model generates good fits in the beginning of the adsorption process but diverges as equilibrium approaches.

As indicated by the concentration decay of TCC seen in figure 48, the rate constant k_2 (min^{-1}) is slightly higher in GW than in MQ water. According to the pseudo second order rate equation , the adsorption may be classified as follows: k_2(MQ TCC 0.07g)<k_2(GW TCC 0.07 g)< k_2(MQ 0.1 g)< k_2 (GW 0.1g). However, the adsorption capacity was higher in MQ than in GW for both instances. This might be caused by the present of other dissolved organic compound in the greywater that takes up adsorption sites. However, the difference is not significant enough to state that higher removal efficiencies could be achieved in neither the one nor the other instances. Also, it seems the adsorption capacity of the carbon increases slightly with decrease of amount of carbon added.

TABLE 14: Adsorption kineticsTCC

		Pseudo 1'			Pseudo 2'			Elovich			
Experiment	**qe,exp**	**qe,calc**	**k_1**	**R^2**	**qe,calc**	**k_2**	**R^2**	**qe,calc**	**a**	**b**	**R^2**
	µg/mg	µg/mg	min^{-1}	%	µg/mg	mg/µg min^{-1}	%	µg/mg			%
MQ TCC (0.1 g AC)	0,046	0,029	0.0100	0.908	0,047	0,995	0.999	0.045	0.522	135.1	0.980
GW TCC (0.1 g AC)	0,041	0,032	0.0138	0.980	0,043	1,098	0.999	0.040	0.572	159.7	0.967
MQ TCC (0.07 g AC)	0,064	0,047	0.0095	0.978	0,067	0.474	0.999	0.061	0.384	86.2	0.982
GW TCC (0.07 g AC)	0,056	0,040	0.0105	0.944	0,057	0.644	1.000	0.053	0.333	99.0	0.982
			Δq (%)	35.1		Δq (%)	5.23			Δq (%)	4.15

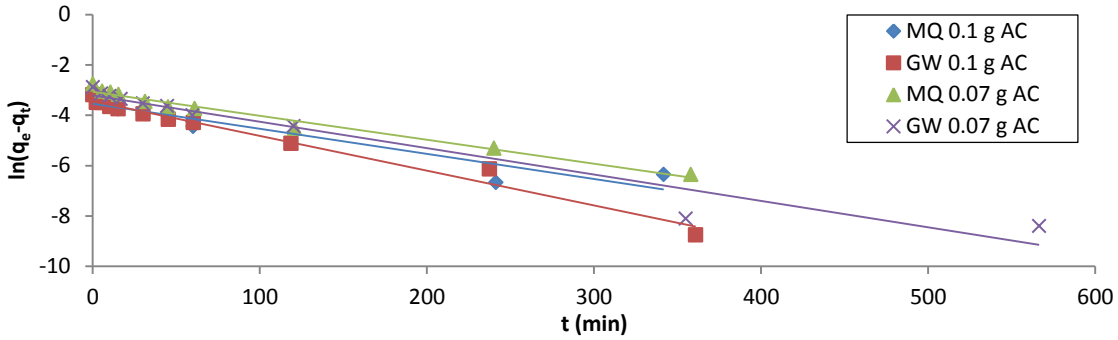

FIGURE 49: TCC pseudo first order rate equation

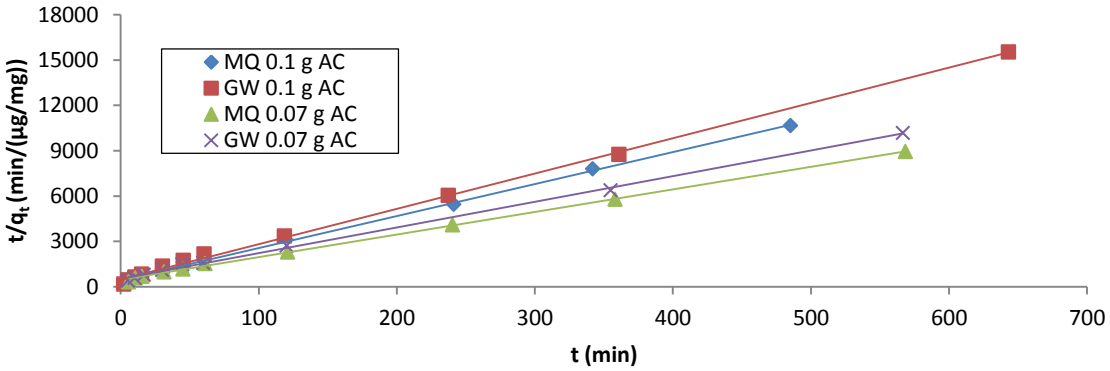

FIGURE 50: TCC pseudo second order rate equation

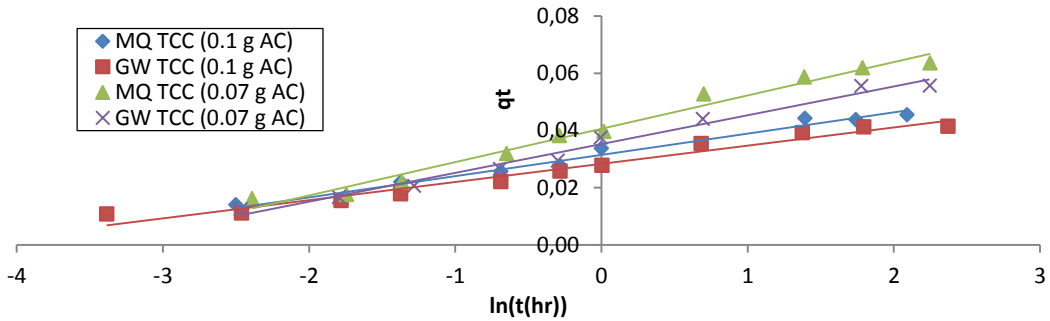

FIGURE 51: TCC Elovich equation

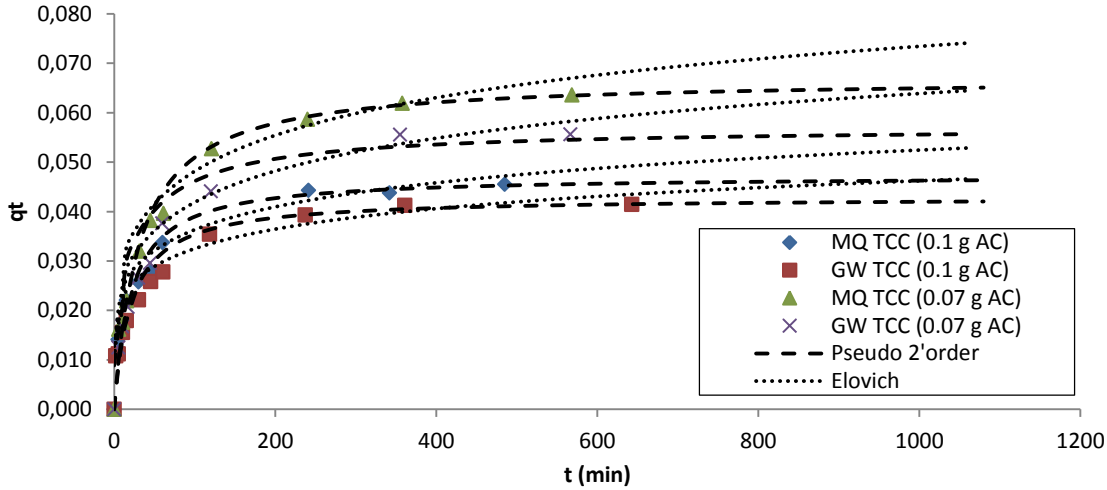

FIGURE 52: Fit of pseudo second order rate equation and Elovich equation to the experimental data of TCC

Adsorption mechanisms

The intraparticle diffusional models of Weber-Morris and Drumwald Wagner were used as an attempt to describe the rate limiting steps of the adsorption process. External adsorption was considered to be neglectable, since it was no instantaneous drop of concentration in the beginning of the adsorption process. Three diffusion stages were identified, as shown in figure 53. The obtained values for k_{int}, C, and R^2 are shown in table 15. In the first stage, intraparticle diffusion was designated to be the rate limiting mechanism as shown by close intersection with the origin (C_1<0.004) and high R^2 values. As the adsorption progresses, the diffusional mechanisms are slowed down due to the decreasing concentration of TCC in the aqueous phase. At stage three, the diffusion is decreased to a minimum rate, due to the extreme low concentration of TCC in the water surrounding. Referring to the figure, it seems that stage three is transferred a bit to the left for increasing ratio of initial solute concentration to added amount of carbon. For the MQ samples with 0.07 g added carbon (highest ratio of solute concentration to added amount of carbon), the last stage is not reached. A reason for this could be that it is the lack of adsorption sites that limit the adsorption process and not the diffusion mechanisms.

The second and third diffusion line of the Weber-Morris plot does not pass through the origin. This might be caused by differences in the mass transfer actions. It indicates that the sorption of TCC is a complex process that involves mechanisms of film diffusion and intraparticle diffusion simultaneously. The Drumwald-Wagner model showed good linearity for the whole adsorption process and close passing through the origin. This might indicates that intraparticel diffusion is in fact the rate dominating mechanism, but that other diffusion processes occurs as well.

TABLE 15: Summary of TCC sorption data evaluated by different intraparticle diffusion models

Weber- Morris		**Stage 1**			**Stage 2**			**Stage 3**		
Experiment	**Ci TCC**	**$k_{int,1}$** µg/mgxmin$^{-1/2}$	**C_1** µg/mg	**R^2**	**$k_{int,2}$**	**C_2**	**R^2**	**$k_{int,3}$**	**C_3**	**R^2**
MQ(0.1 g AC)	19.04	0,004	0,0030	0,958	0,0014	0,023	1,000	0,00020	0,041	0,547
GW (0.1 g AC)	16.81	0,0033	0,0036	0,957	0,0015	0,018	0,917	0,00020	0,037	0,665
MQ(0.07 g AC)	19.84	0,0048	0,0031	0,981	0,0008	0,045	0,924	-	-	-
GW (0.07 g AC)	17,2	0,0046	0,0013	0,989	0,0016	0,026	0,994	0,00005	0,055	1,000
Drumwald -Wagner										
Experiment		**K** min^{-1}	**C**	**R^2**						
MQ(0.1 g AC)		0,0017	0,0556	0,921						
GW (0.1 g AC)		0,0023	0,0232	0,972						
MQ(0.07 g AC)		0,0015	0,0134	0,996						
GW (0.07 g AC)		0,0018	0,0098	0,946						

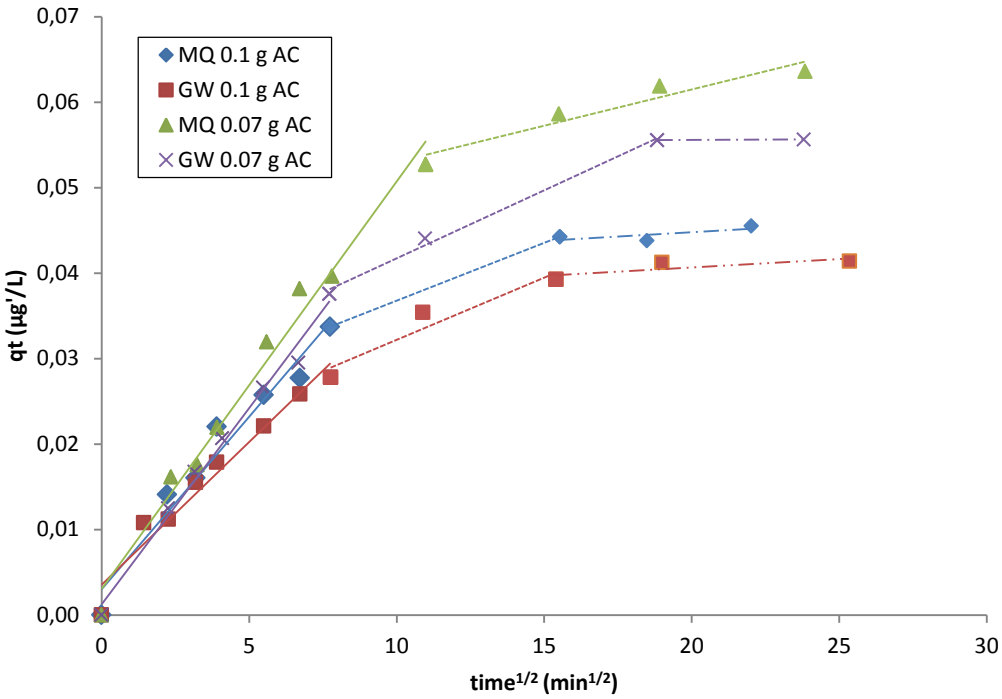

FIGURE 53: Multilinear intraparticle diffusion model of Weber-Morris applied to TCC adsorption

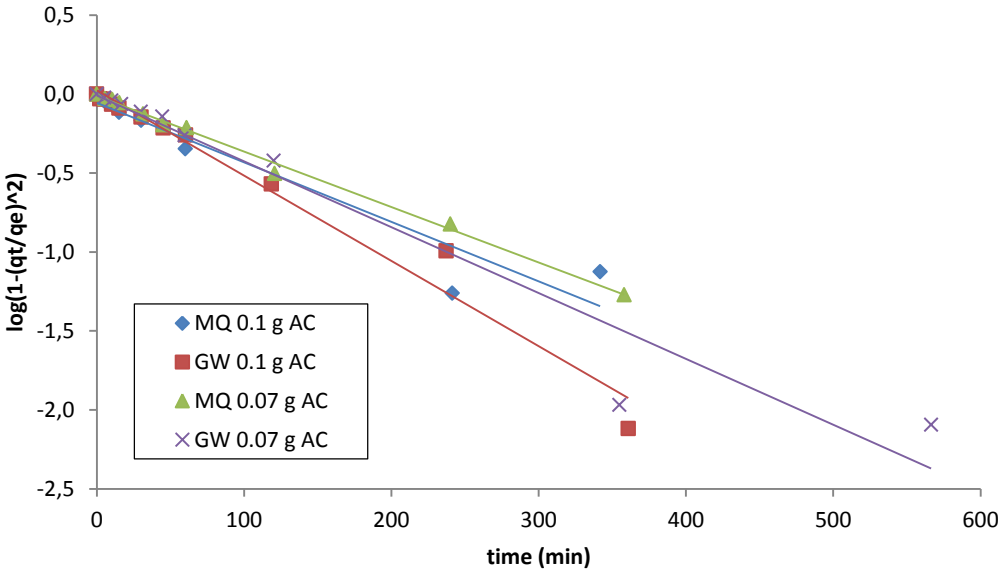

FIGURE 54: Intraparticle diffusion model of Drumwald-Wagner applied to TCC adsorption

7.2.2 Diethyl Phthalate and dissolved organic carbon

Adsorption curves

The adsorption decays of DEP in GW and MQ water for 0.1 g added carbon are shown in figure 55. The adsorption of the dissolved organic carbon in the GW is also shown on the figure. A closer look on the adsorption decay of DEP in the last time period is shown in figure 56. The figure shows that after about 6 hours (360 min) the adsorption rate of DEP begins to decrease. After 24 hours, the equilibrium state is reached and almost no further removal of DEP is seen. The curve indicates that the adsorption decay in MQ is a little bit faster than the one experienced in GW. Also, the curve implements that higher removal of DEP is expected compared to the DOC in the GW. The concentration of DOC was almost twice as high as DEP, thus, longer contact time is needed to achieve high removal efficiencies. By observing figure 55, it doesn't seem like the equilibrium has been reached for the DOC in the GW. The equilibrium time required for DEP is much higher than for TCC. It has already been shown that the adsorption rate of DEP onto activated carbon decreases with increasing initial concentration (Venkata Mohan et al., 2007). The initial concentration of DEP is 250 times the initial concentration of TCC. Thus, it is logical that longer contact time is required for the DEP molecules to diffuse into the activated carbon pores. Another reason for the longer equilibrium time could be that DEP is less hydrophobic, more water soluble, and more polar than TCC, and therefore, possess larger affinity to the water phase.

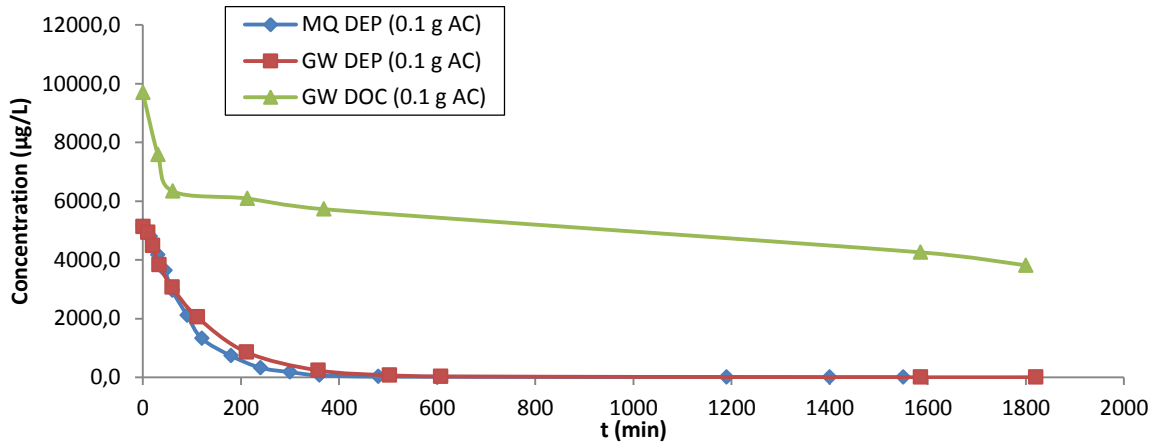

FIGURE 55: Concentration decay of DEP and DOC over time by addition of 0.1 g AC

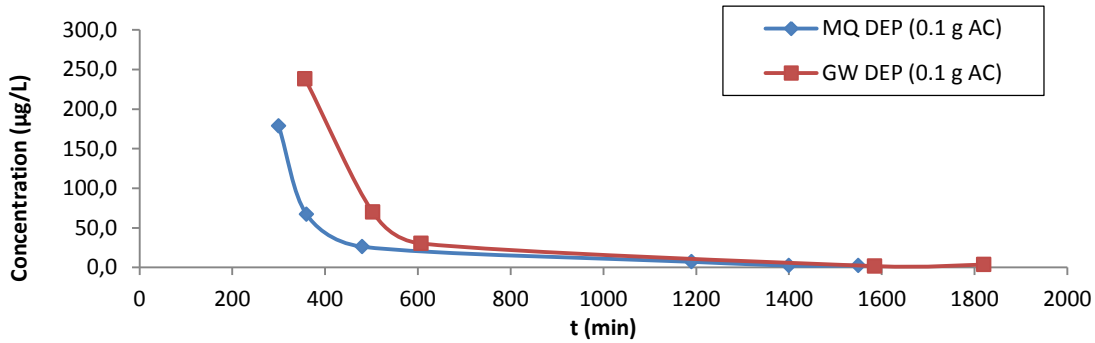

FIGURE 56: Closer look at sorption decay of DEP in MQ and GW over time

Adsorption kinetics

The kinetic results of DEP adsorption onto F400 are summarized in table 16. The plots of the pseudo equations and the elovich equation are shown in figure 57, 58 and 59, respectively. The pseudo first order equation showed the worst fit to the data, with lowest R^2 values and a very high Δq of 47 %. It seems this model is not suitable in predicting the sorption of DEP onto F400. The pseudo second order equation generated the best fit of the three models tested, seen by the highest R^2 values (>0.98) and the lowest Δq of 7.54%. The predicted equilibrium adsorption capacities by the pseudo order rate model, correlated well with the experimental adsorption capacities obtained. The elovich model was the next best fit with R^2 values around 0.9 and a Δq of 17%. Figure 52 is a plot of the experimental data (seen as points) versus the values obtained with the pseudo second rate equation (shown as stippled lines). Referring to the figure, it appears that the pseudo second order model is a good fit, but that it has some anomalous shape around the point where the adsorption capacity is decreasing. It seems the predicted rate constants are too low at this point, and that the equilibrium adsorption capacities should have been higher than what was found. The selected agitation time might not have been sufficient enough for equilibrium to be reached or analytical error in the lowest concentration range has led to too high detected values

Also for DEP, the rate constant k_2 is slightly higher in GW than in MQ water. According to the pseudo second order rate equation, the adsorption may be classified as follows: k_2(MQ DOC)<k_2(MQ DEP)< k_2(GW DEP). However, by looking at figure 60, it seems the k_2 value in MQ should have been higher than in GW. This fits better with the fact that GW contains other organic compounds that compete for adsorption sites. But even though the calculated k values are a bit wrong, just by looking at the experimental data, it doesn't seem like the present of other organic compounds have a great impact on the sorption of DEP.

TABLE 16: Summary of adsorption kinetics of DEP and DOC

			Pseudo 1'			Pseudo 2'			Elovich		
Experiment	**qe,exp**	**qe,calc**	**k_1**	**R^2**	**qe,calc**	**k_2**	**R^2**	**qe,calc**	**a**	**b**	**R^2**
	µg/mg	µg/mg	(mg/µg) min^{-1}		µg/mg	mg/µg min^{-1}		µg/mg			
MQ DEP (0.1 g AC)	12.873	9,563	0.0087	0.976	13,947	0.00076	0.987	15,20	23.11	0.343	0.887
GW DEP (0.1 g AC)	12.813	6,522	0.0049	0.904	13,624	0.00090	0.995	14,68	20.27	0.348	0.914
GW DOC (0.0 g AC)	14.698	9,150	0.0014	0.904	14,933	0.00063	0.993	13,69	65.47	0.492	0.942
			Δq (%)	47.41		Δq (%)	7.54			Δq (%)	17.12

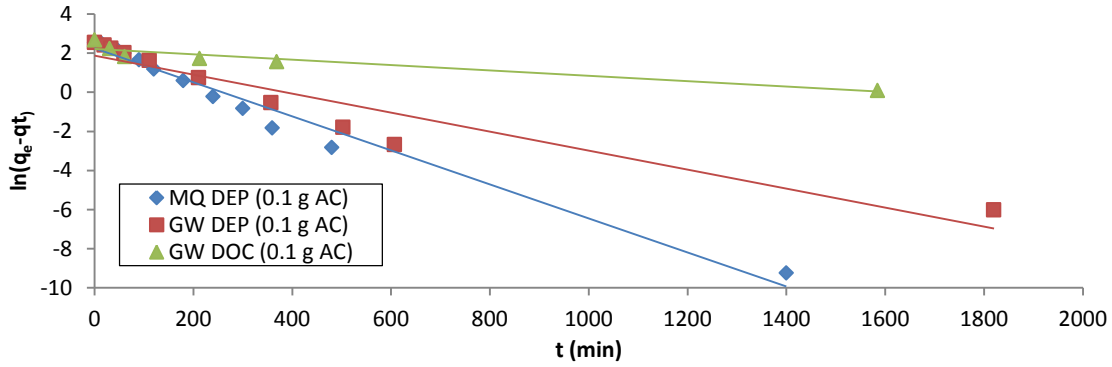

FIGURE 57: DEP pseudo first order equation

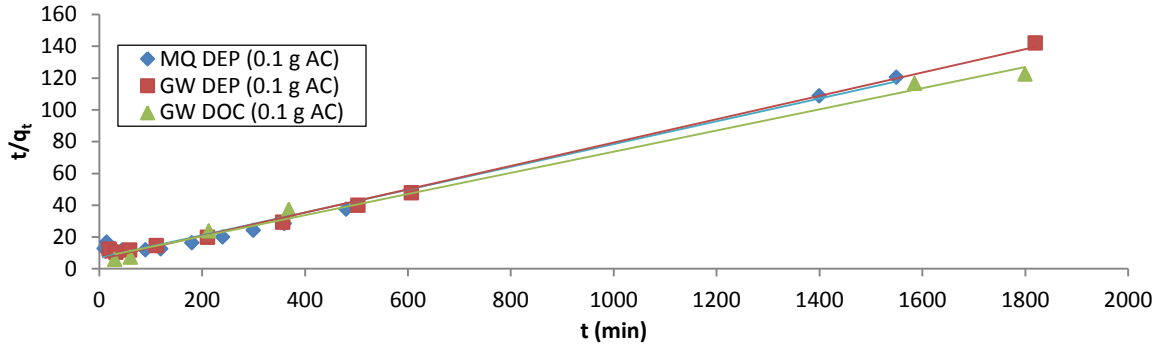

FIGURE 58: DEP pseudo second order equation

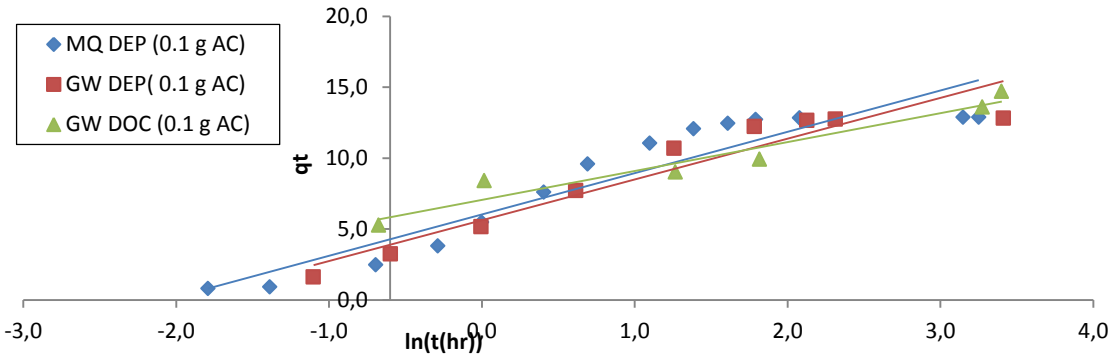

FIGURE 59: DEP Elovich equation

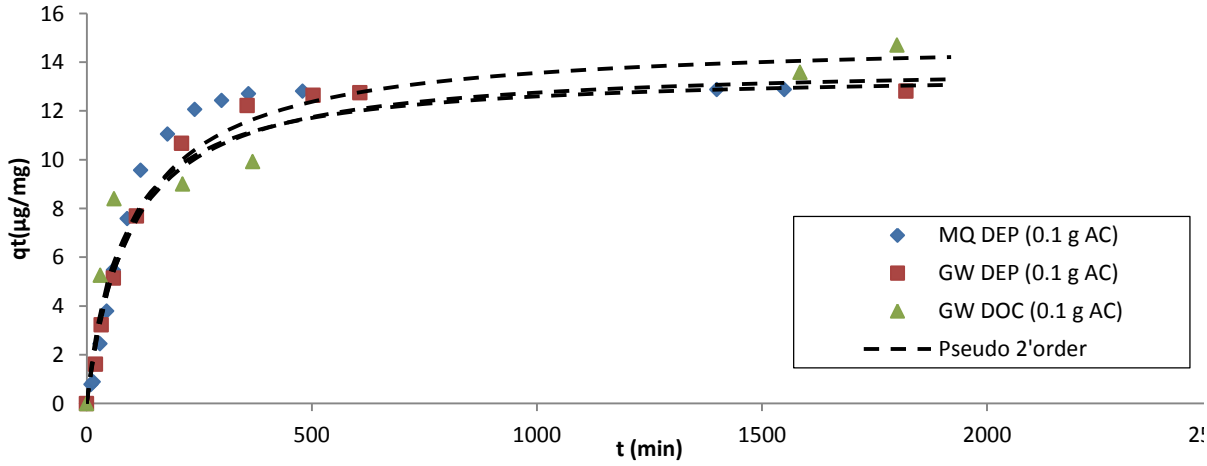

FIGURE 60: Fit of pseudo second order equation to DEP experimental data

Adsorption mechanisms

The intraparticle diffusional models of Weber-Morris and Drumwald-Wagner were used as an attempt to describe the rate limiting steps for sorption of DEP and DOC onto F400. Also for DEP, the external adsorption was considered to be not important. For adsorption of DOC it might seems as external adsorption leads to an instant drop of concentration in the beginning of the adsorption process. Three diffusion stages were identified, as shown in figure 53. The obtained values for ki_{nt}, C, and R^2 are shown in table 17. The Weber-Morris model did not fitted very well with the sorption of DEP. The lines of the first stage intersect the y-axis at negative values. The Weber-Morris model fits better to the sorption of DOC, with closer passing through the origin and a high correlation factor of 0.97. The results from the Drumwald Wagner model showed better fit with the DEP data and might indicate that intraparticle diffusion is the rate limiting mechanism. However, it is more likely that the diffusion process of DEP is a complex process that involves both film diffusion and intraparticle diffusion.

TABLE 17: Summary of the DEP sorption data fitted to the intraparticle diffusion models

Weber-Morris	**Stage 1**			**Stage 2**			**Stage 3**		
Experiment	**$k_{int,1}$** µg/mgxmin$^{-1/2}$	**C_1** µg/mg	R^2	$k_{int,2}$	C_2	R^2	$k_{int,3}$	C_3	R^2
MQ(0.1 g AC)	0,9434	1,7510	0,947	0,1986	8,754	0,819	0,00380	12,729	1,000
GW (0.1 g AC)	0,7778	0,8495	0,974	0,205	7,946	0,891	0,00370	12,652	1,000
GW DOC (0.1 g AC)	1,0525	0,1244	0,992	0,182	6,615	0,986	-	-	-
Drumwald- Wagner									
	K min^{-1}	**C**	R^2						
MQ(0.1 g AC)	0,0036	0,0111	0,986						
GW (0.1 g AC)	0,0020	0,1452	0,924						
GW DOC (0.1 g AC)	0,0005	0,0724	0,974						

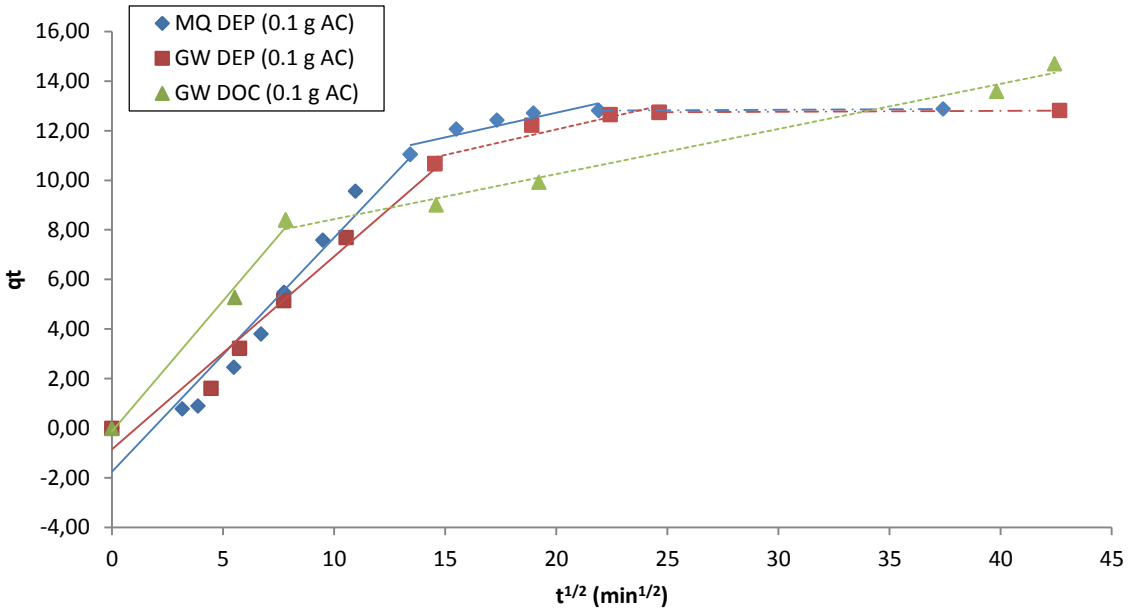

FIGURE 61: The multilinear intraparticle diffusion model of Weber-Morris on the sorption of DEP and DOC

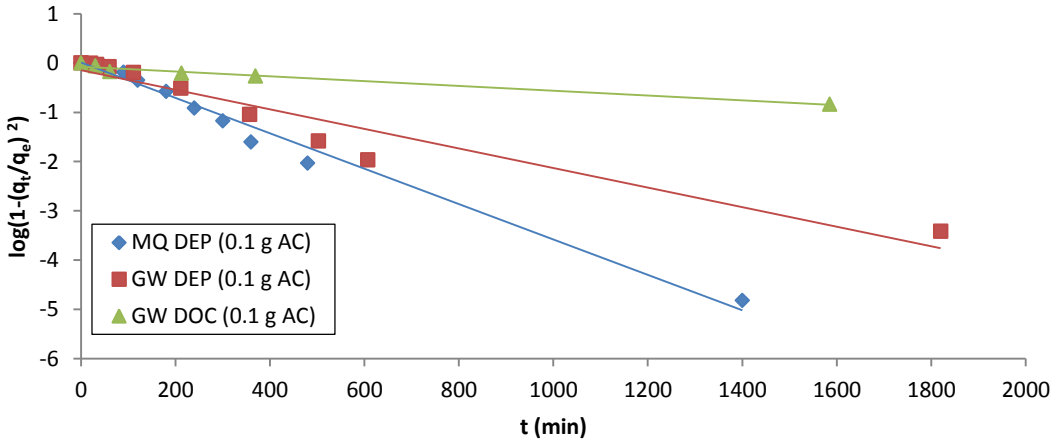

FIGURE 62: The intraparticle diffusion model of Drumwald-Wagner applied to the sorption data of DEP and DOC

7.2.3 Comparison DEP and TCC kinetics

The adsorption rate constants of DEP and DOC are much smaller than the ones found for TCC. This supports that TCC probably possess much greater affinity to the activated carbon surface compared to DEP due to its high hydrophobicity and very low water solubility. The initial concentration of DEP was much higher than the one of TCC and this might have contributed to the need of longer equilibrium time. For both DEP and TCC it seems like the sorption rates are not much affected by the present of other organic compounds in the GW. The sorption rates obtained for MQ and GW did differ much for neither TCC nor DEP. High removal efficiencies appears to be achieved for both compounds.

7.3 Adsorption isotherms

7.3.1 Triclocarban

The linear and non- linear form of the Langmuir and Freundlich equations were used to model the isotherm data of TCC. The linear plots of the Langmuir and Freundlich model are presented in figure 63 and 64. A summary of the results is shown in table 17. The results varied some between the different experiments conducted and it is not a significant difference between the Langmuir and Freundlich model. Based on the average obtained R^2 and Δq value, the Langmuir non-linear model seems to generate the best fit with the experimental data. However, it is difficult to say if the adsorption is monolayered (the energy is the same for each adsorption site) or multilayered (the energy differ between the adsorption sites), since good fits also are obtained by the Freundlich model. Figure 65 shows the plot of experimental and calculated equilibrium adsorption isotherm model of TCC onto F400. As seen by the figure the Freundlich non-linear and linear model don't differ much, while a distinct difference is seen between the non-linear and linear Langmuir model. The reason for this is not known, but it is obvious that the non-linear Langmuir approach better fits the experimental data.

According to the Langmuir model and the R_L values, the adsorption of TCC is considered as favorable (<1). The values indicate that the adsorption is more favorable in MQ compared to GW, but only slightly. The maximum adsorption capacity Q_0 is slightly higher in GW than in MQ. As for the adsorption kinetics, this is probably caused by the lower initial concentration of TCC in GW. It appears like the adsorption capacity increases for decreasing initial concentration of TCC. More experiments have to be done to state this. No significant difference is observed for the TCC alone and the TCC in mixture with DEP. It does not appear that TCC and DEP have the same mode of action when it comes to adsorption or if this is the case, the TCC molecules outdistance the DEP molecules for adsorption sites. Otherwise, the much higher initial concentration of DEP would have affected the adsorption efficiency of TCC.

TABLE 18: Summary of TCC isotherm data onto F400 by using linear and non-linear Langmuir and Freundlich model

Linear	**Langmuir**					**Freundlich**			
Experiment	**Q_0** µg/mg	**K_L** L/µg	**R_L**	**R^2**	**Δq** %	**K_F** (µg/mg)x $(L/mg)^{1/n}$	**n**	**R^2**	**Δq** %
MQ TCC (alone)	0,548	0,1880	0,224	0,924	17,10	0,08	1,563	0,941	19.92
GW TCC (alone)	1,051	0,1337	0,310	0,972	16,17	0,11	1,382	0,980	13.86
MQ TCC(mixture)	2,098	0,0786	0,409	0,905	45,16	0,17	1,491	0,909	23.12
GW TCC (mixture)	2,811	0,0558	0,554	0,824	34,24	0,14	1,368	0,916	31.22
Average R^2 and Δq				0.906	28.17			0.936	22.03
Non Linear	**Langmuir**					**Freundlich**			
Experiment	**Q_0** µg/mg	**K_L** L/µg	**R_L**	**R^2**	**Δq** %	**K_F** µg/mg)x $(L/mg)^{1/n}$	**n**	**R^2**	**Δq** %
MQ TCC (alone)	0,564	0,1820	0,229	0,959	17,24	0,10	1,826	0,935	29.59
GW TCC (alone)	1,401	0,0740	0,448	0,987	22,90	0,12	1,400	0,987	14.82
MQ TCC(mixure)	1,093	0,1914	0,221	0,926	22,35	0,18	1,659	0,930	27.85
GW TCC (mixture)	1,200	0,1400	0,331	0,933	30,53	0,15	1,426	0,949	33.24
Average R^2 and Δq				0.951	23.26			0.950	26.37

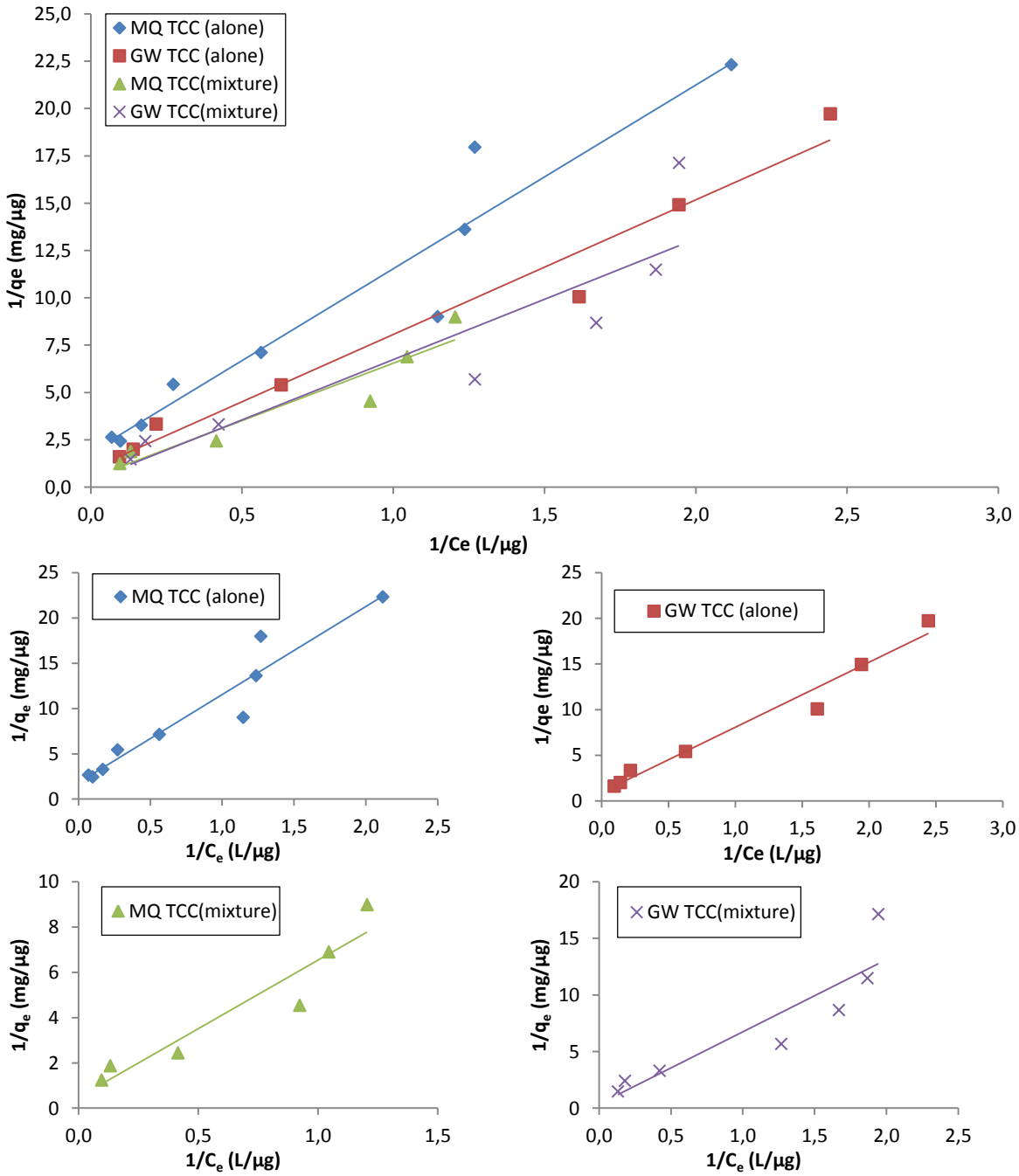

FIGURE 63: Equilibrium adsorption isotherms of TCC onto F400 fitted to the linear Langmuir model

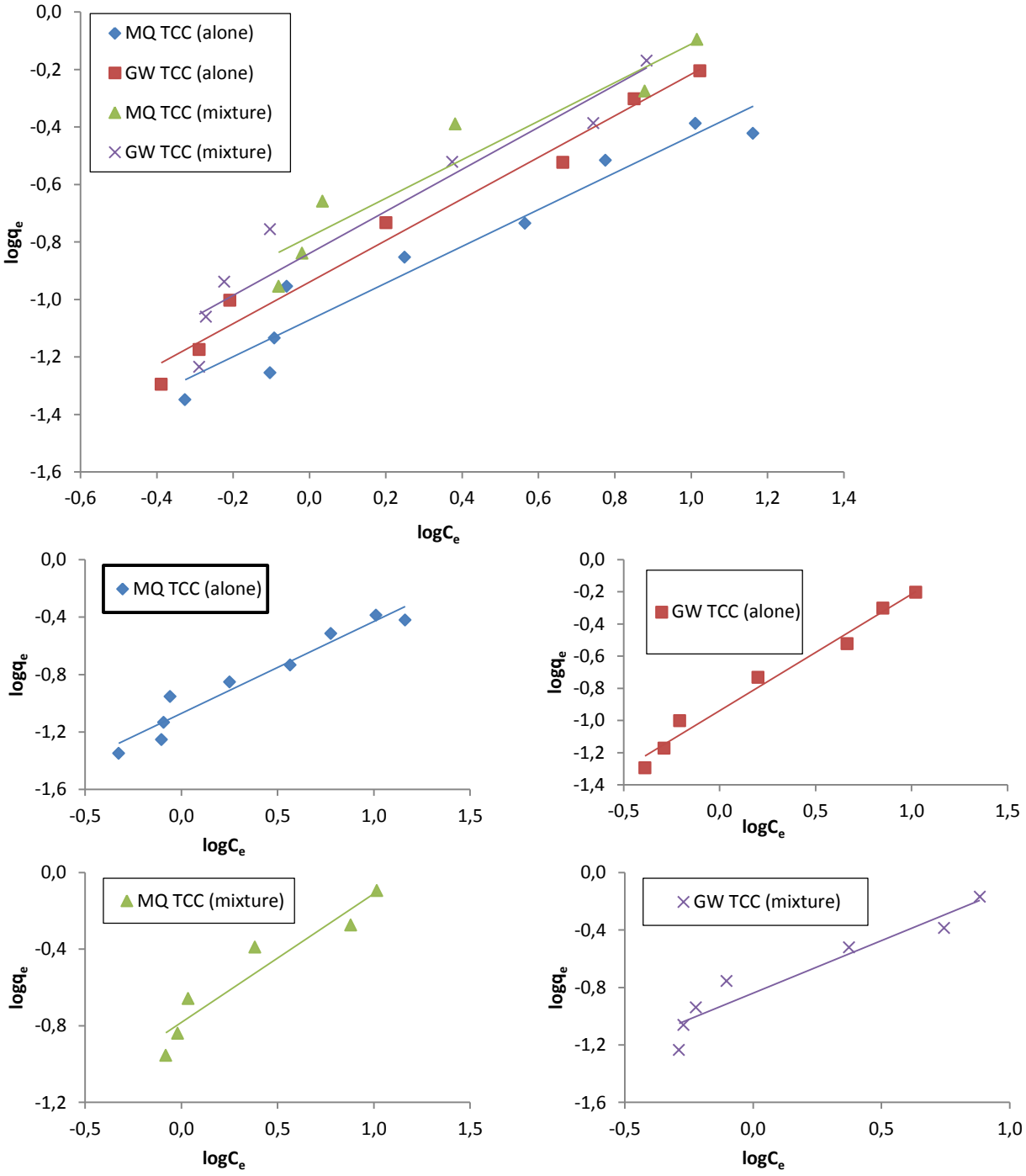

FIGURE 64: Equilibrium adsorption isotherms of TCC onto F400 fitted to the linear Freundlich model

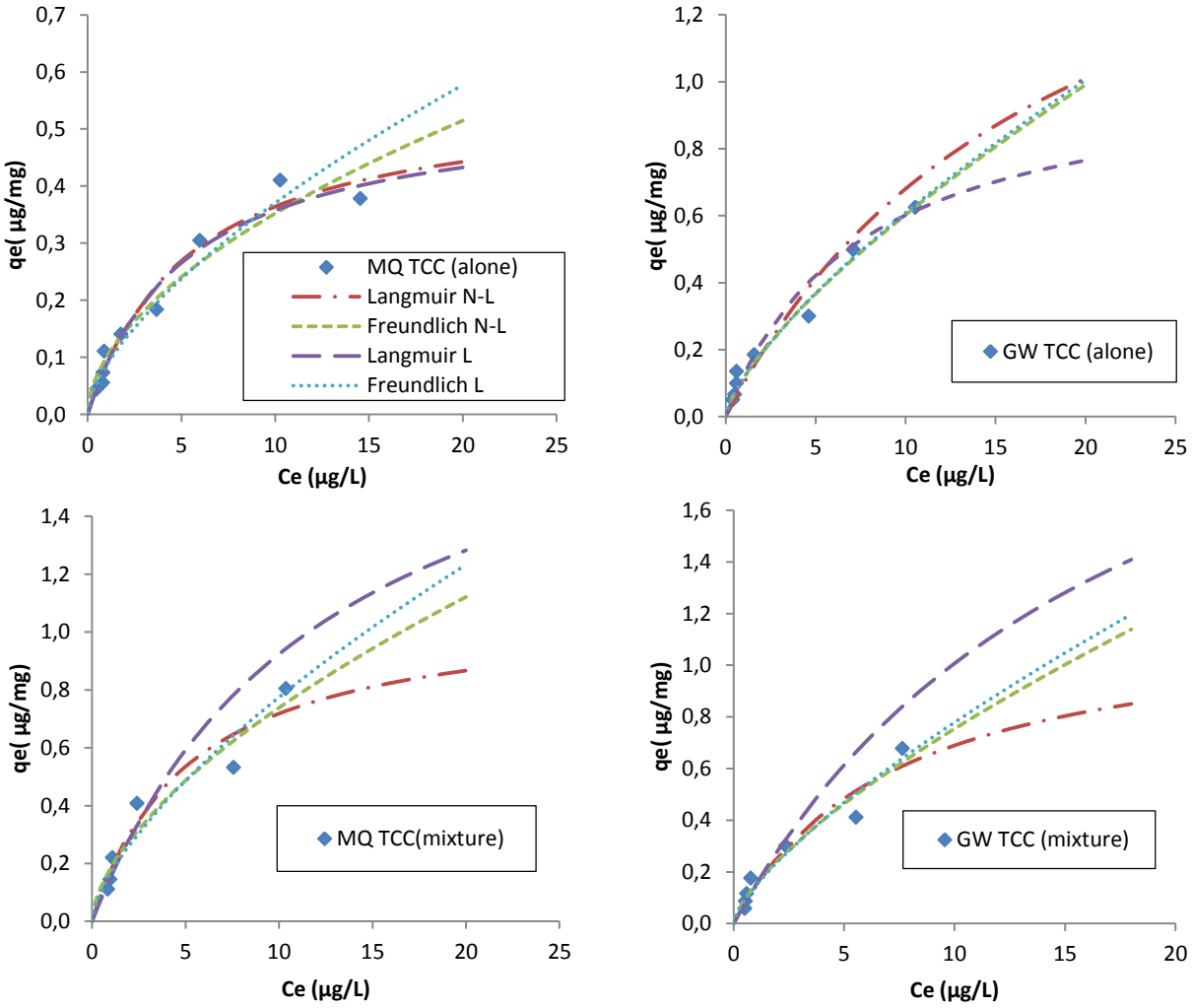

FIGURE 65: Experimental and calculated equilibrium adsorption isotherms (N-L =non linear, L=linear)

7.3.2 Diethyl Phthalate

The linear and non- linear form of the Langmuir and Freundlich equations were used to model the equilibrium adsorption isotherms of DEP onto F400. The linear plots of the Langmuir and Freundlich model are illustrated in figure 66 and 67. A summary of the results is shown in table 17. The results show that the adsorption of DEP onto F400 is best fitted with the Freundlich model. This differs from other literature that found DEP equilibrium adsorption isotherms to be of Langmuir type (Venkata Mohan et al., 2007, Medellin-Castillo et al., 2013, de Oliveira et al., 2012). Both the linear and non-linear Freundlich model generates good fits with the experimental data with R^2 values larger than 0.97 and Δq values of 10.6 and 12.7%, respectively. The linear Freundlich model was the best out of the two approaches. The experimental and calculated adsorption isotherms are plotted and shown in figure 68. By looking at the figure, it is obvious that the experimental values are best fitted with the Freundlich model and that the Langmuir model seems less suitable in describing the equilibrium process of DEP.

The Freundlich model indicates that the adsorption is multilayered and the adsorption is heterogeneous. The closer the slope of the linear equation is to 0, which is given by 1/n, the more heterogeneous the system is. The slope of the Freundlich DEP equation varies from 0.23-0.30 indicating a high heterogeneity of the DEP sorption onto F400.

In the Freundlich model, the K_F constant is a measure on the adsorption capacity and intensity of sorption. According to the linear K_F constants, the adsorption of DEP can be categorized as follows: K_F(GW DEP(mix))<K_F(MQ DEP(mix))<K_F(GW DEP(alone))<K_F(MQ DEP(alone). The result indicates that the adsorption capacity of DEP is affected by both the present of DOC in the greywater and the TCC in the mixture solutions. In the conducted experiments, the initial concentration of TCC was 250 times less than the one of DEP. If the initial concentration of DEP had been decreased to the same level as TCC, a clearer picture on the competition between them could have been obtained.

TABLE 19: Summary of DEP isotherm data onto F400 by using linear and non-linear Langmuir and Freundlich model

Linear	**Langmuir**					**Freundlich**			
Experiment	**Q_0**	**K_L**	**R_l**	**R^2**	**Δq**	**K_F**	**n**	**R^2**	**Δq**
	µg/mg	L/µg			%	(µg/mg)x (L/mg)$^{1/n}$			%
MQ DEP (alone)	59,524	0,2283	0,00085	0,909	28,66	16,58	4,348	0.981	9,61
GW DEP (alone)	40,816	0,2094	0,00093	0,779	35,2	11,04	4,214	0.996	4,5
MQ DEP (mixture)	84,746	0,0568	0,00345	0,942	34,9	11,78	3,339	0.979	12,68
GW DEP (mixture)	64,103	0,0419	0,00472	0,893	35,14	8,62	3,317	0.958	15,48
Average R^2 and Δq				0.881	33.48			0.978	10.57
Non Linear	**Langmuir**					**Freundlich**			
Experiment	**Q_0**	**K_L**	**R_l**	**R^2**		**K_F**	**n**	**R^2**	**Δq**
	µg/mg	L/µg				(µg/mg)x (L/mg)$^{1/n}$			%
MQ DEP (alone)	99,917	0,0110	0,017	0,862	59,04	18,83	4,761	0,972	14,070
GW DEP (alone)	75,542	0,0080	0,024	0,826	53,57	11,29	4,277	0,992	4,680
MQ DEP (mixture)	151,627	0,0020	0,090	0,898	59,79	10,75	3,179	0,984	12,900
GW DEP (mixture)	120,000	0,0018	0,1015	0,811	55,98	6,03	2,832	0,928	19,000
Average R^2 and Δq				0.849	57.10			0.969	12.66

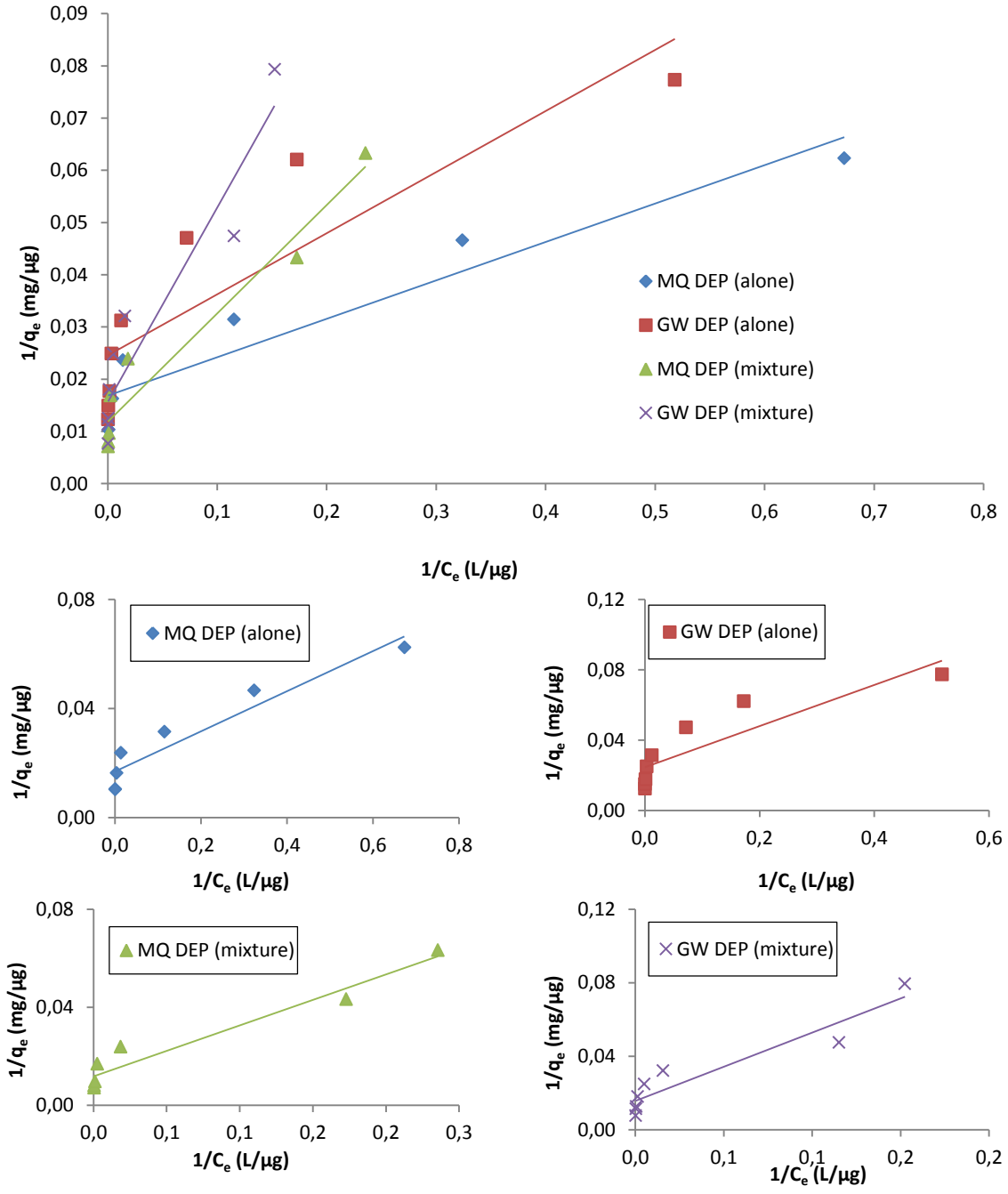

FIGURE 66: Equilibrium adsorption isotherm of DEP fitted to the linear Langmuir model

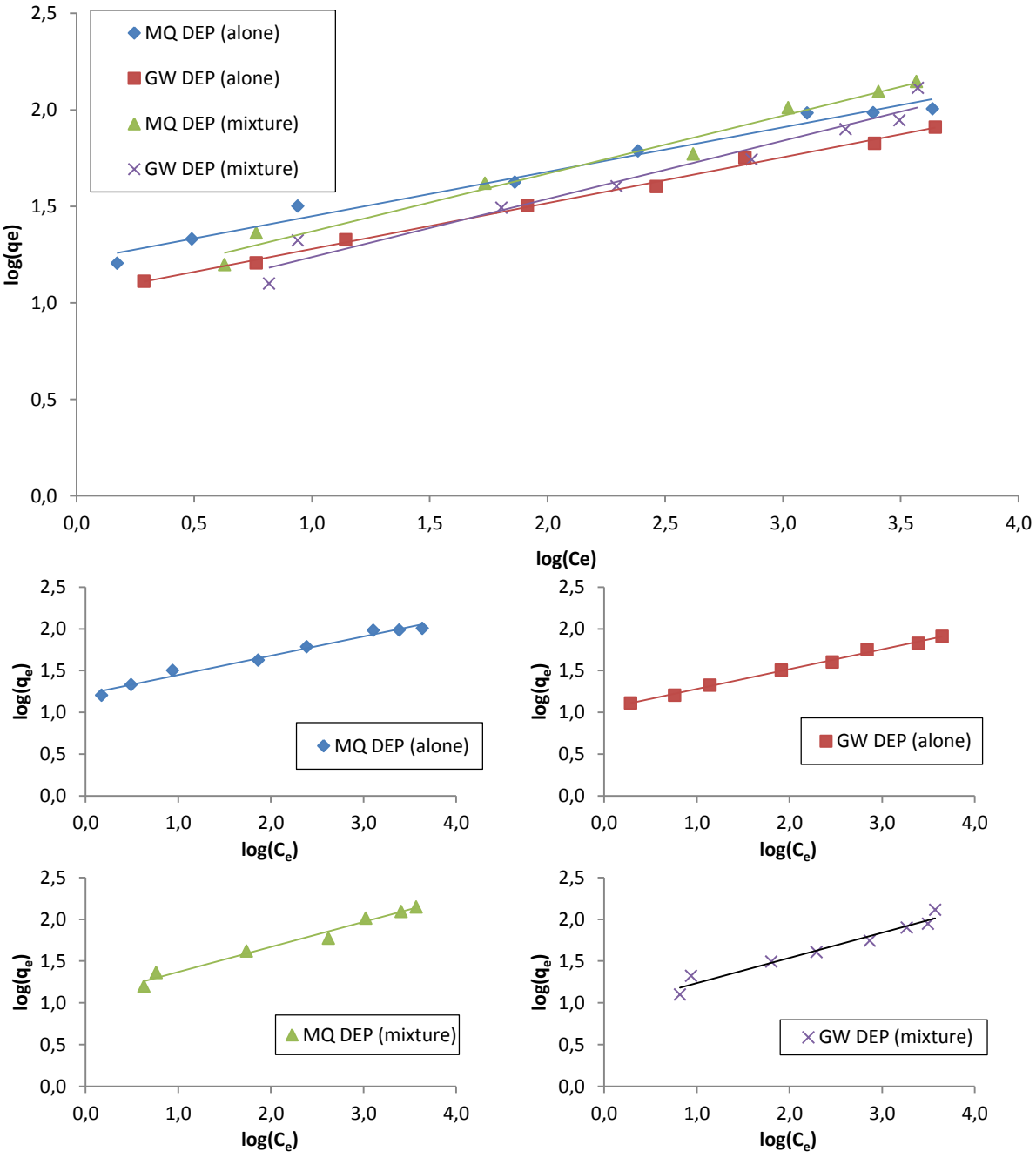

FIGURE 67: Equilibrum adsorption isotherm of DEP fitted to the linear Freundlich model

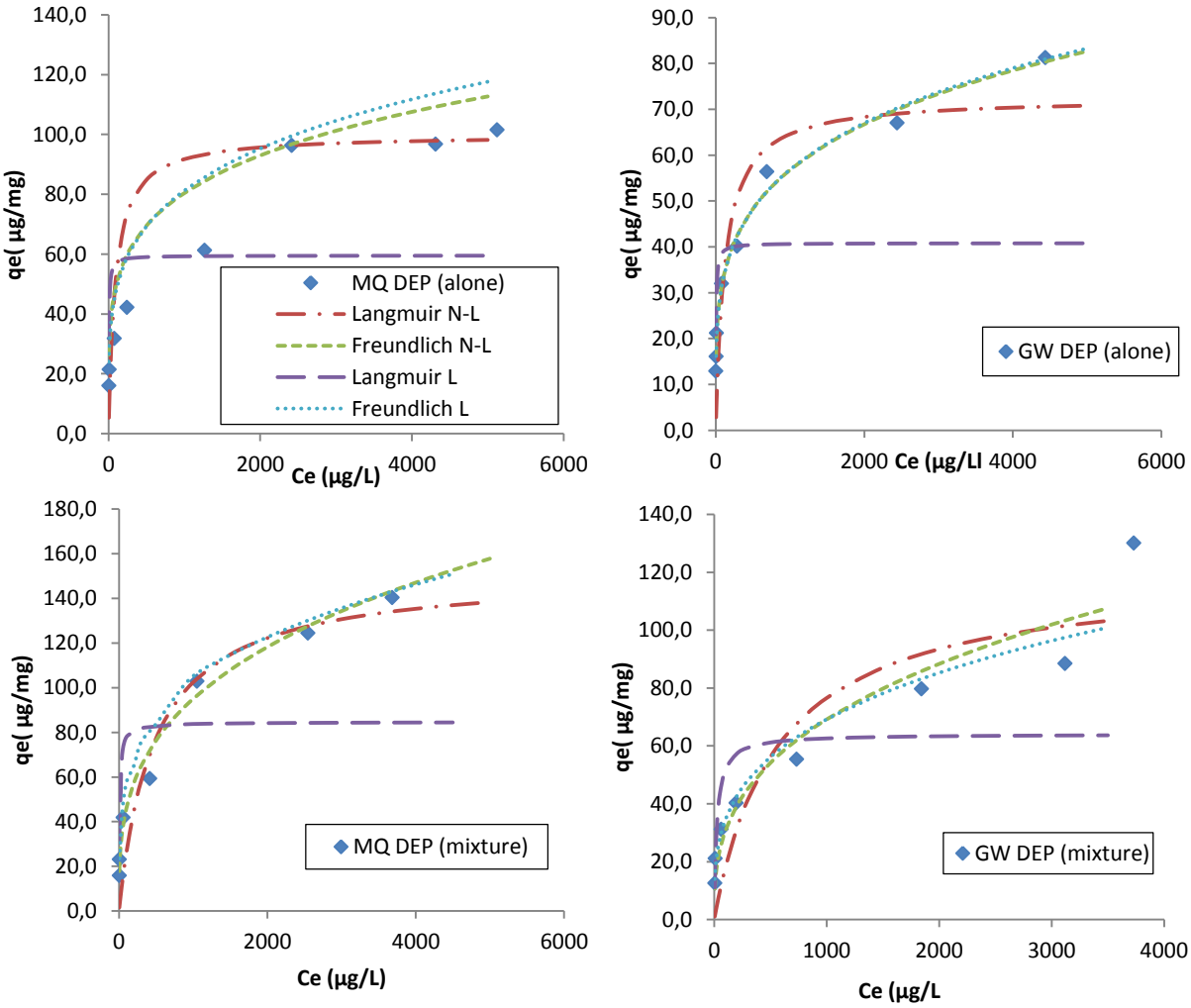

FIGURE 68: Experimental and calculated equilibrium adsorption isotherms of DEP (N-L =non linear, L=linear)

7.3.3 Dissolved organic carbon

The results from the DOC adsorption decay in GW spiked with DEP are summarized in table 19. The adsorption of DOC seems to follow the Freundlich model, which had the highest R^2 values and lowest Δq. Since the DOC constitutes of several different organic and non-organic compound, which originates from the PCPs added to the GW, it seems rational that the adsorption of DOC follows the heterogenous Freundlich model instead of the homogenous Langmuir model. The plots of the linear Langmuir and Freundlich model fitted to the experimental data are presented in figure 69 and 70. The experimental data points and the different calculated adsorption isotherms are shown in figure 71. The K_f constant obtained for DOC is in the same range as the one obtained for DEP.

It must be noted that the data points obtained from the DOC experiment were very scattered and without a clear pattern. Only four datapoints out of ten were used to model the isotherms. It is therefore recommended to repeat the DOC experiments.

TABLE 20: Equilibrium adsorption isotherms of DOC in GW fitted to the Langmuir and Freundlich models

Linear	**Langmuir**					**Freundlich**			
Experiment	**Q_0**	**K_L**	**R_l**	**R^2**	**Δq**	**K_F**	**n**	**R^2**	**Δq**
	µg/mg	L/µg			%	log(µg/mg)			%
GW DOC (with DEP)	59,524	0,2283	0,00085	0,909	28,66	16,58	4,348	0,981	9,61
Non Linear	**Langmuir**					**Freundlich**			
Experiment	**Q_0**	**K_L**	**R_l**	**R^2**	**Δq**	**K_F**	**n**	**R^2**	**Δq**
	µg/mg	L/µg			%	log(µg/mg)			%
GW DOC (with DEP)	99,917	0,0110	0,017	0,862	59,04	18,83	4,761	0,972	14,07

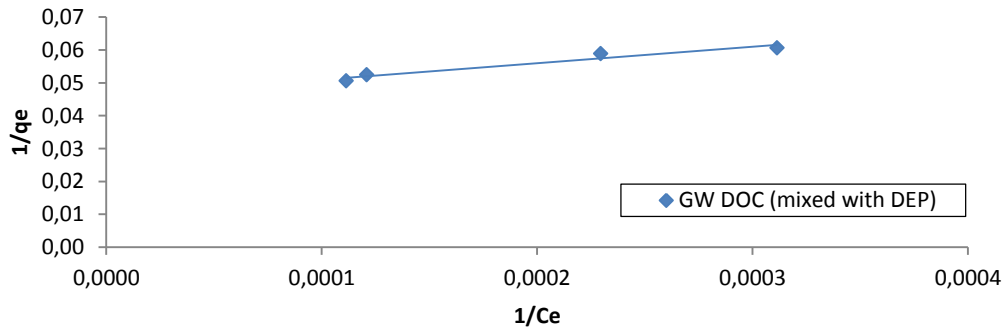

FIGURE 69: Adsorption isotherm of DOC in GW mixed with DEP fitted to the Langmuir model

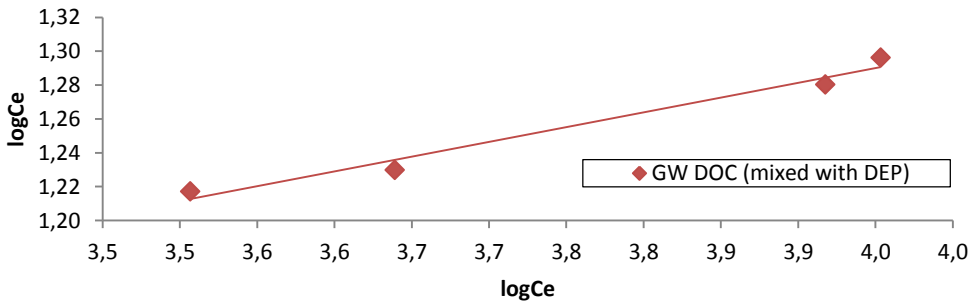

FIGURE 70: Adsorption isotherm of DOC in GW mixed with DEP fitted to the Langmuir model

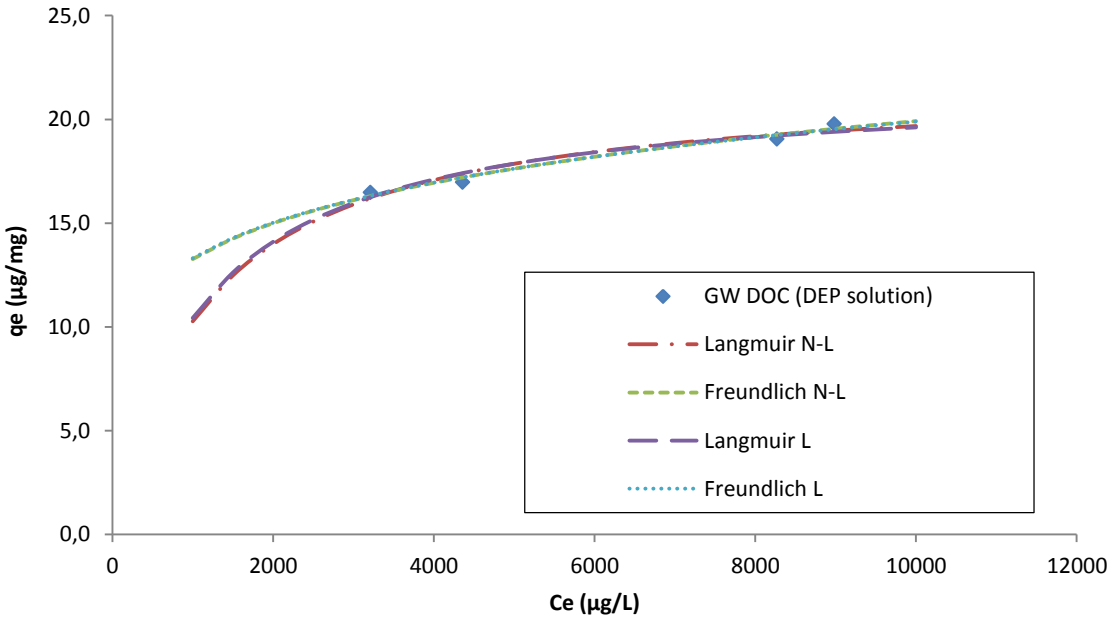

FIGURE 71: The experimental and modelled adsorption isotherms of DOC in GW mixed with DEP

7.3.4 Comments on the adsorption data

Figure 72 shows the experimental data points that were out of trend and not included in the isotherm calculations. The points that were taken out are marked with red on the graphs. In almost all instances, it was the points obtained for the highest amount of carbon added (low Ce) or the lowest amounts of carbon (high Ce) that didn't fit the patterns. The explanation to this could be as follows:

1) For the highest amount of carbon added very high removal efficiencies followed and low concentration of TCC and DEP were detected. As pointed out in the discussion on the analytical method, the lowest concentration range showed asymmetric peak shape, tailing effect and potential interference from other compounds or the baseline. This can have led to overestimated areas and too high concentrations for the highest amount of carbon added. The quantification limit of the analytical method might not have been as low as indicated by the calibration curve.

2) For the lowest amount of carbon added, the difference in particle size can have led to different conditions for the adsorption process and unstable results. Only a few carbon particles made up the lowest weights. Thus, the ratio of external surface area and internal surface area might have differed a lot depended on the particle size of the weighed carbon. From theory it is known that the internal surface area is crucial for the adsorption of substances and that this increases with decreasing particle size. From literature it was noted that many sieved their carbon or grinded it before use to make sure the particle size and adsorption conditions were as uniform as possible. This was not done for this thesis and might explain why the highest Ce values were out of trend.

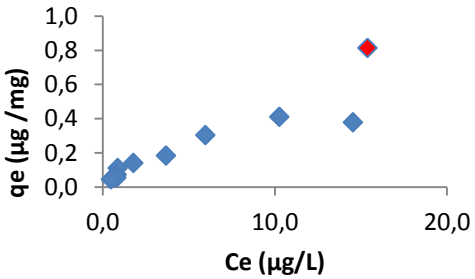

MQ TCC (alone)

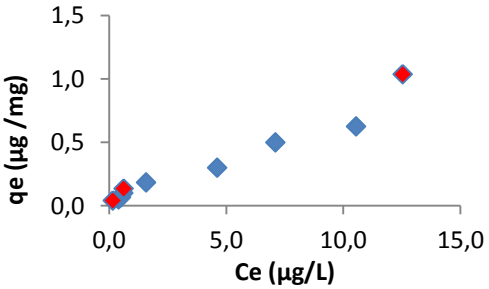

GW TCC (alone)

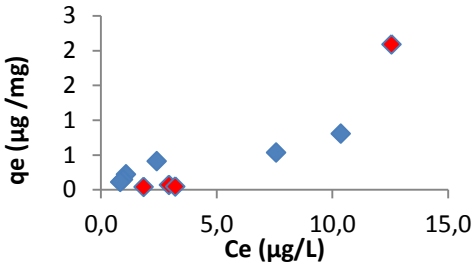

MQ TCC (mixture)

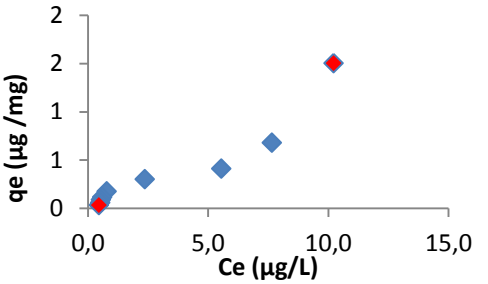

GW TCC (mixture)

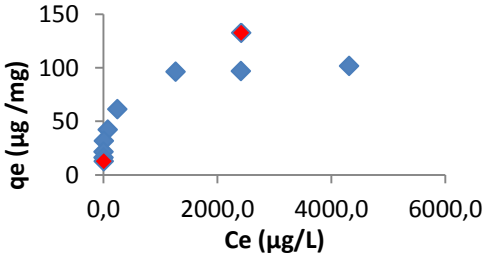

MQ DEP (alone)

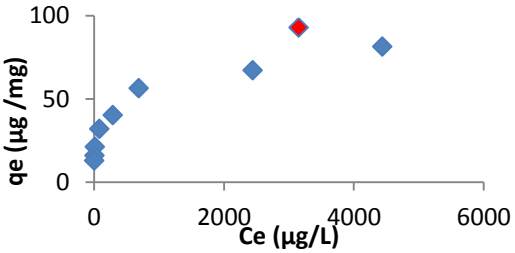

GW DEP (alone)

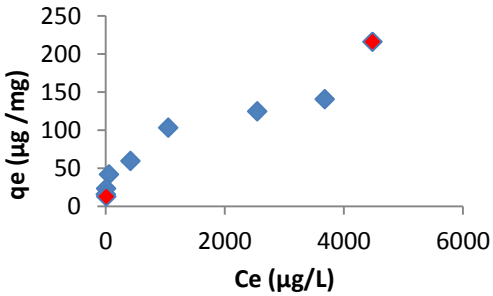

MQ DEP (mixture)

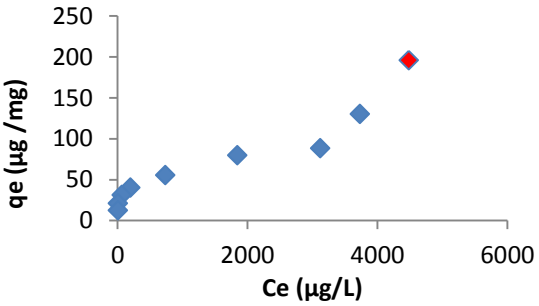

GW DEP (mixture)

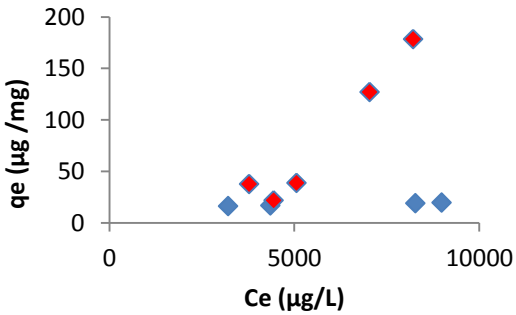

GW DOC (mixed with DEP)

FIGURE 72: Datapoints not included for the isotherms

7.4 How to use the isotherm results on pilot-scale adsorption systems

The results from the isotherm studies can be used to predict the removal of DEP and TCC with activated carbon F400 for an adsorption system. It seems the highly microporous F400 is a suitable adsorbent chose for both of the compounds. For a batch system, the needed amount of carbon to achieve wanted removal efficiency can be directly found from the isotherm curve, given that the conditions in the bacth system (pH, temp, concentration DOC etc) are the same. When designing a best fit adsorption system, it is essential to have the most suitable adsorption equilibrium correlation. The isotherms can provide information on the dominating adsorption mechanisms pathways, and give an indication of the surface properties and capacity of the adsorbent. Isotherms can also be used for quantitative comparison of adsorption behavior and selectivity for different types of adsorbents. However, an isotherm cannot provide definitive scale- up data for a granular carbon adsorption system. For this, the breakthrough curve is needed, which most commonly is obtained by a column test as explained in section 5.8. So mainly, the isotherm results obtained in this thesis can be used to plan the optimal conditions for the column test, which will be further used to design the granular pilot- scale system. Further isotherm testing such as varying the pH, testing different types of carbon, and increasing temperature etc, should be conducted to find the optimal adsorption conditions for DEP and TCC before continuing with a column test.

8. Conclusion

For this thesis, the micropollutants triclocarban and diethyl phthalate were selected as potential model pollutants for a greywater recycling scheme. From the literature search done in the specialization project and during this thesis, it was concluded that these two compounds are likely to be present in greywater and that they possess a potential threat to the environment and humans. They are both suspected of being endocrine disrupting to humans and other living organisms. Based on the literature search, it seems little or no studies have been conducted on the removal of DEP and TCC from greywater. In fact, on TCC, only one article was found that on the removal of TCC from water. This is probably due to its very low water solubility, which makes it difficult to work with. DEP on the other hand, is often selected as a model pollutant for the phthalate group due to its relative high water solubility. A concluding mark on the selected pollutants is therefore that DEP is the easiest choice for coming studies in a pilot- greywater recycling scheme, while TCC is the most interesting choice to continue with.

This thesis examined the removal of TCC and DEP from greywater and ultra-pure water with adsorption onto activated carbon. The adsorption kinetic and isotherm experiments were conducted in the lab. The analytical method RP-HPLC with UV-DAD detection was found to suitable in detecting and quantifying TCC and DEP in greywater in very low concentrations.

The results indicated that high removal efficiencies can be expected for both DEP and TCC by adsorption onto activated carbon. However, longer contact time seems to be necessary to achieve the wanted removal of DEP compared to TCC. Based on the isotherm results it seems the adsorption efficiency of TCC is not affected by other dissolved organic compounds. The removal efficiency of DEP seems to be affected by other dissolved organic compounds. This has to be accounted for when planning an adsorption system for DEP. The competition between DEP and TCC seems to be in favor of TCC. The TCC adsorption was not affected when DEP and TCC were mixed together, even though the concentration of DEP was 250 times higher.

The activated carbon F400, which is commonly applied to the sorption of micropollutants, appeared to be a suitable adsorbent for both DEP and TCC. It has a low content of acidic functional groups, which favor the sorption of hydrophobic compounds such as TCC and DEP. It seems reasonable to continue with the F400 for the coming adsorptions experiments on TCC and DEP.

8.1 Future research proposal

- Do equilibrium adsorption isotherm of DEP and TCC for different pH's and temperature. This to find the optimal conditions for the adsorption process
- Test different initial concentrations of TCC and DEP to see if this affect the adsorption rate
- Do a pre-column test to obtain the breakthrough curve for DEP and TCC
- Design a pilot-scale adsorption system based on the column test obtain
- For the analytical method it is proposed to look into solid phase extraction to decrease the injection volume and obtain better peak shapes

Bibliography

AGILENT 2011. The LC Hanbook *Guide to LC Columns and Method Development.* 5990-7595EN ed. the United States: Agilent Technologies, Inc.

AHN, K. C., KASAGAMI, T., TSAI, H. J., SCHEBB, N. H., OGUNYOKU, T., GEE, S. J., YOUNG, T. M. & HAMMOCK, B. D. 2012. An immunoassay to evaluate human/environmental exposure to the antimicrobial triclocarban. *Environ Sci Technol,* 46**,** 374-81.

ALFA AESAR. 2013. *Sikkerhetsdatablad Diethyl Phthalate* [Online]. Available: http://www.alfa.com/content/msds/norwegian/A17529.pdf [Accessed 20.09 2013].

ALSHOULI, M. M. 2012. *Wastewater Tracer Study Utilizing Carbamazepine, Triclocarban and Triclosan in the Philadelphia Waterway.* Master in Analytical Chemistry, Drexel University.

API, A. M. 2001. Toxicological profile of diethyl phthalate: a vehicle for fragrance and cosmetic ingredients. *Food and Chemical Toxicology,* 39**,** 97-108.

BADIA-FABREGAT, M., RODRÍGUEZ-RODRÍGUEZ, C. E., GAGO-FERRERO, P., OLIVARES, A., PIÑA, B., DÍAZ-CRUZ, M. S., VICENT, T., BARCELÓ, D. & CAMINAL, G. 2012. Degradation of UV filters in sewage sludge and 4-MBC in liquid medium by the ligninolytic fungus Trametes versicolor. *Journal of Environmental Management,* 104**,** 114-120.

BARANOWSKA, I., MAGIERA, S. & BORTNICZUK, K. 2010. Reverse-phase HPLC method for the simultaneous analysis of triclosan and triclocarban in surface waters. *Water Science & Technology: Water Supply,* 10**,** 173.

BARANOWSKA, I. & WOJCIECHOWSKA, I. 2012. Development of SPE/HPLC-DAD to determine residues of selected disinfectant agents in surface water. *Polish Journal of Environmental Studies,* 21**,** 269-277.

BLAIR, B. D., CRAGO, J. P., HEDMAN, C. J., TREGUER, R. J. F., MAGRUDER, C., ROYER, L. S. & KLAPER, R. D. 2013. Evaluation of a model for the removal of pharmaceuticals, personal care products, and hormones from wastewater. *Science of The Total Environment,* 444**,** 515-521.

BONO-BLAY, F., GUART, A., DE LA FUENTE, B., PEDEMONTE, M., PASTOR, M. C., BORRELL, A. & LACORTE, S. 2012. Survey of phthalates, alkylphenols, bisphenol A and herbicides in Spanish source waters intended for bottling. *Environmental Science and Pollution Research,* 19**,** 3339-3349.

BOONYAROJ, V., CHIEMCHAISRI, C., CHIEMCHAISRI, W., THEEPHARAKSAPAN, S. & YAMAMOTO, K. 2012. Toxic organic micro-pollutants removal mechanisms in long-term operated membrane bioreactor treating municipal solid waste leachate. *Bioresource Technology,* 113**,** 174-180.

BOYD, G. E., ADAMSON, A. W. & MYERS JR, L. S. 1947. The exchange adsorption of ions from aqueous solutions by organic zeolites. II. Kinetics. *Journal of the American Chemical Society,* 69**,** 2836-2848.

BOYJOO, Y., PAREEK, V. K. & ANG, M. 2013. A review of greywater characteristics and treatment processes. *Water Science and Technology,* 67**,** 1403-1424.

BRENNAN, J. K., BANDOSZ, T. J., THOMSON, K. T. & GUBBINS, K. E. 2001. Water in porous carbons. *Colloids and Surfaces A: Physicochemical and Engineering Aspects,* 187–188**,** 539-568.

CAI, Y.-Q., JIANG, G.-B., LIU, J.-F. & ZHOU, Q.-X. 2003. Multi-walled carbon nanotubes packed cartridge for the solid-phase extraction of several phthalate esters from water samples and their determination by high performance liquid chromatography. *Analytica Chimica Acta,* 494**,** 149-156.

CALGONCARBON. 2012. *FILTRASORB 400* [Online]. CalgonCarbon. Available: http://www.calgoncarbon.com/media/images/site_library/25_Filtrasorb_400_1019web.pdf [Accessed 02.11 2013].

CAMERON CARBON 2006. Activated carbon Manufacture, Structure and Properties. Cameron Carbon.
CHEN, F., YING, G.-G., YANG, J.-F., ZHAO, J.-L. & WANG, L. 2010. Rapid resolution liquid chromatography-tandem mass spectrometry method for the determination of endocrine disrupting chemicals (EDCs), pharmaceuticals and personal care products (PPCPs) in wastewater irrigated soils. *Journal of Environmental Science and Health, Part B,* 45**,** 682-693.
CHIAIA-HERNANDEZ, A. C., ASHAUER, R., MOEST, M., HOLLINGSHAUS, T., JEON, J., SPAAK, P. & HOLLENDER, J. 2013. Bioconcentration of organic contaminants in Daphnia resting eggs. *Environmental Science and Technology,* 47**,** 10667-10675.
CLARA, M., WINDHOFER, G., HARTL, W., BRAUN, K., SIMON, M., GANS, O., SCHEFFKNECHT, C. & CHOVANEC, A. 2010. Occurrence of phthalates in surface runoff, untreated and treated wastewater and fate during wastewater treatment. *Chemosphere,* 78**,** 1078-1084.
CLARK, L. B., ROSEN, R. T., HARTMAN, T. G., LOUIS, J. B. & ROSEN, J. D. 1991. Application of Particle Beam LC/MS for the Analysis of Water from Publicly Owned Treatment Works. *International Journal of Environmental Analytical Chemistry,* 45**,** 169-178.
COOGAN, M. A., EDZIYIE, R. E., LA POINT, T. W. & VENABLES, B. J. 2007. Algal bioaccumulation of triclocarban, triclosan, and methyl-triclosan in a North Texas wastewater treatment plant receiving stream. *Chemosphere,* 67**,** 1911-1918.
COONEY, D. O. 1998. *Adsorption Design for Wastewater Treatment,* Florida, CRC Press.
CUDERMAN, P. & HEATH, E. 2007. Determination of UV filters and antimicrobial agents in environmental water samples. *Analytical and Bioanalytical Chemistry,* 387**,** 1343-1350.
DARGNAT, C., TEIL, M.-J., CHEVREUIL, M. & BLANCHARD, M. 2009. Phthalate removal throughout wastewater treatment plant: Case study of Marne Aval station (France). *Science of The Total Environment,* 407**,** 1235-1244.
DE OLIVEIRA, T. F., CAGNON, B., FAUDUET, H., LICHERON, M. & CHEDEVILLE, O. 2012. Removal of Diethyl Phthalate from Aqueous Media by Adsorption on Different Activated Carbons: Kinetic and Isotherm Studies. *Separation Science and Technology,* 47**,** 1139-1148.
DE OLIVEIRA, T. F., CHEDEVILLE, O., CAGNON, B. & FAUDUET, H. 2011. Degradation kinetics of DEP in water by ozone/activated carbon process: Influence of pH. *Desalination,* 269**,** 271-275.
DE RIDDER, D. J. 2012. *Adsorption of organic micropollutants onto activated carbon and zeolites.* PhD, Delft University of Technology.
DESILVA, F. 2000. ACTIVATED CARBON FILTRATION. *Water Quality Products Magazine.*
DÍAZ-CRUZ, M. S., GAGO-FERRERO, P., LLORCA, M. & BARCELÓ, D. 2012. Analysis of UV filters in tap water and other clean waters in Spain. *Analytical and Bioanalytical Chemistry,* 402**,** 2325-2333.
DONNER, E., ERIKSSON, E., SCHOLES, L. & REVITT, M. 2008. Priority pollutant behaviour in treatment and reuse systems for household wastewater. *In:* SCOREPP (ed.).
DULEBA, A. J., AHMED, M. I., SUN, M., GAO, A. C., VILLANUEVA, J., CONLEY, A. J., TURGEON, J. L., BENIRSCHKE, K., GEE, N. A., CHEN, J., GREEN, P. G. & LASLEY, B. L. 2011. Effects of triclocarban on intact immature male rat: augmentation of androgen action. *Reprod Sci,* 18**,** 119-27.
DVORAK, B. I. & SKIPTON, S. O. 2013. *Drinking Water Treatment: Activated Carbon Filtration* [Online]. Nebraska: University of Nebraska Lincoln. Available: http://www.ianrpubs.unl.edu/pages/publicationD.jsp?publicationId=293 [Accessed 21.12 2013].
ERIKSSON, E., AUFFARTH, K., EILERSEN, A. M., HENZE, M. & LEDIN, A. 2003. Household chemicals and personal care products as sources for xenobiotic organic compounds in grey wastewater. *Water Sa,* 29**,** 135-146.
ERIKSSON, E., AUFFARTH, K., HENZE, M. & LEDIN, A. 2002. Characteristics of grey wastewater. *Urban Water,* 4**,** 85-104.

ESBENSHADE, J. L., CARDOSO, J. C. & ZANONI, M. V. B. 2010. Removal of sunscreen compounds from swimming pool water using self-organized TiO2 nanotubular array electrodes. *Journal of Photochemistry and Photobiology A: Chemistry,* 214**,** 257-263.

ESSANDOH, H. M., TIZAOUI, C., MOHAMED, M. H., AMY, G. & BRDJANOVIC, D. 2010. Fate of triclocarban during soil aquifer treatment: soil column studies. *Water Sci Technol,* 61**,** 1779-85.

FATOKI, O. S. & NOMA, A. 2002. Solid phase extraction method for selective determination of phthalate esters in the aquatic environment. *Water, Air, and Soil Pollution,* 140**,** 85-98.

FAUST, B. 1997. Modern Chemical Techniques. The Royal Society of Chemistry.

FENT, K., ZENKER, A. & RAPP, M. 2010. Widespread occurrence of estrogenic UV-filters in aquatic ecosystems in Switzerland. *Environmental Pollution,* 158**,** 1817-1824.

FERRER, I., ZWEIGENBAUM, J. A. & THURMAN, E. M. 2010. Analysis of 70 Environmental Protection Agency priority pharmaceuticals in water by EPA Method 1694. *J Chromatogr A,* 1217**,** 5674-86.

FOO, K. Y. & HAMEED, B. H. 2010. Insights into the modeling of adsorption isotherm systems. *Chemical Engineering Journal,* 156**,** 2-10.

GAGO-FERRERO, P., MASTROIANNI, N., DÍAZ-CRUZ, M. S. & BARCELÓ, D. 2013. Fully automated determination of nine ultraviolet filters and transformation products in natural waters and wastewaters by on-line solid phase extraction–liquid chromatography–tandem mass spectrometry. *Journal of Chromatography A,* 1294**,** 106-116.

GE, D. & LEE, H. K. 2012. A new 1-hexyl-3-methylimidazolium tris(pentafluoroethyl)trifluorophosphate ionic liquid based ultrasound-assisted emulsification microextraction for the determination of organic ultraviolet filters in environmental water samples. *Journal of Chromatography A,* 1251**,** 27-32.

GIOKAS, D. L., SAKKAS, V. A. & ALBANIS, T. A. 2004. Determination of residues of UV filters in natural waters by solid-phase extraction coupled to liquid chromatography–photodiode array detection and gas chromatography–mass spectrometry. *Journal of Chromatography A,* 1026**,** 289-293.

GIOKAS, D. L., SAKKAS, V. A., ALBANIS, T. A. & LAMPROPOULOU, D. A. 2005. Determination of UV-filter residues in bathing waters by liquid chromatography UV-diode array and gas chromatography-mass spectrometry after micelle mediated extraction-solvent back extraction. *Journal of Chromatography A,* 1077**,** 19-27.

GIUDICE, B. D. & YOUNG, T. M. 2010. The antimicrobial triclocarban stimulates embryo production in the freshwater mudsnail Potamopyrgus antipodarum. *Environmental Toxicology and Chemistry,* 29**,** 966-970.

GONZALEZ-MARINO, I., QUINTANA, J. B., RODRIGUEZ, I. & CELA, R. 2009. Simultaneous determination of parabens, triclosan and triclocarban in water by liquid chromatography/electrospray ionisation tandem mass spectrometry. *Rapid Commun Mass Spectrom,* 23**,** 1756-66.

GRANT. 2013. *PSU-20i Orbital Shaking Platform* [Online]. Grant. Available: http://www.grantinstruments.com/psu-20i-orbital-shaking-platform/ [Accessed 08.01 2013].

GRASSI, M., KAYKIOGLU, G., BELGIORNO, V. & LOFRANO, G. 2012. Removal of Emerging Contaminants from Water and Wastewater by Adsorption Process. *In:* LOFRANO, G. (ed.) *Emerging Compounds Removal from Wastewater.* Springer Netherlands.

GUO, Z. Y., GAI, P. P., DUAN, J., ZHAI, J. X., ZHAO, S. S., WANG, S. & WEI, D. Y. 2010. Simultaneous determination of phthalates and adipates in human serum using gas chromatography-mass spectrometry with solid-phase extraction. *Biomedical Chromatography,* 24**,** 1094-1099.

HADJMOHAMMADI, M. R. & RANJBARI, E. 2012. Utilization of homogeneous liquid–liquid extraction followed by HPLC-UV as a sensitive method for the extraction and determination of phthalate esters in environmental water samples. *International Journal of Environmental Analytical Chemistry,* 92**,** 1312-1324.

HALDEN, R. U. & PAULL, D. H. 2004. Analysis of triclocarban in aquatic samples by liquid chromatography electrospray ionization mass spectrometry. *Environmental Science and Technology,* 38**,** 4849-4855.
HALDEN, R. U. & PAULL, D. H. 2005. Co-Occurrence of Triclocarban and Triclosan in U.S. Water Resources. *Environmental Science & Technology,* 39**,** 1420-1426.
HAMEED, B. H., TAN, I. A. W. & AHMAD, A. L. 2008. Adsorption isotherm, kinetic modeling and mechanism of 2,4,6-trichlorophenol on coconut husk-based activated carbon. *Chemical Engineering Journal,* 144**,** 235-244.
HARRIS, P. J. F., LIU, Z. & SUENAGA, K. 2008. Imaging the atomic structure of activatedcarbon. *Journal of Physics Condensed Matter,* 20.
HEIDLER, J., SAPKOTA, A. & HALDEN, R. U. 2006. Partitioning, Persistence, and Accumulation in Digested Sludge of the Topical Antiseptic Triclocarban during Wastewater Treatment. *Environmental Science & Technology,* 40**,** 3634-3639.
HIGGINS, C. P., PAESANI, Z. J., CHALEW, T. E. A. & HALDEN, R. U. 2009. Bioaccumulation of triclocarban in Lumbriculus variegatus. *Environmental Toxicology and Chemistry,* 28**,** 2580-2586.
HINTHER, A., BROMBA, C. M., WULFF, J. E. & HELBING, C. C. 2011. Effects of triclocarban, triclosan, and methyl triclosan on thyroid hormone action and stress in frog and mammalian culture systems. *Environ Sci Technol,* 45**,** 5395-402.
HO, Y. S. & MCKAY, G. 1999. Pseudo-second order model for sorption processes. *Process Biochemistry,* 34**,** 451-465.
HOWARD, P. H. & MUIR, D. C. G. 2010. Identifying New Persistent and Bioaccumulative Organics Among Chemicals in commerce. *Environmental Science & Technology 44(7).*
HUBINGER, J. C. & HAVERY, D. C. 2006. Analysis of consumer cosmetic products for phthalate esters. *Journal of Cosmetic Science,* 57**,** 127-137.
JULINOVA, M. & SLAVIK, R. 2012. Removal of phthalates from aqueous solution by different adsorbents: a short review. *J Environ Manage,* 94**,** 13-24.
JUNG, Y. J., OH, B. S., KIM, K. S., KOGA, M., SHINOHARA, R. & KANG, J. W. 2010. The degradation of diethyl phthalate (DEP) during ozonation: Oxidation by-products study. *Journal of Water and Health,* 8**,** 290-298.
KAMAREI, F., EBRAHIMZADEH, H. & YAMINI, Y. 2011. Optimization of ultrasound-assisted emulsification microextraction with solidification of floating organic droplet followed by high performance liquid chromatography for the analysis of phthalate esters in cosmetic and environmental water samples. *Microchemical Journal,* 99**,** 26-33.
KARANFIL, T. & KILDUFF, J. E. 1999. Role of Granular Activated Carbon Surface Chemistry on the Adsorption of Organic Compounds. 1. Priority Pollutants. *Environmental Science & Technology,* 33**,** 3217-3224.
KLEIN, D. R., FLANNELLY, D. F. & SCHULTZ, M. M. 2010. Quantitative determination of triclocarban in wastewater effluent by stir bar sorptive extraction and liquid desorption–liquid chromatography–tandem mass spectrometry. *Journal of Chromatography A,* 1217**,** 1742-1747.
KONIECKI, D., WANG, R., MOODY, R. P. & ZHU, J. 2011. Phthalates in cosmetic and personal care products: concentrations and possible dermal exposure. *Environ Res,* 111**,** 329-36.
KUMAR, K. S., PRIYA, S. M., PECK, A. M. & SAJWAN, K. S. 2010. Mass loadings of triclosan and triclocarbon from four wastewater treatment plants to three rivers and landfill in Savannah, Georgia, USA. *Arch Environ Contam Toxicol,* 58**,** 275-85.
KUMAR, K. V., SUBANANDAM, K., RAMAMURTHI, V. & SIVANESAN, S. 2004. *Solid Liquid Adsorption for Wastewater Treatment: Principle Design and Operation* [Online]. Eco Service International. Available: http://www.eco-web.com/edi/040201.html [Accessed 28.12 2013].
KUPIEC, T. 2004. Quality-Control Analytical Methods High-Performance Liquid Chromatography. *International Journal of Pharmaceutical Compounding,* 8.
LEAL, L. H. 2010. Removal of micropollutants from grey water (PHD). Wageningen: Wageningen University.

LI, J., CAI, Y., SHI, Y., MOU, S. & JIANG, G. 2008. Analysis of phthalates via HPLC-UV in environmental water samples after concentration by solid-phase extraction using ionic liquid mixed hemimicelles. *Talanta,* 74**,** 498-504.

LI, L., ZHU, W., ZHANG, P., ZHANG, Z., WU, H. & HAN, W. 2006. Comparison of AC/O3-BAC and O3-BAC processes for removing organic pollutants in secondary effluent. *Chemosphere,* 62**,** 1514-22.

LI, W., MA, Y., GUO, C., HU, W., LIU, K., WANG, Y. & ZHU, T. 2007. Occurrence and behavior of four of the most used sunscreen UV filters in a wastewater reclamation plant. *Water Research,* 41**,** 3506-3512.

LIU, T. & WU, D. 2011. Simultaneous determination of some ultraviolet-absorbing chemicals in sunscreen cosmetics using a high-performance liquid chromatography method. *Int J Cosmet Sci,* 33**,** 408-15.

LIU, T. & WU, D. 2012. High-performance liquid chromatographic determination of triclosan and triclocarban in cosmetic products. *Int J Cosmet Sci,* 34**,** 489-94.

MALVIYA, R., BANSAL, V., PAL, O. P. & SHARMA, P. K. 2010. HIGH PERFORMANCE LIQUID CHROMATOGRAPHY: A SHORT REVIEW. *Journal of Global Pharma Technology,* 10**,** 22-26.

MANKIDY, R., WISEMAN, S., MA, H. & GIESY, J. P. 2013. Biological impact of phthalates. *Toxicol Lett,* 217**,** 50-8.

MANSOURI, L. & BOUSSELMI, L. 2012. Degradation of diethyl phthalate (DEP) in aqueous solution using TiO2/UV process. *Desalination and Water Treatment,* 40**,** 63-68.

MATTA, G. K. L., BARROS, M. A. S. D., LAMBRECHT, R., SILVA, E. A. D. & LIMA, O. C. D. M. 2008. Dynamic isotherms of dye in activated carbon. *Materials Research,* 11**,** 365-369.

MEDELLIN-CASTILLO, N. A., OCAMPO-PEREZ, R., LEYVA-RAMOS, R., SANCHEZ-POLO, M., RIVERA-UTRILLA, J. & MENDEZ-DIAZ, J. D. 2013. Removal of diethyl phthalate from water solution by adsorption, photo-oxidation, ozonation and advanced oxidation process (UV/H2O2, O-3/H2O2 and O-3/activated carbon). *Science of the Total Environment,* 442**,** 26-35.

MEINZINGER, F. & OLDENBURG, M. 2009. Characteristics of source-separated household wastewater flows: A statistical assessment. *Water Science and Technology,* 59**,** 1785-1791.

MOLDOVEANU, S. C. & DAVID, V. 2013a. Chapter 1 - Basic Information about HPLC. *In:* MOLDOVEANU, S. C. & DAVID, V. (eds.) *Essentials in Modern HPLC Separations.* Elsevier.

MOLDOVEANU, S. C. & DAVID, V. 2013b. Chapter 2 - Parameters that Characterize HPLC Analysis. *In:* MOLDOVEANU, S. C. & DAVID, V. (eds.) *Essentials in Modern HPLC Separations.* Elsevier.

MOLDOVEANU, S. C. & DAVID, V. 2013c. Chapter 6 - Stationary Phases and Their Performance. *In:* MOLDOVEANU, S. C. & DAVID, V. (eds.) *Essentials in Modern HPLC Separations.* Elsevier.

MOLDOVEANU, S. C. & DAVID, V. 2013d. Chapter 7 - Mobile Phases and Their Properties. *In:* MOLDOVEANU, S. C. & DAVID, V. (eds.) *Essentials in Modern HPLC Separations.* Elsevier.

MONTAGNER, C. & JARDIM, W. 2011. Spatial and Seasonal Variations of Pharmaceuticals and Endocrine Disruptors in the Atibaia River, São Paulo State (Brazil). *J. Braz. Chem. Soc.,* 22**,** 1452-1462.

MORLAY, C. & JOLY, J.-P. 2009. Contribution to the textural characterisation of Filtrasorb 400 and other commercial activated carbons commonly used for water treatment. *Journal of Porous Materials,* 17**,** 535-543.

MORLAY, C., QUIVET, E., PILSHOFER, M., FAURE, R. & JOLY, J.-P. 2011. Adsorption of Imazamox herbicide onto Filtrasorb 400 activated carbon. *Journal of Porous Materials,* 19**,** 79-86.

NAVACHAROEN, A. & VANGNAI, A. S. 2011. Biodegradation of diethyl phthalate by an organic-solvent-tolerant Bacillus subtilis strain 3C3 and effect of phthalate ester coexistence. *International Biodeterioration & Biodegradation,* 65**,** 818-826.

NELSON, E. D., DO, H., LEWIS, R. S. & CARR, S. A. 2010. Diurnal Variability of Pharmaceutical, Personal Care Product, Estrogen and Alkylphenol Concentrations in Effluent from a

Tertiary Wastewater Treatment Facility. *Environmental Science & Technology,* 45**,** 1228-1234.
NORIT. 2001. GRANULAR ACTIVATED CARBON EVALUATION. Available: http://www.norit.com/files/documents/Pilot_Col_Testing_rev2.pdf.
OH, B. S., JUNG, Y. J., OH, Y. J., YOO, Y. S. & KANG, J.-W. 2006. Application of ozone, UV and ozone/UV processes to reduce diethyl phthalate and its estrogenic activity. *Science of The Total Environment,* 367**,** 681-693.
OLIVER, R., MAY, E. & WILLIAMS, J. 2005. The occurrence and removal of phthalates in a trickle filter STW. *Water Research,* 39**,** 4436-4444.
OLUJIMI, O., FATOKI, O. S. & ODENDAAL, J. P. 2011. Method development for simultaneous determination of phthalate and eleven priority phenols as tert-butyldimethylsilyl derivatives in grab samples from wastewater treatment plants using GC-MS in Cape Town, South Africa. *Fresenius Environmental Bulletin,* 20**,** 69-77.
ORGANISATION FOR ECONOMIC COOPERATION AND DEVELOPMENT. 2004. *The 2004 OECD List of High Production Volume Chemicals* [Online]. Paris. Available: http://www.oecd.org/chemicalsafety/risk-assessment/33883530.pdf.
PEDROUZO, M., BORRULL, F., MARCÉ, R. M. & POCURULL, E. 2009. Ultra-high-performance liquid chromatography-tandem mass spectrometry for determining the presence of eleven personal care products in surface and wastewaters. *Journal of Chromatography A,* 1216**,** 6994-7000.
PEDROUZO, M., BORRULL, F., MARCÉ, R. M. & POCURULL, E. 2011. Analytical methods for personal-care products in environmental waters. *TrAC Trends in Analytical Chemistry,* 30**,** 749-760.
POOLE, C. F. 2003. Chapter 4 - The Column in Liquid Chromatography. *In:* POOLE, C. F. (ed.) *The Essence of Chromatography.* Amsterdam: Elsevier Science.
PRAPATPONG, P. & KANCHANAMAYOON, W. 2010. Determination of phthalate esters in drinking water using solid-phase extraction and gas chromatography. *Journal of Applied Sciences,* 10**,** 1987-1990.
QIU, H., LV, L., PAN, B. C., ZHANG, Q. J., ZHANG, W. M. & ZHANG, Q. X. 2009. Critical review in adsorption kinetic models. *Journal of Zhejiang University: Science A,* 10**,** 716-724.
RAILSBAKC, B. L. 2006. *An explanation of "point of zero charge" - Part I* [Online]. Available: http://www.gly.uga.edu/railsback/Fundamentals/8150PointofZeroCharge05Pt1P.pdf [Accessed 06.01 2013].
REINERT, A. M. 2013. *Granular Activated Carbon Adsorption of Micropollutants from Surface Waters: Field-scale Adsorber Performance and Scale-up of Bench-scale Data.* Master of Science, North Carolina State Univeristy.
REINHARD, M. & DEBROUX, J.-F. 1999. Identifying Future Drinking Water Contaminants. *In:* SCIENCES, N. A. O. (ed.). The National Academies.
RIBEIRO DA SILVA, M. D. D. M. C., RIBEIRO DA SILVA, M. A. V., FREITAS, V. L. S., ROUX, M. V., JIMÉNEZ, P., DÁVALOS, J. Z., CABILDO, P., CLARAMUNT, R. M., PINILLA, E., ROSARIO TORRES, M. & ELGUERO, J. 2010. Energetic studies of urea derivatives: Standard molar enthalpy of formation of 3,4,4′-trichlorocarbanilide. *Journal of Chemical Thermodynamics,* 42**,** 536-544.
RIVERA-UTRILLA, J. & SÁNCHEZ-POLO, M. 2002. Ozonation of 1,3,6-naphthalenetrisulphonic acid catalysed by activated carbon in aqueous phase. *Applied Catalysis B: Environmental,* 39**,** 319-329.
RODIL, R., MOEDER, M., ALTENBURGER, R. & SCHMITT-JANSEN, M. 2009a. Photostability and phytotoxicity of selected sunscreen agents and their degradation mixtures in water. *Analytical and Bioanalytical Chemistry,* 395**,** 1513-1524.
RODIL, R., QUINTANA, J. B., LÓPEZ-MAHÍA, P., MUNIATEGUI-LORENZO, S. & PRADA-RODRÍGUEZ, D. 2009b. Multi-residue analytical method for the determination of emerging pollutants in water by solid-phase extraction and liquid chromatography-tandem mass spectrometry. *Journal of Chromatography A,* 1216**,** 2958-2969.

RODIL, R., QUINTANA, J. B., LÓPEZ-MANÍA, P., MUNIATEGUI-LORENZO, S. & PRADA-RODRÍGUEZ, D. 2008. Multiclass determination of sunscreen chemicals in water samples by liquid chromatography-tandem mass spectrometry. *Analytical Chemistry,* 80**,** 1307-1315.

RUSSO, M. V., NOTARDONATO, I., CINELLI, G. & AVINO, P. 2012. Evaluation of an analytical method for determining phthalate esters in wine samples by solid-phase extraction and gas chromatography coupled with ion-trap mass spectrometer detector. *Analytical and Bioanalytical Chemistry,* 402**,** 1373-1381.

SALVADOR, A. & CHISVERT, A. 2005. An environmentally friendly ("green") reversed-phase liquid chromatography method for UV filters determination in cosmetics. *Analytica Chimica Acta,* 537**,** 15-24.

SÁNCHEZ-AVILA, J., FERNANDEZ-SANJUAN, M., VICENTE, J. & LACORTE, S. 2011. Development of a multi-residue method for the determination of organic micropollutants in water, sediment and mussels using gas chromatography-tandem mass spectrometry. *Journal of Chromatography A,* 1218**,** 6799-6811.

SÁNCHEZ-AVILA, J., TAULER, R. & LACORTE, S. 2012. Organic micropollutants in coastal waters from NW Mediterranean Sea: Sources distribution and potential risk. *Environment International,* 46**,** 50-62.

SAPKOTA, A., HEIDLER, J. & HALDEN, R. U. 2007. Detection of triclocarban and two co-contaminating chlorocarbanilides in US aquatic environments using isotope dilution liquid chromatography tandem mass spectrometry. *Environmental Research,* 103**,** 21-29.

SCIFINDER. 2013. *Triclocarban* [Online]. The American Chemical Society. Available: https://scifinder.cas.org.

SHEN, H. Y., JIANG, H. L., MAO, H. L., PAN, G., ZHOU, L. & CAO, Y. F. 2007. Simultaneous determination of seven phthalates and four parabens in cosmetic products using HPLC-DAD and GC-MS methods. *Journal of Separation Science,* 30**,** 48-54.

SHEN, J. Y., CHANG, M. S., YANG, S. H. & WU, G. J. 2012. Simultaneous and rapid determination of triclosan, triclocarban and their four related transformation products in water samples using SPME-HPLC-DAD. *Journal of Liquid Chromatography and Related Technologies,* 35**,** 2280-2293.

SIGMA ALDRICH. 2013. *Material Data Safety Sheet Diethyl Phthalate* [Online]. Available: http://www.sigmaaldrich.com/MSDS/MSDS/DisplayMSDSPage.do?country=NO&language=no&productNumber=W512206&brand=ALDRICH&PageToGoToURL=http%3A%2F%2Fwww.sigmaaldrich.com%2Fcatalog%2Fproduct%2Faldrich%2Fw512206%3Flang%3Den [Accessed 20.09 2013].

SKÅR, I. F. 2013. *Priority Micropollutants in Greywater from Personal Care Products.* Master Specialization project, NTNU.

SNYDER, E. H. & O'CONNOR, G. A. 2013. Risk assessment of land-applied biosolids-borne triclocarban (TCC). *Science of The Total Environment,* 442**,** 437-444.

SNYDER, E. H., O'CONNOR, G. A. & MCAVOY, D. C. 2010. Measured physicochemical characteristics and biosolids-borne concentrations of the antimicrobial Triclocarban (TCC). *Science of the Total Environment,* 408**,** 2667-2673.

SNYDER, E. H., O'CONNOR, G. A. & MCAVOY, D. C. 2011. Toxicity and bioaccumulation of biosolids-borne triclocarban (TCC) in terrestrial organisms. *Chemosphere,* 82**,** 460-467.

STUBIN, A. I., BROSNAN, T. M., PORTER, K. D., JIMENEZ, L. & LOCHAN, H. 1996. Organic Priority Pollutants in New York City Municipal Wastewaters: 1989-1993. *Water Environment Research,* 68**,** 1037-1044.

SUPELCO. 1998. Bulletin 910 Guide to solid phase extraction. Available: http://www.sigmaaldrich.com/Graphics/Supelco/objects/4600/4538.pdf [Accessed 15.9.2013].

TAN, B. L. L., HAWKER, D. W., MÜLLER, J. F., TREMBLAY, L. A. & CHAPMAN, H. F. 2008. Stir bar sorptive extraction and trace analysis of selected endocrine disruptors in water, biosolids and sludge samples by thermal desorption with gas chromatography-mass spectrometry. *Water Research,* 42**,** 404-412.

TCC CONSORTIUM. 2002. *IUCLID data set* [Online]. EPA. Available: http://epa.gov/chemrtk/pubs/summaries/tricloca/c14186rs.pdf.

THOMAS, B. 2010. *Sizing is critical with carbon media* [Online]. Water Technology. Available: http://www.watertechonline.com/articles/150507 [Accessed 18.12 2013].

TIZAOUI, C., GRIMA, N. & HILAL, N. 2011. Degradation of the antimicrobial triclocarban (TCC) with ozone. *Chemical Engineering and Processing: Process Intensification,* 50**,** 637-643.

TRENHOLM, R. A., VANDERFORD, B. J., DREWES, J. E. & SNYDER, S. A. 2008. Determination of household chemicals using gas chromatography and liquid chromatography with tandem mass spectrometry. *Journal of Chromatography A,* 1190**,** 253-262.

UNITED STATES ENVIRONMENTAL PROTECTION AGENCY. 2006a. *1990 HPV Challenge Program Chemical List* [Online]. Available: http://www.epa.gov/hpv/pubs/update/hpv_1990.pdf.

UNITED STATES ENVIRONMENTAL PROTECTION AGENCY. 2006b. *1994 HPV Additions Chemical List* [Online]. Available: http://www.epa.gov/hpv/pubs/update/hpv_1994.pdf.

VENKATA MOHAN, S., SHAILAJA, S., RAMA KRISHNA, M. & SARMA, P. N. 2007. Adsorptive removal of phthalate ester (Di-ethyl phthalate) from aqueous phase by activated carbon: A kinetic study. *Journal of Hazardous Materials,* 146**,** 278-282.

VERMA, K. S. & XIA, K. 2010. Analysis of triclosan and triclocarban in soil and biosolids using molecularly imprinted solid phase extraction coupled with HPLC-UV. *Journal of AOAC International,* 93**,** 1313-1321.

VETHAAK, A. D., LAHR, J., SCHRAP, S. M., BELFROID, A. C., RIJS, G. B. J., GERRITSEN, A., DE BOER, J., BULDER, A. S., GRINWIS, G. C. M., KUIPER, R. V., LEGLER, J., MURK, T. A. J., PEIJNENBURG, W., VERHAAR, H. J. M. & DE VOOGT, P. 2005. An integrated assessment of estrogenic contamination and biological effects in the aquatic environment of The Netherlands. *Chemosphere,* 59**,** 511-524.

VIRKUTYTE, J., VARMA, R. S. & JEGATHEESAN, V. 2010. *Treatment of Micropollutants in Water and Wastewater,* London, IWA Publishing.

VOSOUGH, M., MOJDEHI, N. R. & SALEMI, A. 2012. Chemometrics assisted dispersive liquid-liquid microextraction for quantification of seven UV filters in urine samples by HPLC-DAD. *J Sep Sci,* 35**,** 3575-85.

WANG, L. H., TSO, M. & CHIN, C. Y. 2005. Simultaneous determination of chlorinated bacteriostats in cosmetic and pharmaceutical products. *Journal of Cosmetic Science,* 56**,** 183-192.

WANG, W., WU, Q., ZANG, X., WANG, C. & WANG, Z. 2012. Extraction of phthalate esters in environmental water samples using layered-carbon magnetic hybrid material as adsorbent followed by their determination with HPLC. *Bulletin of the Korean Chemical Society,* 33**,** 3311-3316.

WEBER JR, W. J. 1974. ADSORPTION PROCESSES. *XXIVth International Congress of Pure and Applied Chemistry.* Butterworth-Heinemann.

WICK, A., FINK, G. & TERNES, T. A. 2010. Comparison of electrospray ionization and atmospheric pressure chemical ionization for multi-residue analysis of biocides, UV-filters and benzothiazoles in aqueous matrices and activated sludge by liquid chromatography–tandem mass spectrometry. *Journal of Chromatography A,* 1217**,** 2088-2103.

XIE, S., DENG, H., XIANG, B. & XIANG, S. 2008. Detection of trace triclocarban in water sample using solid-phase extraction - Liquid chromatography with stochastic resonance algorithm. *Environmental Science and Technology,* 42**,** 2988-2991.

YANG, L., CHENG, S. & WU, Z. 2009. Anthropogenic organic contaminants in water and surface sediments of large shallow eutrophic Chaohu Lake, China. *Fresenius Environmental Bulletin,* 18**,** 2048-2054.

YAO, J., XU, H., LV, L., SONG, D., CUI, Y., ZHANG, T. & FENG, Y. Q. 2008. A novel liquid-phase microextraction method combined with high performance liquid chromatography for analysis of phthalate esters in landfill leachates. *Anal Chim Acta,* 616**,** 42-8.

ZAFRA-GOMEZ, A., BALLESTEROS, O., NAVALON, A. & VILCHEZ, J. L. 2008. Determination of some endocrine disrupter chemicals in urban wastewater samples using liquid chromatography-mass spectrometry. *Microchemical Journal,* 88**,** 87-94.

ZECHMEISTER, L. 1948. HISTORY, SCOPE, AND METHODS OF CHROMATOGRAPHY. *Annals of the New York Academy of Sciences,* 49**,** 145-160.

ZHANG, D., LIU, H., LIANG, Y., WANG, C., LIANG, H. & CAI, H. 2009. Distribution of phthalate esters in the groundwater of Jianghan plain, Hubei, China. *Frontiers of Earth Science in China,* 3**,** 73-79.

ZHU, S. & CHEN, H. 2013. The fate and risk of selected pharmaceutical and personal care products in wastewater treatment plants and a pilot-scale multistage constructed wetland system. *Environ Sci Pollut Res Int*.

ZIMMERMAN, D. C., ROSSI, H. F., RIZZO, J., KEATING, D. W. & USHER, K. M. 2013. Analysis of Phthalates in Body Wash using Solid-Supported Liquid-Liquid Extraction. Available: https://www.chem.agilent.com/Library/applications/5991-2734EN.pdf [Accessed 16.09.2013].

List of figures

List of tables

Appendix A

HPLC literature Triclocarban

Article reference	(Liu and Wu, 2012)
Equiptment	RP-HPLC UV-DAD, Agilent 1200 series
Sample matrix	Cosmetics
Extraction method	Sonication
Detection limit	Good linear regression between test range of 0-110 mg/mL. LOD= 5 µg/g. LOQ=17 µg/g
Mobile phase	Isocratic elution. Buffer solution of methanol and 0.01 mol/L phosphate (72:28, V/V). pH 3
Column	Agilent Zorbax SB-C8 (250x4.6mm, 5µm). Temperature 35°C
Detector	Wavelength 280 nm. TCC found to have an max absorbance at 205 and 264 nm
Injection volume	10 µL
Flowrate, t_R	1 mL/min, 11 min
Article reference	(Baranowska et al., 2010)
Equiptment	RP- HPLC UV-DAD, Merck system
Sample matrix	Surface waters
Extraction method	SPE, 87% extraction efficiency
Detection limit	LOD= 0.17ng/mL. LOQ=0.50ng/mL
Mobile phase	Isocratic elution. Methanol:Water ratio 90:10, v/v
Column	Develosil RP Aqueous AR5 RP-30 (250x4.6mm, 5.8 µm), Temperature 25°C
Detector	Wavelength 265
Injection volume	20 µL
Flowrate, t_R	1 mL/min, 8.13 min
Article reference	(Shen et al., 2012)
Equiptment	RP-HPLC UV-DAD, Agilent series 1100HPLC
Sample matrix	Milli-Q water and river water
Extraction method	SPME
Detection limit	MDL (MQ)= 0.06 ng/mL, MDL (river water)= 0.47 ng/mL
Mobile phase	Gradient elution. Acetonitrile and deionized water
Column	HC-C18 (150 mmx4.6mm, 5µm)
Detector	Wavelength at 265 nm for quantitative analysis and 266 nm for qualitative analysis
Injection volume	-
Flowrate, t_R	1 mL/min, 6.9 min
Article reference	(Baranowska and Wojciechowska, 2012)
Equiptment	RP-HPLC UV-DAD, La Chrom ELITE Hitachi
Sample matrix	River water and wastewater
Extraction method	SPE
Detection limit	MDL (MQ)= 0.06 ng/mL, MDL (river water)= 0.47 ng/mL
Mobile phase	Gradient elution, Methanol:Water
Column	Develosil RP Aqueous AR5 RP-30 (250x4.6mm, 5.0 µm), pre-column Devosil RP Aqueous AR RP-30(10x4.0mm, 5.0 µm). Temp 20-22°C
Detector	Wavelength 265 nm
Injection volume	20 µL
Flowrate, t_R	0.9 mL/min, 9.39 min
Article reference	(Xie et al., 2008)
Equiptment	RP-HPLC UV-Vis
Sample matrix	Distilled water
Extraction method	SPE
Detection limit	LOD (without stochastic resonance)=10 ng/L, LOQ(without stochastic resonance)= 50 ng/L, LOD (with stochastic resonance)=1 ng/L, LOQ (with stochastic resonance)= 5 ng/L
Mobile phase	Isocratic elution, Methanol: Distilled water (80:20, v/v)
Column	Dikma Diamonsil C18(250mmx4.6mm, 5.0 µm)
Detector	Wavelength at 281 nm
Injection volume	20 µL
Flowrate, t_R	1 mL/min, 18 min

Article reference	(Wang et al., 2005)
Equiptment	RP-HPLC UV-RI
Sample matrix	-
Extraction method	SPME
Detection limit	-
Mobile phase	Methanol: Water with 0.3 M sodium perchlorate (80:20, v/v), pH 4.95 Acetonitrile:water with 0.05M potassium dihydrogen phosphate (70:30, 60:40, 50:50, v/v), pH 3.05
Column	Nucleosil (250x4.6mm, 5 µm, pore size 10 nm), µBondapack, Hypersil, and a Vydack C18column
Detector	Differential refractometer RI, wavelength at 214 nm and 260 nm
Injection volume	250 µL
Flowrate, t_R	1.5 mL/min, 1.0 mL/min
Article reference	(Verma and Xia, 2010)
Equiptment	RP-HPLC UV-DAD, Waters system alliance 2695
Sample matrix	Soil and biosolids
Extraction method	MISPE
Detection limit	MDL (MQ)= 0.06 ng/mL, MDL (river water)= 0.47 ng/mL
Mobile phase	Isocratic elution, Acetonitrile: Water(70:30, v/v)
Column	Xterra C18 RP (150x4.6mm, 5.0 µm)
Detector	Wavelength 260 nm
Injection volume	-
Flowrate, t_R	1 mL/min
Article reference	(Tizaoui et al., 2011)
Equiptment	RP-HPLC UV-Vis, Waters 2695
Sample matrix	acetonitrile:milliQ water (70:30, v/v)
Extraction method	-
Detection limit	LOD= 20 ng/L, LOQ= 66.7 ng/L
Mobile phase	Isocratic elution, Acetonitrile:Water (70:30, v/v)
Column	Hypersil Gold column C18 (150 × 4.6 mm, 5 µm)
Detector	Wavelength 265 nm
Injection volume	20 µL
Flowrate, t_R	1 mL/min, 4.6 min
Article reference	(Alshouli, 2012)
Equiptment	RP-HPLC UV-DAD, Hitachi
Sample matrix	Surface water
Extraction method	SPE
Detection limit	Linearity from 1-100µg/L
Mobile phase	Isocratic elution, Acetonitrile:Water (70:30, v/v)
Column	Thermo Hypersil Gold C-18 (150 × 4.6 mm, 5 µm), Temperature 40°C
Detector	Wavelength 231 nm
Injection volume	40 µL
Flowrate, t_R	1 mL/min, 7.39 min

HPLC litterature diehtyl phtalate

Article reference	(Zimmerman et al., 2013)
Equiptment	RP-HPLC UV-DAD, Agilent series 1200LC
Sample matrix	Body Wash
Extraction method	SLE and LLE
Detection limit	-
Mobile phase	Gradient elution. Water with 10% Acetonitrile:Acetonitrile
Column	Agilent Zorbax eclipse plus C18 (4.6mmx150mm, 5µm)
Detector	Wavelength 230 nm
Injection volume	1.7 µL
Flowrate, t_R	2 mL/min
Article reference	(Li et al., 2008)

Equiptment	RP- HPLC UV-DAD, Merck system
Sample matrix	Different water samples
Extraction method	SPE using ionic liquid mixed hemimicelles
Detection limit	LOD = 0.17 µg/L
Mobile phase	Isocratic elution. Acetonitrile:Water (75:25,v/v)
Column	Dikma Diamonsil-C18 (250mmx4.6mm, 4µm)
Detector	Wavelength 226
Injection volume	-
Flowrate, t_R	1 mL/min
Article reference	(Oh et al., 2006)
Equiptment	RP-HPLC UV-Vis
Sample matrix	-
Extraction method	SPE
Detection limit	-
Mobile phase	Isocratic elution. Methanol:10mM phosphoric acid-buffered water (40:60)
Column	C18, Waters
Detector	Wavelength at 275
Injection volume	300 µL
Flowrate, t_R	1 mL/min
Article reference	(de Oliveira et al., 2011)
Equiptment	HPLC UV-Vis, Kontron 325 system
Sample matrix	-
Extraction method	-
Detection limit	-
Mobile phase	Acetonitrile:Water (70:30)
Column	Hypersil C18 column (250mmx4.6mm)
Detector	Wavelength 228 nm
Injection volume	-
Flowrate, t_R	1 mL/min
Article reference	(Medellin-Castillo et al., 2013)
Equiptment	RP-HPLC UV-Vis
Sample matrix	Water
Extraction method	-
Detection limit	-
Mobile phase	Isocratic elution, Methanol:Milli-Q water (50:50, v/v)
Column	Nova-Pak C18 (150mmx3.9mm, 4µm)
Detector	Wavelength at 224 nm
Injection volume	-
Flowrate, t_R	1 mL/min
Article reference	(Navacharoen and Vangnai, 2011)
Equiptment	RP-HPLC UV-Vis, Shimadzu
Sample matrix	-
Extraction method	Same as (Li et al., 2008)
Detection limit	-
Mobile phase	Isocratic eluiton, Acetonitrile:Water (70:30)
Column	Hyperclone C18 (250mmx4.6mm, 5µm), Temperature 30°C
Detector	Wavelength at 226 nm
Injection volume	-
Flowrate, t_R	1 mL/min, 4.38 min
Article reference	(Wang et al., 2012)
Equiptment	RP-HPLC UV-Vis, Shimadzu
Sample matrix	River water, reservoir water
Extraction method	MSPE
Detection limit	LOD = 0.1ng/mL
Mobile phase	Isocratic elution, Acetoniltrile:Water (65:35, v/v)
Column	Centurysil C18 EPS (250mmx4.6mm, 5 µm)
Detector	Wavelength 225 nm
Injection volume	-

Flowrate, t_R	1 mL/min
Article reference	(Hubinger and Havery, 2006)
Equiptment	RP- HPLC UV-DAD, Agilent 1100 series
Sample matrix	Cosmetics
Extraction method	-
Detection limit	LOQ= 10 ppm
Mobile phase	Gradient elution, Water:Acetonitrile:2-propanol:Methanol
Column	Whatman partisil ODS (250mmx4.6mm, 3.5 µm)
Detector	Wavelength 230 nm
Injection volume	20 µL
Flowrate, t_R	1 mL/min, 9 min
Article reference	(Shen et al., 2007)
Equiptment	RP- HPLC UV-DAD, Agilent 1100 series
Sample matrix	Cosmetics
Extraction method	Sonication-assisted extraction with methanol and clean-up with C18 SPE
Detection limit	-
Mobile phase	Gradient elution, Methanol: Water
Column	Zorbax C8 (150mmx4.6mm, 3 µm), Temperature 30°C
Detector	Wavelength 230 nm
Injection volume	-
Flowrate, t_R	1 mL/min
Article reference	(Hadjmohammadi and Ranjbari, 2012)
Equiptment	RP-HPLC UV-Vis
Sample matrix	Different water samples
Extraction method	HLLE
Detection limit	LOD = 0.18 µg/L
Mobile phase	Isocratic elution, Acetoniltrile:Water (65:35, v/v)
Column	Waters column C18 (250mmx4.6mm, 10 µm)
Detector	Wavelength 286 nm
Injection volume	20 µL
Flowrate, t_R	1 mL/min
Article reference	(Kamarei et al., 2011)
Equiptment	RP-HPLC UV-DAD, Shimadzu
Sample matrix	Different water samples
Extraction method	USAEME-SFO
Detection limit	LOD = 0.005 µg/L
Mobile phase	Isocratic elution, Water:Methanol (24:76)
Column	Capital HPLC ODS-H C18 (250mmx4.6mm, 5 µm)
Detector	Wavelength 205 nm
Injection volume	10 µL
Flowrate, t_R	1 mL/min, 6 min
Article reference	(Cai et al., 2003)
Equiptment	RP-HPLC UV-DAD, Shimadzu
Sample matrix	River water
Extraction method	SPE and adsorption on multi-walled carbon nanotubes
Detection limit	LOD = 0.18 ng/mL
Mobile phase	Isocratic elution, Acetonitrile:water (67:33, v/v)
Column	Zorbax Eclipse XDB-C8 (150mmx4.6mm, 5 µm)
Detector	Wavelength 226 nm
Injection volume	-
Flowrate, t_R	1 mL/min
Article reference	(Ranjbari and Hadjmohammadi, 2012)
Equiptment	RP-HPLC UV
Sample matrix	Surface water
Extraction method	SPE
Detection limit	LOD=33 ng/L, LOQ=110 ng/L
Mobile phase	Gradient elution, Acetonitrile: Acidified water

Column	Capcell Pack C18 AG120 (250mmx4.6mm, 5 µm)
Detector	Wavelength 225 nm
Injection volume	20 µL
Flowrate, t_R	0.8 mL/min, 24.3 min
Article reference	(Yao et al., 2008)
Equiptment	RP-HPLC VWD, Agilent 1100 series
Sample matrix	Landfill leachates
Extraction method	LPME
Detection limit	LOD=0.0014mg/L
Mobile phase	Isocratic elution, Methanol: Water (80:20, v/v)
Column	Venusil, XBP C18 column (250mmX4.6mm, 5 µm), Temperature 25°C
Detector	Wavelength 280 nm
Injection volume	20 µL
Flowrate, t_R	1 mL/min
Article reference	(Montagner and Jardim, 2011)
Equiptment	RP-HPLC VWD, Agilent 1100 series
Sample matrix	Landfill leachates
Extraction method	LPME
Detection limit	LOD=0.0014mg/L
Mobile phase	Isocratic elution, Methanol: Water (80:20, v/v)
Column	Venusil, XBP C18 column (250mmX4.6mm, 5 µm), Temperature 25°C
Detector	Wavelength 280 nm
Injection volume	20 µL
Flowrate, t_R	1 mL/min

HPLC literature 4-MBC

Article reference	(Badia-Fabregat et al., 2012)
Equiptment	HPLC UV, Dionex 3000 , same method as (Salvador and Chisvert, 2005)
Sample matrix	Sterile sewage sludge
Extraction method	PLE, pressurized liquid extraction
Detection limit	-
Mobile phase	Gradient elution, Ethanol and acetic acid (1%): MilliQ water
Column	LiChrosphere RP-18 (12.5 mm x4mm, 5µm particle size)
Detector	-
Injection volume	-
Flowrate, t_R	0.5 ml/min, 8 min
Article reference	(Salvador and Chisvert, 2005)
Equiptment	HPLC UV-Vis, Hitachi
Sample matrix	Lotion
Extraction method	-
Detection limit	LOD= 0.4 µg/ml
Mobile phase	Ethanol:Water with 1% Acetic acid (70:30, v/v), pH 4.75, Temperature 45°C,
Column	LiChrosphere RP-18 (C-18) (12.5 mm x 4mm, 5µm particle size)
Detector	Wavelength 313 nm
Injection volume	20 µl
Flowrate, t_R	0.5 mL/min, 8 min
Article reference	(Fent et al., 2010)
Equiptment	HPLC UV- Vis Agilent 1100 system coupled to an LC/MSD Trap XCT plus
Sample matrix	River water
Extraction method	SPE
Detection limit	LOD= 200-400 pg
Mobile phase	-
Column	Zorbax SB-C18 coloumn (150 mmx3.0mm, 3.5µm) and, Temperature 30 C°
Detector	-
Injection volume	-

Flowrate, t_R	-
Article reference	(Rodil et al., 2009a)
Equiptment	HPLC MS, Hewlett Packard 1100 series
Sample matrix	MQ-water
Extraction method	SBSE
Detection limit	-
Mobile phase	Gradient elution, Water: Methanol
Column	LUNA C8(20x2.0mm, 5µm) Mercury MS Cartridge system phenomenex
Detector	MS
Injection volume	5 µl
Flowrate, t_R	0.4ml/min
Article reference	(Giokas et al., 2005)
Equiptment	HPLC UV-DAD, Shimadzu
Sample matrix	Bathing water
Extraction method	Cloud point extraction (CPE)
Detection limit	LOD =0.14 µg/l
Mobile phase	Isocratic elution , Aquatic mixture of 100 mM SDS:Acetonitrile (20/80%, v/v), pH 3
Column	Discorvery C18 (25 cmx 4.6mm, 5 µm), Temperature at 30 C°
Detector	-
Injection volume	20 µl
Flowrate, t_R	-
Article reference	(Giokas et al., 2004)
Equiptment	HPLC UV-DAD, Shimadzu
Sample matrix	Natural waters
Extraction method	SPE
Detection limit	LOQ = 8 ng/l
Mobile phase	Isocratic elution, Aquatic mixture of 3.5 mM SDS:Acetonitrile (20/80%, v/v), pH 3
Column	Discorvery C18 (25 cmx 4.6mm, 5 µm), Temperature at 30 C°
Detector	Wavelength 300 nm
Injection volume	20 µl
Flowrate, t_R	-
Article reference	(Esbenshade et al., 2010)
Equiptment	HPLC UV-DAD
Sample matrix	Svimming pool water
Extraction method	-
Detection limit	-
Mobile phase	Isocratic elution, Methanol:water (88:12, v/v), pH 9
Column	Shimatzy CLC-ODS C18 column (25 cm x4.6mm, 100 å), Ambient temperature
Detector	Wavelength 320 nm
Injection volume	20 µL
Flowrate, t_R	1 ml/min, 12.6 min
Article reference	(Liu and Wu, 2011)
Equiptment	RP-HPLC UV-DAD, Agilent 1100 series
Sample matrix	Cosmetics
Extraction method	Sonication
Detection limit	LOQ= 800 ng/ml, LOD=250 ng/ml
Mobile phase	Gradient elution, Methanol:Tetrahydrofuran:Perchlorid acid aqueous solution (0.2ml $HClO_4$ + 300 ml H20) Acidic mobile phase
Column	Agilent SB-C18 (25x4.6mm, 5µm), Temperature 30°C
Detector	Wavelength 311 nm
Injection volume	10 µL
Flowrate, t_R	1 ml/min, 6.3 min
Article reference	(Vosough et al., 2012)

Equiptment	RP-HPLC UV-DAD, Agilent 1200 series
Sample matrix	Urine
Extraction method	Dispersive liquid-liquid micro-extraction (DLLME)
Detection limit	LOQ=0.003 µg/mL, LOD=1.0-13.8 ng/mL
Mobile phase	Isocratic elution, Water:Methanol: Acetonitrile (8:42:50; v/v/v)
Column	Octadecylsilane column (7cmx0.46cm, 5-µm), Temperature 25°C
Detector	Wavelength 300 nm
Injection volume	20 µl
Flowrate, t_R	1 ml/min, 4 min
Article reference	(Ge and Lee, 2012)
Equiptment	HPLC UV-Vis, Waters system
Sample matrix	Milli-Q water
Extraction method	IL-USAEME
Detection limit	LOD=1ng/ml
Mobile phase	Isocratic elution, Ethanol: 1%acetic acid (60:40, v/v)
Column	Metaphase C18 packed column (25 cmx4.6mm internal diameter, 5-µm)
Detector	Wavelength 289 nm
Injection volume	20 µl
Flowrate, t_R	1.5 ml/min

Appendix B

SPE literature triclocarban

Report	Step 1 Equipment	Step 2 Condition	Step 3 Add the sample	Step 4 Wash the packing	Step 5 Elute the compounds
(Baranowska and Wojciechowska, 2012)	Bakerbond Speedisc Octadecyl (C18) (50 mm) discs	10 mL methanol and 10 mL water (pH 5), flowrate 2 mL/min	3 L of filtered water sample added to the disc at a flowrate of 10-15 ml/min. Dried for 2 min		10 mL of methanol at a flowrate of 1 mL/min
(Baranowska et al., 2010)	Bakerbond spe-12G system with cartridges (C18; 6mL, 500 mg)	5 mL methanol and 4 mL of water , flowrate of 2 mL/min	1 L of filtered water sample added, dried under vacuum for 10 min		7 mL methanol. Evaporated to dryness and dissolved in 1 mL methanol
Algorithm (Xie et al., 2008)	Oasis HLB (60 mg) cartridges	2 mL methanol in acetone (50%) followed by 2 mL methanol and 6 mL water.	200 mL	1 mL water containing 5% methanol by volume	3 mL methanol in acetone (50%), flowrate 0.5 mL/min. Extracts dried and reconstituted in 200µL methanol
(Halden and Paull, 2005)	Oasis HLB (3 cm^3, 60 mg)				4 mL of 50:50 methanol:acetone with 10mM AcOH Dried and reconstituted with 1 mL of 50:50 methanol:acetone
(Nelson et al., 2010)	OASIS HLB 200 mg polymeric cartridges		200 mL of sample, Flowrate 10 ml/min	Rinsed, dried	Methanol followed by methanol: dichloromethanol (70:30) Extracts reduced to 1 mL afterwards
(Essandoh et al., 2010)	6 cm^3 Envi-chrom P cartrigdes (from supelco)	2 mL methanol 2 mL 50:50 acetone: methanol 6 mL MQ water	500 mL at flowrate 5 mL/min by vacuum manifold	Dried in between	4 mL 50:50 acetone:methanol with 10 mM AcOH. Dried, reconstituted in 1 mL 50:50 acetone:methanol
(Zhu and Chen, 2013)	Oasis HLB cartridges (6 mL, 500 mg, waters)	10 mL methanol and 10 mL MQ water	250 mL-500 mL of sample volume. Flowrate 2 mL/min	Rinsed with 20 mL ultrapure wter and dried under nitrogen gas for 15 min	4 mL of methanol:acetonitrile (1:1, v/v) x2. Elutes dried to 1 mL
(Chen et al., 2010)	Oasis HLB SPE cartridges	10 mL methanol followed by 10 mL Milli-Q	Flowrate 10 mL/min	Rinced twice with 50 mL Milli-Q water with 5% methanol (v/v) Dried	4X3 mL of methanol followed by 3x2 mL of dichloromethane Concentrated under nitrogen gas, redissolved in 1 mL of methanol
(Ferrer et al., 2010)	Oasis HLB cartridges (500 mg, 6 mL, from waters)	4 mL methanol followed by 6 mL of HPLC-grade water	200 mL sample	Dried for 3 min	5 mL methanol. Evaporated to volume of 0.5 mL

Report	Step 1 Equipment	Step 2 Condition	Step 3 Add the sample	Step 4 Wash the packing	Step 5 Elute the compounds
(Pedrouzo et al., 2009)	Oasis HLB 500 mg	5 mL of MeoH and 2 mL of Milli-Q water	100 mL influent, 200 mL effluent, Flowrate 10-15 mL/min	Clean-up step 15% MeOH in 5 mL water solution. Cartridges dried for 5 min	5 mL MeOH, complete drying, Adding 5 mL DCM. Extracts reduced to ca. 3-4 mL. Diluted to 5 mL with Milli-Q water
(Wick et al., 2010)	Oasis HLB cartridges (200 mg, 30µm, from waters)	1x2 mL heptane followed by 1x2mL acetone, 2x3mL methanol and 4x2mL groundwater	Water samples volume 100 mL, 200 mL and 1000 mL Flowrate at 5mL/min	Dried by nitrogen stream for ca 1 hour	4X2mL mixture of methanol:acetone (60:40, v/v). Extracts evaporated to 500 µL and filled up to volume of 1 mL with 0.1% formic acid
(Gonzalez-Marino et al., 2009)	Oasis HLB cartridges (3mL, 60 mg)	Sequentially 3 mL methanol and 3 mL water	200 mL for sewage. Flowrate 10 mL/min	Dried under vacuum for 30 min	4 mL methanol. Concentrated down to 0.5 mL and diluted to a final volume of 1 mL with ultrapure water
(Trenholm et al., 2008)	200 mg HLB glass cartridges	Sequentially, 5mL MTBE, 5mL methanol, 5 mL reagent water	500 mL added at flowrate 15 mL/min	5 mL reagent water. Dried	5 mL methanol, followed by 5 mL of 10:90 (v/v) methanol/MTBE. Reduced to 500 µL
(Halden and Paull, 2004)	Oasis HLB $3cm^3$/60 mg				4 mL, 50:50 methanol:acetone containing 10 mM acetic acid. Eluates dried, reconstituted (1mL, 50:50 methanol:acetone),

SPE literature diethyl phthalate

Report	Step 1 Equiptment	Step 2 Condition	Step 3 Add the sample	Step 4 Wash the packing	Step 5 Elute the compounds
(Oh et al., 2006)	1 g of reversed phase C18nec (6 mL reservoir) from Sepak Waters	3x3 mL methanol	500 mL, flowrate 10-15 mL/min under 5 in Hg of a vacuum manifold	3x3 mL deionized water (pH 2)	2x5 mL acetone. Evaporated to dryness under nitrogen. Then 0.5 mL ethanol
(Bono-Blay et al., 2012)	Oasis HLB 200 mg sorbent in 6 mL syringe cartridges	10 mL hexane, 10 mL dichloromethane, 10 mL methanol, and 15 mL of HPLC-grade water	1000 mL samples spiked with surrogate solution. Flowrate 8-13 mL/min	Dried by vacuum system for about 60 min	10 mL dichloromethane: hexane (1:1, v/v) at 1 mL/min and 10 mL of acetone: dichloromethane (1:1, v/v) at 1 mL/min Dried. Reconstituted with 250 µL acetate and 10 µL of 10 ng/µL deuterated internal standard
(Sánchez-Avila et	Oasis HLB 200 mg	10 mL Hexane	250 mL added 10	5 mL x 3	10 mL

Report	Step 1 Equiptment	Step 2 Condition	Step 3 Add the sample	Step 4 Wash the packing	Step 5 Elute the compounds
al., 2012)		10 mL dichloromethane, 10 mL methanol 15 mL MQ water. Flowrate 5 mL/min	ng/L surrogate standard. Flowrate 10 mL/min	ultrapure water and dried under vacuum for 30 min	dichloromethane :hexane (1:1, v/v) then 10 mL acetone: dichloromethane (1:1, v/v). Evaporated to dryness. Reconstituted with 250µL ethyl acetate.
(Boonyaroj et al., 2012)	C18 bond elut SPE resin with 500 mg SPE sorbent	6 mL methanol, 6 mL pure water	100 mL leachate. Flow rate 1 mL/min	Dried with clean air	2x3mL dichloromethane :methanol mixture (1:9, v/v). Reduced to 0.5 mL by nitrogen.
(Montagner and Jardim, 2011)	Oasis HLB 500 mg (Waters)	6 mL methanol, 6 mL water, 6 mL acidified water (pH 3)	1000 mL (pH 3) Flowrate 10 mL/min		4X3 mL methanol. Concentrated until dryness and reconstituted with 0.5 mL acetonitrile
(Prapatpong and Kanchanamayoon, 2010)	3.0 mL LC-18 (500 mg) and and 6.0 mL Florisil (1 g) column	5 mL methanol under vacuum, followed by 5 mL deionized water	100 mL deionized water Flowrate 1 mL/min		Diff. kind of solvents:
(Russo et al., 2012)	Carbograph 1 (250 mg, 80-100 mesh size) packed in a poly-propylene tube (6.0x0.8 cm)	3 mL n-hexane, 3 mL acetone and 3 mL carbon disulfide	100 mL 5-6 mL/min		3X 5mL n-hexane Combined organic extract were dried and, after I.S addition, concentrated under nitrogen flow.
(Guo et al., 2010)	Waters Oasis MAX SPE cartridges	Equilibrated by 1 mL acetonitrile and then conditioned by 1 mL ultrapure water	1 mL human serum, gravity	1 mL 5% acetonitrile aqueous solution	2 mL 100% acetonitrile. Evaporated to dryness reconstituted in 1 mL acetonitrile with 3 min vortex
(Yang et al., 2009)	Oasis HLB (500 mg, 6CC, from waters)	6 ml n-hexane, methylene dichloride, and ethyl acetate followed by methanol	4000 mL surface water. Flowrate 5 mL/min	Dried under vacuum for 5 min	4 x 2mL aliquots n-hexane, methylene, dichloride, ethyl acetate and methanol at flowrate of 5 mL/min. Concentrated to 1 mL using nitrogen
(Zhang et al., 2009)	Agilent SPE cartridge (500 mg, 6 mL)	2 mL methylene chloride, 1 mL acetone, 2 mL methanol and 2 mL organic free-water, respectively	1000 mL groundwater Flowrate 4 mL/min	Dried for about 3 min	Elution passed through the cartridge, didn't say anything about which elutions
(Fatoki and Noma, 2002)	Envi C18 (1 g packing) solid phase column	Deionized water followed by 2 mL CH3OH	1000 mL Flowrate 1mL/min	2 mL CH3OH: CH2Cl2 (50:50, v/v)	

SPE literature 4-MBC

Report	Step 1 Equiptment	Step 2 Condition	Step 3 Add the sample	Step 4 Wash the packing	Step 5 Elute the compounds
(Giokas et al., 2005)	Supelco vacuum apparaturs 500 mg C18 disks (47mm) (from Empore)	5 mL ethyl acetate:dichloro methane (1:1, v/v) 10 mL methanol 5 mL of MQ water	500 ml (pH 3)	Disk was dried for 5 min under vacuum	Two aliquots 5 mL of ethyl acetate: dichloromethane (1:1, v/v) Evaporated to dryness and redissolved in scaled micro vials to 0.050 mL with methanol
(Fent et al., 2010)	500 mg Phenomenex strata-X-CW cartridge	Dichloro-methane, MeOH MQ water	1000 mL		Dichloromethane and MeOH. Dried and resolved in ethanol
(Gago-Ferrero et al., 2013)	PLRP-s cartridge (cross-linked styrene-divinyl-benzene polymer, 15-25µm particle size)	1 mL MeOH, 1 mL ACN, 1 mL HPLC grade water Flow rate 5 mL/min	5 mL sample. Flowrate 1 mL/min	0.5 mL HPLC water at flowrate 5 mL/min	On line SPE, eluted from cartridge by the mobile phase used in the chromatographic analysis
(Díaz-Cruz et al., 2012)	Isolute SPE Columns C18 (500 mg)	5 mL CH_2Cl_2:AcEt (1:1), 5 mL MeOH and 5 mL HPLC-grade water	Aliquots of 200 mL water sample Flowrate 1 mL/min	Dried under vacuum for 30 min	Four successive 2.5 mL aliquots of CH2CL2:AcEt (1:1). Flowrate of 0.5 mL/min Evaporated under nitrogen at 25°C, reconstituted in 0.5 mL n-hexane plus 0.1 mL of a solution of benzyl cinnamate in n-hexane
(Cuderman and Heath, 2007)	SPE cartridges Strata X (60mg/3 mL)	1.5 mL ethyl acetate:dichloro methane (1:1, v/v), 1.5 mL methanol 1.5 mL MQ water	500 mL (pH 3) 5 ml/min	1.5 mL methanol (1%, v/v). Column left to dry for 2 min	1:1 (v/v) ethyl acetate-dichloromethane (3x0.5 mL). Evaporated in dryness before dissolution in 0.4 mL toluene
(Rodil et al., 2009b)	Visiprep SPE Oasis HLB 200 mg	Sequentially, 5 mL MeOH and 5 mL pure water	200-500 mL. pH 7	3 mL Milli-Q water. Dried with nitrogen	Mehtanol (3 x10 mL) Concentrated by evaporation to 0.2 mL and made to final volume of 1 mL with methanol:water (1:1)
(Rodil et al., 2008)	Visiprep SPE manifold. Oasis HLB 60 mg	Sequentially, 3 mL MeOH, 3 mL pure water, 3 mL buffer	200 mL with addition of 20 mL ion-pair buffer solution (2% MeOH, 50 mM TrBA, pH 4.5 formic acid)	3 mL buffer, 3 mL Milli-Q water Dried with nitrogen	Methanol (3 x 10 mL) Concentrated by evaporation to 0.2 mL and made to final volume of 1 mL with methanol:water (1:1)
(Li et al., 2007)	C18 cartridge (200mg/3mL, from Agela technologies	5 mL ethylacetate :dichloro-methane (1:1) 5 mL methanol 5 mL deionized water	1000 mL sample (pH 3) Flowrate 10 mL/min.	Dried for about 5 min under vacuum.	5 mL aliquots ethylacetate/dichloromethan e (1:1, v/v). Evaporated to dryness under ethylacetate:dichloromethan e (1:1, v/v). Redissolved with n-hexane to 1 mL

Appendix C

Filter test of TCC

The filter test was conducted by first preparing a solution with TCC in MQ water of concentration 20 µg/L. First, the initial area (concentration) was measured without the use of any filters. Then increasing volumes of the solution where filtered through a cellulose, Teflon and GF filter. Samples of filtered solution were taken at set intervals. Recoveries were plotted as a function of volume solution gone through the filters. The aim was to see if full recoveries could be achieved after saturation of the filters. The test showed that:

- the cellulose filter adsorbed most of the TCC. The recovery did not increase with increasing volume through filter
- the telfon filter showed increasing recovery with increasing volume through filter, but still only 80% recovery was reached
- the GF filter showed high recovery after only 5 mL volume had gone through the filter.

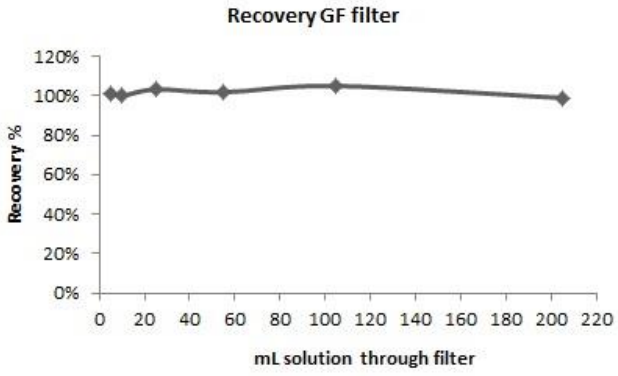

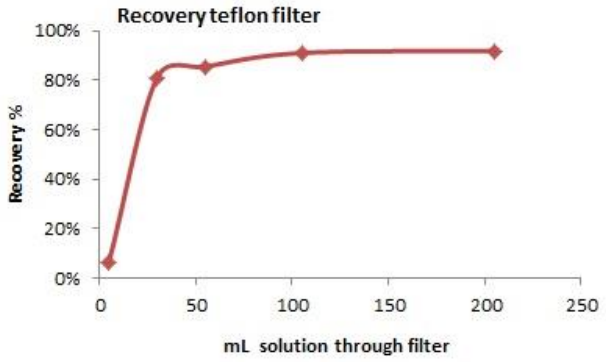

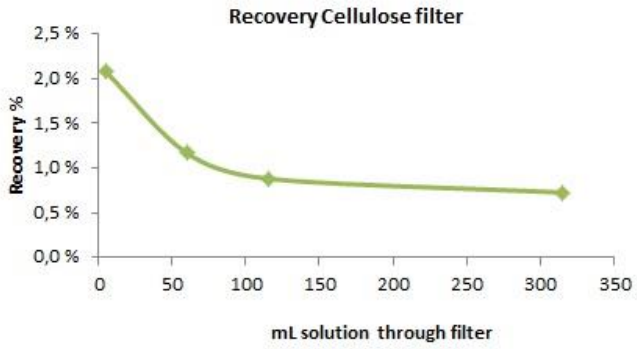

Appendix D

Time schedules adsorption kinetic experiments

		Greywater TCC	MQ TCC	Greywater TCC	MQ TCC
Time (min)	Amount withdrawn per sample (mL)	Real time	Real time	Real time ref1	Real time ref2
0	5				
5	5				
10	5				
15	5				
30	5				
45	5				
60 (1 hr)	5				
120 (2 hr)	5				
240 (4 hr)	5				
360 (6 hr)	5				
480(8 hr)	5				
600(10 hr)	5				
1440(24 hr)	5				
Total amount	65				

		Greywater DEP	Greywater DOC	MQ DEP	Greywater DEP ref	MQ DEP ref
Time (min)	Max amount withdrawn (only GW) (mL)	Real time	Real time	Real time	Real time	Real time
0	20+5					
5	5					
10	5					
15	5					
30	20+5					
45	5					
60 (1 hr)	20+5					
120 (2 hr)	20+5					
240 (4 hr)	20+5					
360 (6 hr)	20+5					
480(8 hr)	5					
600(10 hr)	20+5					
1200(20 hr)	5					
1440(24 hr)	20+5					
1620(27 hr)	20+5					
Total amount	30					

Appendix E

Data calibration curves

Triclocarban		**Diehtyl Phthalate**	
Concentration	Area	Concentration	Area
µg/L	mAu	µg/L	mAu
0	0	0	0
0,05	0,63	0,001	1,13
0,1	0,94	0,005	3,11
0,5	2,9	0,01	5,62
1	5	0,02	9,72
2	9,4	0,03	15,81
3	13,5	0,05	26,73
5	23,3	0,07	35,74
10	47,2	0,1	52,29
15	70,4	0,3	155,3
20	93,3	0,5	263,42
25	120,8	0,7	350,88
		1	531,64
		2	1066,07
		4	2018,37
		5	2619,43

Appendix F

Data TCC adsorption kinetic experiments

The lines marked with red were taken out of the calculations

Water	MQ		
Amount carbon	100	mg	
Volume	0,25	L	
Ci	19,038	µg/L	
Ce	0,830	µg/L	
Qe	0,046	µg /mg	
Time (min)	**Area (mAU/s)**	**Conc (µg/L)**	**Qt (µg/mg)**
0,00	90,4	19,038	0,000
4,92	63,6	13,397	0,014
10,17	59,9	12,618	0,016
15,20	48,5	10,218	0,022
30,17	41,5	8,745	0,026
45,25	37,7	7,945	0,028
60,02	26,3	5,545	0,034
241,30	6,3	1,335	0,044
341,73	7,2	1,525	0,044
485,17	3,9	0,830	0,046

Water	GW		
Amount carbon	100	mg	
Volume	0,25	L	
Ci	16,807	µg/L	
Ce	0,241	µg/L	
Qe	0,041	µg /mg	
Time (min)	**Area (mAU/s)**	**Conc (µg/L)**	**Qt (µg/mg)**
0,00	79,8	16,807	0,0000
2,03	59,3	12,492	0,0108
5,12	58,5	12,323	0,0112
10,12	50,3	10,597	0,0155
15,20	45,8	9,650	0,0179
30,17	37,8	7,966	0,0221
45,17	30,7	6,471	0,0258
60,23	27	5,693	0,0278
118,63	12,5	2,640	0,0354
237,33	5,2	1,104	0,0393
360,90	1,4	0,304	0,0413
643,00	1,1	0,241	0,0414

Water	MQ		
Amount carbon	252	mg	
Volume	0,9	L	
Ci	19,838	µg/L	
Ce	2,030	µg/L	
Qe	0,064	µg /mg	
Time (min)	**Area (mAU/s)**	**Conc (µg/L)**	**Qt (µg/mg)**
0	94,2	19,84	0,000
6	72,7	15,31	0,016
11	70,8	14,91	0,018
15	65	13,69	0,022
31	51,7	10,89	0,032
45	43,4	9,14	0,038
61	41,5	8,74	0,040
121	24,1	5,08	0,053
240	16,2	3,42	0,059
358	11,9	2,51	0,062
568	9,6	2,03	0,064
1590	12,6	2,66	0,061

Water	GW		
Amount carbon	252	mg	
Volume	0,9	L	
Ci	17,207	µg/L	
Ce	1,567	µg/L	
Qe	0,056	µg /mg	
Time (min)	**Area (mAU/s)**	**Conc (µg/L)**	**Qt (µg/mg)**
0	81,7	17,21	0,0000
5	65,1	13,71	0,0125
10	59,4	12,51	0,0168
17	54,2	11,42	0,0207
30	46,3	9,76	0,0266
45	42,4	8,93	0,0295
60	31,7	6,68	0,0376
120	23,1	4,87	0,0441
355	7,8	1,65	0,0556
567	7,7	1,63	0,0556
1590	7,4	1,57	0,0559

Data DEP adsorption experiments

Water	MQ			
Amount carbon	200	mg		
Volume	0,5	L		
Ci	5151,64	µg/L		
Ce	2,37	µg/L		
Qe	12,87	µg /mg		
Time (min)	**Area (mAU/s)**	**Conc (µg/L)**	**Qt (µg/mg)**	
0	2668,6	5151,64		0,000
5	2647,6	5111,10		0,101
10	2505,6	4836,97		0,787
15	2482,4	4792,19		0,899
30	2159,9	4169,61		2,455
45	1881,6	3632,36		3,798
60	1533,7	2960,75		5,477
90	1095,7	2115,21		7,591
120	686,8	1325,84		9,564
180	379,3	732,23		11,049
240	169,5	327,21		12,061
300	92,6	178,76		12,432
360	34,7	66,99		12,712
480	13,6	26,25		12,813
1190	3,7	7,14		12,861
1400	1,25	2,41		12,873
1550	1,23	2,37		12,873

Water	GW		
Amount carbon	200	mg	
Volume	0,5	L	
Ci	5127,70	µg/L	
Ce	1,72	µg/L	
Qe	12,81	µg /mg	
Time (min)	**Area (mAU/s)**	**Conc (µg/L)**	**Qt (µg/mg)**
0	2656,2	5127,70	0,000
10	2556,4	4935,04	0,482
20	2321,7	4481,96	1,614
33	1987,8	3837,38	3,226
60	1590,5	3070,40	5,143
111	1062,6	2051,31	7,691
211	444,8	858,67	10,673
357	123,4	238,22	12,224
503	36,1	69,69	12,645
607	15,7	30,31	12,743
1585	0,9	1,72	12,815
1820	1,9	3,67	12,810

Appendix G

Data adsorption isotherm experiments

MQ TCC (alone)			
Conc carbon	**Ce**	**Adsorbed TCC**	**Qe**
mg/250mL	µg/L	mg/L	µg/mg
0	18,47	0,00	
0,95	15,38	3,09	0,8143
2,6	14,53	3,94	0,3785
5	10,26	8,21	0,4105
10,25	5,97	12,50	0,3050
20,1	3,67	14,80	0,1841
29,7	1,78	16,69	0,1405
39,6	0,87	17,60	0,1111
60,1	0,81	17,66	0,0735
79,4	0,79	17,68	0,0557
100,4	0,47	18,00	0,0448

GW TCC (alone)			
Conc carbon	**Ce**	**Adsorbed TCC**	**Qe**
mg/250mL	µg/L	mg/L	µg/mg
0	16,680	0,00	
1	12,534	4,15	1,0367
2,45	10,555	6,13	0,6250
4,8	7,103	9,58	0,4988
10,05	4,619	12,06	0,3000
20,4	1,588	15,09	0,1850
29,6	0,620	16,06	0,1356
40,4	0,620	16,06	0,0994
60,3	0,514	16,17	0,0670
80,2	0,409	16,27	0,0507
98,7	0,157	16,52	0,0419

MQ TCC(mixture)			
Conc carbon	**Ce**	**Adsorbed TCC**	**Qe**
mg/250mL	µg/L	mg/L	µg/mg
0	18,410	0,00	
0,7	12,555	5,86	2,0912
2,5	10,366	8,04	0,8044
5,1	7,566	10,84	0,5316
9,8	2,409	16,00	0,4082
19,7	1,083	17,33	0,2199
30,1	0,956	17,45	0,1450
39,5	0,830	17,58	0,1113
55	2,935	15,47	0,0703
80,4	3,209	15,20	0,0473
99,3	1,840	16,57	0,0417

GW TCC (mixture)			
Conc carbon	**Ce**	**Adsorbed TCC**	**Qe**
mg/250mL	µg/L	mg/L	µg/mg
0	14,43	0,00	
0,7	10,22	4,21	1,5042
2,5	7,65	6,78	0,6780
5,4	5,55	8,88	0,4113
10	2,37	12,06	0,3016
19,4	0,79	13,64	0,1758
30	0,60	13,83	0,1153
39,9	0,54	13,89	0,0871
59,6	0,51	13,92	0,0584
99,7	0,45	13,98	0,0351

MQ DEP (alone)			
Conc carbon	**Ce**	**Adsorbed DEP**	**Qe**
mg/250mL	µg/L	mg/L	µg/mg
0	5122,870	0,00	
2	4310,535	812,34	101,5419
5,1	2415,977	2706,89	132,6909
7	2412,502	2710,37	96,7989
10	1267,157	3855,71	96,3928
19,9	242,273	4880,60	61,3140
29,9	72,585	5050,28	42,2265
40,2	8,687	5114,18	31,8046
59,7	3,089	5119,78	21,4396
79,8	1,486	5121,38	16,0444
100,5	3,668	5119,20	12,7343

GW DEP (alone)			
Conc carbon	**Ce**	**Adsorbed DEP**	**Qe**
mg/250mL	µg/L	mg/L	µg/mg
0	5155,50	0,00	
2,2	4440,07	715,43	81,2990
5,4	3149,75	2005,75	92,8590
10,1	2445,32	2710,18	67,0837
19,8	689,18	4466,32	56,3930
30,3	290,15	4865,35	40,1432
39,6	82,04	5073,46	32,0294
60,5	13,90	5141,60	21,2463
79,9	5,79	5149,71	16,1130
99,6	1,93	5153,57	12,9357

MQ DEP (mixture)			
Conc carbon	**Ce**	**Adsorbed DEP**	**Qe**
mg/250mL	µg/L	mg/L	µg/mg
0	5085,230	0,00	
0,7	4480,415	604,81	216,0052
2,5	3681,782	1403,45	140,3448
5,1	2547,055	2538,17	124,4203
9,8	1051,138	4034,09	102,9105
19,7	415,629	4669,60	59,2589
30,1	54,246	5030,98	41,7856
55	5,791	5079,44	23,0884
80,4	4,247	5080,98	15,7991
99,3	9,073	5076,16	12,7799

GW DEP (mixture)			
Conc carbon	**Ce**	**Adsorbed DEP**	**Qe**
mg/250mL	µg/L	mg/L	µg/mg
0,0	5031,76	0,00	
0,7	4483,12	548,64	195,9435
2,5	3730,62	1301,14	130,1137
5,4	3121,18	1910,58	88,4530
10,0	1844,95	3186,81	79,6704
19,4	735,31	4296,45	55,3666
30,0	196,33	4835,43	40,2953
39,9	63,71	4968,05	31,1282
59,6	8,69	5023,07	21,0699
99,7	6,56	5025,20	12,6008

GW DOC(mixed with DEP) Conc carbon	Ce	Adsorbed DOC	Qe
mg/250mL	µg/L	mg/L	µg/mg
0	9780,00	0,00	
2,2	8209,00	1571,00	178,5227
5,4	7033,00	2747,00	127,1759
10,1	8981,00	799,00	19,7772
19,8	8270,00	1510,00	19,0657
30,3	5057,00	4723,00	38,9686
39,6	3776,00	6004,00	37,9040
60,5	4439,00	5341,00	22,0702
79,9	4356,00	5424,00	16,9712
99,6	3211,00	6569,00	16,4885